The Metallurgy and Processing Science of Metal Additive Manufacturing

W.J. Sames[1,2], F.A. List,[2,3] , S. Pannala, R.R. Dehoff[2,3], and S.S. Babu[2,4]

[1] Department of Nuclear Engineering, Texas A&M University, College Station, TX;
[2] Manufacturing Demonstration Facility, Oak Ridge National Laboratory, Knoxville, TN;
[3] Materials Science and Technology Division, Oak Ridge National Laboratory, Oak Ridge, TN;
[4] Department of Aerospace and Biomedical Engineering, University of Tennessee, Knoxville, TN

Contents

Abstract

Additive Manufacturing (AM), widely known as 3D printing, is a method of manufacturing that forms parts from powder, wire, or sheets in a process that proceeds layer-by-layer. Many techniques (using many different names) have been developed to accomplish this via melting or solid-state joining. In this review, these techniques for producing metal parts are explored, with a focus on the science of metal AM: processing defects, heat transfer, solidification, solid-state precipitation, mechanical properties, and post-processing metallurgy. The various metal AM techniques are compared, with analysis of the strengths and limitations of each. Few alloys have been developed for commercial production, but recent development efforts are presented as a path for the ongoing development of new materials for AM processes.

1. Introduction & History

Additive Manufacturing (AM), or 3D printing, has grown and changed tremendously in the past 30 years since researchers in Austin, TX started development of what is arguably the first machine in the lineage of metal AM: a laser used to selectively melt layers of polymer and, later, metal. [1] The development of metal AM techniques has made great progress since then, but faces unique processing and materials development issues. Understanding the various processes used to make metal AM parts, and the issues associated with them, is critical to improving the capabilities of the hardware and the materials that are produced. This paper overviews metal AM processes, discusses material processing defects, summarizes the resulting microstructures and mechanical properties of current research, and discusses the future of the field of metal AM.

The first experiments with metal AM grew out of efforts originally targeted at forming polymer powder into 3D parts. [2-5] This research focused on powder bed laser sintering, which was patented and copyrighted as Selective Laser Sintering (SLS). This technique is still used today (the term “sintering” is now used loosely, as many processes use complete melting) under license by EOS GmbH. Shortly after SLS was patented, a group of researchers at MIT patented a process called “three-dimensional printing”, which used inkjet printing to deposit binder. The use of “3D printing” has grown to describe all forms of AM, while the MIT method has become known as binder jetting (BJ). BJ can be used to create metal parts, in addition to other materials. In 1993, research in Sweden led to the patent of another powder bed technique: Electron Beam Melting (EBM). This process was later licensed and developed by Arcam AB. Another class of printers deposit feedstock directly into a molten pool, as opposed to selective melting of a powder bed. Known as Direct Energy Deposition (DED), some of these machines fed by wire trace their history to welding technologies. In 1995, Sandia National Laboratories developed a different approach to feed powder into DED with a laser heat source. This technology was first commercialized and trademarked as Laser Engineered Net Shaping (LENS), a sub-set of DED. The last major category of metal AM, sheet lamination (SL), welds together sheets of feedstock to form parts. A process that uses ultrasonic welding and CNC to accomplish this was originally developed and patented by Dawn White of Solidica in 1999. This metal AM history is more concisely presented as a timeline (Figure 1), with significant patents highlighted in Table 1.

Since the invention of the various metal AM processes, rigorous R&D and industry efforts have found some niche applications. Part repairs, biomedical implants, aerospace structures, and high temperature components highlight some of the current production use of the technologies. Metal AM has received increasing attention for direct production of end-use parts, even being highlighted by U.S. President Barack Obama in a 2014 speech on manufacturing. [6] Despite the recent attention, some big questions remain: What are the current limitations of the technology? Can those limits be overcome?

- Timeline: "30 Years of 3D Metal Printing"
  - 1984 – Deckard & Beaman begin work on technology to build 3D parts out of powder, using a 100W YAG laser heat source[2]
  - 1986 - Deckard & Beaman start Betsy, continue research into "SLS"[2]
  - 1986 – SLS patented by Deckard at University of Texas [7]
  - 1989 - Original "3D Printing", or inkjet binder deposition, patented by Sachs & Cima at MIT [8]
  - 1993 – EBM patented by Larson with no affiliation [9]
  - 1995 – EOS launches EOSINT M 250 for direct metal laser sintering (DMLS) [10]
  - 1995 – Sandia National Laboratories begins LENS development [11]
  - 1997 – EOS licenses SLS rights from 3D Systems and focuses on powder bed technology [10]
  - 1999 – Ultrasonic consolidation patented by Dawn White of Solidica [12]
  - 2001 – 3D Systems acquires rights to SLS technology through acquisition of company holding original patents by Deckard [2]
  - 2002 – Arcam launches first commercial machine, the S12 [13]
  - 2007 – CE-certification of hip implant manufactured by EBM [13]
  - 2012 – 3D Systems acquires Z-Corp, holder of original patent on inkjet binder process[2]

2. Classification of Technologies

Metal AM has entered a period characterized by competing technologies, niche adoption, testing, and research. To understand the competing technologies available, various categories of metal AM will be addressed. Much progress is being made in testing and research of metal AM. The underlying processing science will be reviewed to help understand where limitations exist and progress has been made. The adoption of metal AM for niche applications will be addressed with processing economics.

History shows a diverse set of processes used to form feedstock (powder, sheets, or wire) into 3D objects. All metal AM processes must bond together the feedstock into a dense part. The metal must be melted at some point in the process to achieve this. In order to discuss distinct classes of machines, the ASTM F42 Committee on Additive Manufacturing has issued a standard on process terminology. [14] Of the seven F42 standard categories, the following four pertain to metal AM:

- ***powder bed fusion (PBF)***
  - laser melting (LM)
  - electron beam melting (EBM)
- ***direct energy deposition (DED)***
  - laser vs. e-beam
  - wire-fed vs. powder-fed
- ***binder jetting***
  - infiltration
  - consolidation
- ***sheet lamination***
  - ultrasonic additive manufacturing (UAM)

The other three categories specified in the standard do not currently apply to metal technologies: material extrusion, material jetting, and vat photopolymerization. There are unique uses, strengths, and challenges for each process. Each category for metal AM is explored, but more depth is given to DED and PBF due to the larger volume of recent work published on those processes.

2.1. Powder Bed Fusion

Powder bed fusion (PBF) includes all processes where focused energy (electron beam or laser beam) is used to selectively melt or sinter a layer of a powder bed. For metals, melting is typically used instead of sintering. The use of laser sintering has been previously reviewed, [15] but much progress has been made since this work to include the use of full melting. Re-melting of previous layers during the melting of the current layer allows for adherence of the current layer to the rest of the part. A schematic of a PBF laser melting (LM) machine is shown in Figure 3. A schematic of PBF electron beam melting (EBM) is shown in Figure 2. Although both systems use the same powder bed principle for layer-wise selective melting, there are significant differences in the hardware setup. The EBM system is essentially a giant scanning electron microscope (SEM), which requires a filament, magnetic coils to collimate and deflect the position of the beam, and an electron beam column. LM typically has a system of lenses and a scanning mirror or galvanometer to maneuver the position of the beam. Powder distribution is handled differently as well; LM systems use a dispersing piston and roller, while EBM systems use powder hoppers and a rake. Both EBM and LM processes require certain steps: machine setup, operation, powder recovery, and substrate removal.

To setup a PBF machine, the build substrate must be positioned. The build substrate, or “start plate”, is used to give mechanical and thermal support to the build material. LM processes bolt or clamp down the substrate, whereas the EBM process typically sinters powder surrounding the plate to provide stability. When successive layers of powder are distributed (rolled or raked out), existing layers of the build must not move. The substrate is thermally necessary, as building overhangs on top of loose powder, while possible for some structures, is prone to swelling and other process defects. Finally, powder containers must be loaded and a number of sensors checked and adjusted.

The operation of a PBF machine is governed by the details of the scan strategy and processing parameters, which will be discussed later in more detail. After the build is complete, excess powder

must be removed from the build chamber. For EBM parts, this powder is run through a powder recovery system to remove and recover sintered powder from around the parts. For LM processes, powder surrounding the parts does not sinter as much and can be sifted directly to remove any sintered clusters. Depending on the PBF process material, the build substrate may adhere to the parts. [16] The substrate must be cut off, with abrasive saws and wire EDM being common methods. For some material combinations like Ti-6Al-4V deposit and stainless steel substrate in EBM, material properties promote poor adherence; the parts fall off the substrate after the build, or can be easily removed by applied force. Parts coming directly out of the machine are considered "as-fabricated".

2.2. Direct Energy Deposition

Direct Energy Deposition (DED) includes all processes where focused energy generates a melt pool into which feedstock is deposited. This process can use a laser, arc, or e-beam heat source. The feedstock used can be either powder (Figure 5) or wire (Figure 4). The origins of this category can be traced to welding technology, which deposits material outside of a build environment by flowing a shield gas over the melt pool.

One of the most studied and commercialized forms of DED is accomplished using a laser heat source to melt a stream of powder feedstock (powder-fed). This technology sub-set has its roots in research at Sandia National Laboratories and was originally patented as the LENS process.[17, 18] Other DED processes feed wire into a molten pool (wire-fed), and are essentially extensions of welding technology. [19, 20] In fact, the use of welding machines to make parts via multi-pass welding is presently being explored. [21]

Machine setup is relatively simple; machine software automatically checks most sensors. As in PBF, powder hoppers must be filled and a build substrate positioned. The substrate can be positioned in a stationary position (3-axis systems) or on rotating axes (5+ axis systems) to increase the ability of the machine to process more complex geometries. In powder-fed systems, the feed rate of the powder must be checked regularly. If flow is impeded, nozzle cleaning or other maintenance may be required. The build chamber is enclosed to provide laser safety, but the chamber is not necessarily filled with inert gas. For non-reactive metals, a shield gas directed at the melt pool may provide enough resistance to oxidation. For more reactive metals, like titanium, the chamber is also flooded with an inert gas (argon or nitrogen). A vacuum pump and purge cycles may be used to reduce oxygen content. Cyclic purging can consume a significant amount of gas, as the build chamber is much larger than those in PBF systems.

As in PBF, a finished DED part is typically attached to the build substrate. Parts are then post-processed both thermally (to reduce residual stress and improve properties) and to achieve the desired final geometry (parts produced using DED are typically near net shapes with a rough finish). Parts may be removed from the substrate using the same processes for an adhered PBF part. Excess powder from machine operation is vacuumed to clean out the machine. Depending on the operator, this powder can may be recovered or disposed. Disposal may be a costly option, as powder costs are typically high.

2.3. Binder Jetting

Binder Jetting (BJ) works by depositing binder on metal powder, curing the binder to hold the powder together, sintering or consolidating the powder, and an optional step to infiltrate with a second metal. A schematic of the binder deposition process is shown in Figure 6. Infiltration achieves dense material by using a lower melting temperature infiltration material, whereas consolidation can achieve uniform composition of a single alloy. Porosity is a major concern with these parts, as BJ is essentially a powder metallurgy process. Future development of binder jetting technology will benefit from extensive previous work in powder metallurgy and ceramics. ExOne is currently the main manufacturer of BJ printers, so discussion of these devices in focused on this hardware.

The most common process used by these printers has focused on bronze infiltration of porous iron produced using a binder-sintering process. BJ printers selectively deposit liquid binder on top of metal powder using an inkjet print head. When the binder dries, a fragile binder-metal mix, or "green body", can be removed from the powder bed system. The green body can then be cured to give mechanical strength, which can take 6-12 hours. After curing, the part is then sintered at ~1100°C for 24-36 hours to sinter the loose powder and to burn off binder, leaving a 60% dense sintered metal part. Infiltration works by infiltrating the sintered part with a second material that has a lower melting temperature than the sintered material. This allows infiltration of the liquid metal into the sintered structure to form a more dense part. Bronze infiltration of stainless steel can achieve a final density of 95%. A furnace cool is used to anneal the part and increase ductility. [22] Infiltration is not unique to binder jetting, but is one of the major methods for production; infiltration has been explored for laser sintering from PBF as well. [23] Bronze infiltration of laser sintered PBF parts has been done, with significant focus on porosity and the amount of infiltration. [24]

Consolidation is an alternate process to infiltration that can be used to produce solid alloys. The process works by designing in distortion of the part geometry to accommodate uniform shrinkage during sintering. This designed distortion is not well defined for the process, so "sagging" or non-uniform consolidation may occur. The part is sintered until the metal consolidates into the desired final part geometry. Inconel 625 has been recently developed for binder jetting by ExOne, and is likely just the start of the development of additional consolidated metals for the platform. The material properties of the consolidated parts have not been published, so the quality cannot be currently compared to other AM methods. Surface finish is in line with many PBF processes. The surface finish of parts after annealing is quoted at 15 micron [Ra], and post processing is quoted to reduce roughness to 1.25 micron [Ra]. [22]

There is less recent published work and research progress on BJ than for PBF and DED. Therefore, a detailed description of processing details is not addressed in this review. There are a number of research areas that need to be addressed in this area, including binder burn off, geometrical accuracy during consolidation, and unique infiltration materials, among others.

2.4. Sheet Lamination

Sheet Lamination (SL) uses stacking of precision cut metal sheets into 2D part slices from a 3D object. [25, 26] After stacking, these sheets are either adhesively joined or metallurgically bonded using

brazing, diffusion bonding [27], laser welding [28], resistance welding [29], or ultrasonic consolidation. A key feature of SL hardware is the order in which sheets are applied and cut/machined. Sheets may be either cut to the specified geometry prior to adhesion or machined post-adhesion. Some of the advantages of the SL process include low geometric distortion (the original metal sheets retain their properties), ease of making large-scale (0.5m x 0.8m x 0.5m) parts, relatively good surface finish, and low costs. However, SL does have some limitations. Adhesively joined parts may not work well in shear and tensile loading conditions. Geometric accuracy in the Z-direction is difficult to obtain due to swelling effects. [30] Finally, anisotropic properties are prevalent in SL builds due to the type of joining processes.

Steps involved in a brazing SL process are shown in Figure 7 [31]. The sheets in this example are coated with flux (or low melting alloy), which acts as a brazing alloy for joining these sheets. In another process, special fixtures (Figure 8) have to be developed for resistance welding SL to enable joining of layers. Due to the previously mentioned limitations with SL methodology, researchers have considered other solid-state joining techniques between sheets to improve the process. In 2003, White developed an innovative SL process in which the sheets were joined together by an ultrasonic seam welding technique known as ultrasonic additive manufacturing (UAM). [32] The UAM process is one of the most used technologies for metal SL, so more technical detail is explored to understand the technology.

Typical UAM process order is to (1) mill the substrate to achieve a flat deposition surface, (2) blow off the substrate to remove tailings, (3) deposit material for a given layer in metal tapes through ultrasonic welding, (4) trim the edges of tape from the given layer to match the desired part geometry, (5) iterate layers until part is finished, and (6) engage milling operations as required to produce channels, holes, or other features. [33] The optional milling or machining operation allows for easy incorporation of cooling channels and embedded structures. A schematic illustration of the process is shown in Figure 9. Extensive research [34-36] has been performed in scaling this process to higher power for difficult to join metals including titanium, copper [37], stainless steel, metal-matrix composites, shape memory alloys [38], and the dissimilar combinations thereof. Schick et al. [39], Dehoff and Babu, [40] and Fujii et al. [41] demonstrated that at the interfaces that have good metallurgical bonding always had a recrystallization grain texture.

The evolution of grain texture in UAM was postulated (Figure 10) as a function of steps. [41] Steps 1-3 show that the interaction of the sonotrode leads to the formation of asperities on the surface of the first tape, as well as associated recrystallization texture due to adiabatic heating. Steps 4-8 postulate different steps that leads to bonding of second tape to the first tape which involves plastic flow of the bottom region of the 2nd tape into the asperities on the top of the 1st tape created in Steps 1-3. This process is iterated to build a 3D component. In the first step, the sonotrode with rough surfaces makes contact with smooth Al-tape. On vibration at 20kHz with normal loading, the surfaces of the Al-tapes deform adiabatically. The deformation-induced local (region of depth ~ 20 μm) heating promotes rapid recrystallization of the deformed grains. In the next step, a 2nd Al-tape is abetted against this 1st tape and the process is repeated. This high-strain rate adiabatic heating and on-set of grain boundary motion across the original interface during recrystallization leads to metallurgical bonding. Interestingly, this sequence of events is supported by the presence of shear texture even at the interfaces. Persistence of

shear texture and its effect on grain growth at high temperatures were analyzed by Sojiphan et al. [42]. Interestingly, the grains with shear texture at the interface were found to be extremely stable.

Although the process introduces high temperature (interface temperature may increase as much as 380°C during consolidation) within the localized region of the interface (~20 μm) [43], the overall temperature increase within the whole build is very low and the process temperature typically remains around room temperature. As a result, this process has been used for AM of dissimilar metals as well as embedding of actuators and sensors into parts. [44]

From this brief summary of SL, it can be seen that there are various techniques to accomplish bonding of metal sheets (brazing, resistance welding, etc.). Consolidation using ultrasonic welding through UAM surfaced as one of the most promising techniques for accomplishing SL, and a significant body of work exists on the subject. Interface metallurgy is particularly important for understanding the properties of the resulting material. SL is particularly useful for making metal composites by alternating sheets of dissimilar metal during consolidation. Pairing of machining with the consolidation process is common (de facto in UAM) and produces parts with machined surface finish directly from the hybrid process. However, the process cannot manufacture complex overhangs, as no support material is deposited to provide mechanical support. [45] Features may be additionally limited by the tool paths available for machining operations.

3. Material Processing Issues

Although PBF and DED processes have significant differences, there are some common materials processing issues that occur in both platforms. These issues are explored, noting differences between categories of equipment where appropriate. As with traditional processing methods (casting, welding, etc.), porosity is a common concern in metal AM. Other defects (residual stress, delamination, cracking, swelling, etc.) are more unique to welding or metal AM. Scan strategy, process temperature, feedstock, build chamber atmosphere, and many other inputs determine the occurrence and quantity of defects. Understanding defects, and how they arise, can help operators improve process reliability and the quality of parts produced.

In order to understand the complex relationship between basic processing science, defects, and the end product of an AM process it is useful to consider a general process flow chart (Figure 11). The process inputs are AM Software & Part Geometry, Scan Strategy, AM Hardware, Build Chamber Atmosphere, and Feedstock Quality. The process outputs are Mechanical Properties, Failed Builds, and Feature Size & Geometry Scaling. A box encloses the thermal and particle physics interaction steps: Applied Energy, Beam Interactions, Heat Transfer, and Process Temperature. These physics interactions, if properly modeled, should be able to describe dynamic process temperature, which is one of (if not the most) defining quantity of metal AM processing.

3.1. Feature Size, Surface Finish, and Geometry Scaling

When printing metal parts, the minimum feature size, surface roughness, and geometrical accuracy of the part are typical concerns for equipment operators, but over-focusing on these properties is not

useful for most applications because the part surface will ultimately be machined during post-processing. The minimum feature size is determined by the minimum diameter of the heat source and the size of the feedstock. This data is summarized in Table 2. It can be seen that PBF fusion typically has the best resolution, with the resolution of LM slightly better than EBM depending on parameters used. Powder-fed DED has better resolution than wire-fed DED, which can be attributed to the use of finer feedstock (powder vs. wire). The feature size of DED systems is so large that parts made with these techniques are limited to more simple geometries than PBF techniques. Smaller feature sizes smaller layer thickness currently comes at the expense of deposition rate. The deposition rates of various technologies are explored in more detail later in this paper. Due to small feature size and the low inertia to changing the position of the beam, PBF techniques can utilize the minimum feature size to print metal mesh or foam structures. These structures melt metal "struts", typically the size of an individual pulse of the heat source. Mesh parts have been well studied and reviewed elsewhere, and will not be covered in detail in this paper. [46, 47]

There are two separate contributors to surface roughness as shown in Figure 12: (1) non-flat layer edges or layer roughness and (2) the actual roughness of the metal surface. The layering effect can be reduced by using smaller layer thickness values. This usually means longer melt times; the layer thickness dictates how many layers a part is divided up into. More layers translate to longer build times. The actual roughness of a material depends upon the details of the machine producing the part. DED typically has larger layer thickness, which mostly limits this technology to near net shapes (shapes produced close to the desired part geometry, but planned for the use of machining to deliver the final geometry and details). Near net shape processing is different from traditional subtractive methods where a full block of material is machined down to a final part. PBF systems typically have finer resolution and layer thickness, but are prone to satellite formation [48] due to the sintering of powder at the part edges. Finer powder means smaller satellites and less surface roughness. LM machines use finer powder and smaller layer thickness than EBM, which results in less surface roughness.

Geometrical accuracy can be measured by taking 3D lasers scans (or similar technique) and calculating the deviation relative to the original part file. Typical corrections are empirical modifications to scale part files in a Cartesian system. For example, an x-axis might be smaller than intended by some scaling factor. The scaling factor is then used to increase the x-axis length in the part file, before printing. This is typically accounted for during machine calibration. Post-fabrication machining is typically needed for LM, EBM, and DED parts, as even the best achievable surface finish is still not as good as a machined finish. If machining is used, the actual part tolerance, surface finish, and minimum feature size of AM parts is dictated by any machining. For this reason, work to refine surface finish using smaller powder particles and smaller layer thicknesses may just add process time and cost (the smaller the layer, the more layers must be processed) without improving the quality of the final part.

3.2. Build Chamber Atmosphere

The atmosphere under which metal is processed can effect chemistry, processability, and heat transfer. Inert gas and vacuum systems are typically used, and each has unique processing concerns. Metal

powders have a tendency to oxidize and collect moisture when exposed to air. At higher temperatures, this oxidation can be accelerated. For this reason, welding machines use inert shield gases. Likewise, AM processes have the same need. As discussed previously, DED typically operates with a shield gas flowing over the melted surface and may also operate in an inert atmosphere. LM processes are typically run in an inert environment, with an atmosphere of Argon or Nitrogen filling or flowing over the build surface. The flow rate of the fill gas and the pathway of the flow have been shown to be important in porosity reduction in LM Ti-6Al-4V. [49] Small features may lead to heat concentration in LM, which can cause localized oxidation.

The EBM process uses a heated filament (usually made of tungsten) to generate electrons, which requires a vacuum-capable build chamber to operate the machine (<5x10-2 Pa chamber pressure, <5x10-4 Pa column pressure). During beam operation, a small quantity of helium is injected to reduce electrical charging of the build volume. This raises the pressure of the build chamber to ~0.3 Pa during beam operation. Operating in a near-vacuum environment leads to increased melt vaporization and has interesting heat transfer applications.

3.3. Feedstock Quality

The quality of the feedstock that is used in the AM process is important to the quality of the final part. The quality of the powder is determined by size, shape, surface morphology, composition, and amount of internal porosity. The quality of powder determines physical variables, such as flowability and apparent density. There are a variety of atomization techniques for producing metal powder, each producing distinct variations in powder quality. There are several unique quality issues related to wire feedstock for DED as well. By understanding feedstock quality, an operator can select the optimal material for processing in a given system. Further information on the standards associated with quantifying powder characteristics and the details of powder science are well described elsewhere. [50]

The quality of powder is directly related to the production technique. A variety of techniques are used: gas atomization (GA), rotary atomization (RA), plasma rotating electrode process (PREP), plasma atomization (PA), and others. Some atomization techniques yield irregular shapes (like RA), others have a large amount of satellites (like GA), and some are highly spherical and smooth (like PREP and PA). Figure 13 shows powder surface morphology and shape, as well as cross-sections to analyze internal porosity. Porosity in the powder feedstock is common for certain production techniques, like gas-atomization (GA), that entrap inert gas during production. This entrapped gas is transferred to the part, due to rapid solidification, and results in *powder-induced porosity* in the fabricated material. These pores are spherical, resulting from the vapor pressure of the entrapped gas. Higher quality powders produced via the plasma rotating electrode process (PREP) do not contain such pores and have been used to eliminate powder-induced porosity in DED and PBF systems. [16, 51, 52]

Flowability (how well a powder flows) and apparent density (how well a powder packs) are important quantitative powder characteristics that are directly related to qualitative characteristics. Spherical particles improve flowability and apparent density. Smooth particle surfaces are better than surfaces with satellites or other defects. Fine particles, or “fines”, typically improve apparent density and flowability, but can become segregated from coarser particles during use.

The particle size distribution of powder used for LM is 10-45um, for EBM is 45-106um [53], and for DED is 20-200um. [54] The main tradeoff with powder size is cost and surface finish. Smaller particles are better for smaller layer thicknesses, but typically cost more as a feedstock (than a larger size range) due to lower yields for smaller particles in powder production. LM uses a fine distribution of powder to improve surface finish by enabling shorter layer thicknesses. EBM uses slightly thicker layers and a correspondingly large size distribution. EBM can use smaller size distributions, with no noticeable effect on chemistry, material properties, or microstructure. [55] The effect of powder flowability on the processability in various hardware is not well published, though it is known in industry. PBF systems typically have a hardware specific flowability that depends on the powder distribution method used. Very fine particles size distributions that do not have a measurable flowability may still be processable in some systems. Powder-fed DED systems must consider the effect of flowability on the ability of powder to feed into the carrier gas stream. Once in the stream, the powder flow rate has been observed to have little effect on particle speed during DED processing. [56]

Additionally, the chemical composition of the powder must remain within alloy-specific specifications. It is important to measure the elemental composition of recycled powder (wire is not recycled), as evaporative losses, contamination from powder recovery (vacuums or grit blaster used in EBM), and reaction with oxygen, nitrogen, or other gases must be considered for quality control. Depending on the feedstock material, oxidation and humidity control may be important for both wire and powder storage. A thorough survey of the many powder types used for laser processes exists [57] and is a good starting point for learning more about the research available on specific powder alloys.

Having addressed powder feedstock in-depth, wire feedstock for wire-fed DED processes is important but less defect prone than powder. Wire feedstock is commonly available from the welding industry. The diameter of wire used for wire-fed DED is typically on the order of 2.4mm. [58] Better quality wire will have less variation in wire diameter, which is the same requirement of plastic extrusions printers that use plastic wire as a feedstock. Porosity is a common welding defect, and the quality of wire is known to affect the amount of porosity in the weld deposit. [59] For reactive metal like titanium, surface adsorption and reactions with atmosphere may also cause defects. More notably, the presence of cracks or scratches on the wire surface may translate directly to porosity formation. Unlike powder production, gas porosity is not an issue in wire production. In a study of both powder and wire feedstock, it was noted that powder had porosity, whereas the wire did not. [60]

3.4. Beam-Powder Interactions

The interaction of the heat source with the feedstock or melt pool impacts the amount of energy utilization and can lead to ejecta and porosity. There are four basic modes of particle ejection during beam melting processes: (1) the convective transport of liquid or vaporized metal out of the melt pool (or spatter ejection), (2) the electrostatic repulsion of powder particles in EBM, (3) the kinetic recoil of powder in DED, and (4) the enhanced convection of powder in gas streams. Lasers must address reflectivity losses and spatter. E-beams must address backscatter losses, the buildup of electrical

charge, and spatter. DED systems must also consider the effective feed rate of the feedstock, as appropriate amounts of deposit material must be delivered.

The convective transport of liquid or vapor out of the melt pool is commonly called “spatter” or “spatter ejection” and is seen in PBF, DED, and welding. This is caused by the application of a high energy beam creating localized boiling, where the energy of the ejecta must overcome surface tension forces. [61] These particles can be identified in PBF and DED by the high temperature emission of white or other light, which is the reason that these ejecta are sometimes referred to as “fireworks”.

A laser beam imparts energy to the powder bed via photons. Laser techniques must therefore compensate for the reflectivity/absorptivity [62]of the metal powder, as some of the applied energy will not be absorbed. Depending on the metal, this may be a significant limitation. Higher power lasers are typically used to overcome this barrier to melting, but the higher laser power can lead to increased spatter ejection. [63] Pulse shaping, or the control of the shape of the laser power profile, has shown promise for increasing energy absorption and decreasing spatter ejection in LM. [48] Pulse shaping can be used to more slowly heat a melt area (effectively a preheat), which can cause a decrease in reflectivity associated with higher temperatures. As laser control software and hardware improves, this technique may prove useful.

In the EBM process, electrons interact with the material to transfer not just energy, but also electrical charge. The powder particles may eject from the powder bed, if repulsive electrostatic forces are greater than the forces holding the particle to the powder bed. [64] This effect can cause the bulk displacement of powder within the powder bed, known as “smoking”, if sintering is not properly achieved. [65, 66] The electrostatic ejection of powder particles can be reduced in EBM by using a diffuse beam, rapidly scanned, to slightly sinter the melt surface prior to melting. Small quantities of helium gas are also injected during melting to dissipate charge from the melt surface. The ratio of the bulk density to the electrical resistivity of the powder has been identified as important for the reduction of powder ejection in EBM. [64] Pre-sintering in LM systems is not necessary, as the photons do not cause charge buildup.

Powder may also be removed by kinetic recoil (powder-fed DED) and convection of powder in the fill or shield gas steam (LM or powder-fed DED). As the stream of powder particles is sprayed into the melt pool during DED, some particles will recoil and avoid deposition. This loss is typically adjusted for experimentally, but can be a significant loss of powder (if not recovered). Small traces of powder may appear as “dust” present in the fill gas of inert atmosphere processes. Particles lost in this way have not been studied, though are probably not significant compared to other loss mechanisms. Both kinetic recoil and convection of powder do not directly remove particles from the melt pool, which means that these mechanisms are not of likely importance for control of porosity. Electrostatic repulsion is mostly an operational concern, but may lead to some porosity. Spatter ejection is known to result in weld defects and is an underlying mechanism for the formation of some forms of process-induced porosity.

3.5. Porosity

Porosity is a common defect in metal AM parts and can negatively affect mechanical properties. Porosity can be either powder-induced or process-induced. [16] As previously discussed, gas pores may form inside the powder feedstock during powder atomization. These spherical, gas pores can translate directly to the as-fabricated parts. For most studies, porosity formation is dominated by processing technique. Process parameters must be properly tuned to avoid a range of mechanisms that can create pores.

Pores formed by processing technique, known as *process-induced porosity*, are formed when the applied energy is not sufficient for complete melting or spatter ejection occurs. These pores are typically non-spherical, and come in a variety of sizes (sub-micron to macroscopic). Different processing issues can create defects in the material, some of which contribute to porosity. When not enough power is supplied to a region of powder, *lack-of-fusion* can occur. Lack-of-fusion regions may be identifiable by un-melted powder particles visible in or near the pore. Another form of process-induced porosity is caused during solidification. *Shrinkage porosity* (sometimes termed "hot tearing") is the incomplete flow of metal into the desired melt region. Spatter ejection may also lead to regions of porosity. Unlike lack-of-fusion regions that are created by insufficient energy application, spattering may also be caused by too much energy application. To limit spatter ejection, an operator will typically watch the process and tune parameters, while developing a new material processing strategy. Process-induced porosity has other contributors, including the effect of powder consolidation from a loosely packed powder bed to a fully dense part. [67] Details of this mechanism are not fully defined. Powder is distributed that includes particles larger than the layer thickness, which upon melting are intended to consolidate into a layer of the correct height. With optimized melting parameters, process-induced porosity can be reduced to very low levels in DED, LM, and EBM (greater than 99% dense). [68-70] The differences in how process-induced porosity forms have not been fully studied; the relationships between lack-of-fusion, shrinkage regions, and cracks have not been studied in AM material. Work has been done to explore the effect of process parameters (beam speed and beam power) on the formation of process-induced and gas-induced porosity. [71]

3.6. Scan Strategy

The tool path that the heat source follows for lasers or electron beams is classified as the *scan strategy*. Various scan strategies have been developed and are depicted in Figure 15. Scan strategies for DED tend to be limited to movement of the powder or wire feeding system and choose relatively simple scan strategies. Unidirectional (Figure 15(a)) and bi-directional (Figure 15(b)) fills are both standard DED processing techniques. These strategies use rectilinear infill to melt a given part layer. Both unidirectional and bidirectional fills are used in LM and EBM, though improvements have been made. In LM, island scanning (Figure 15(c)) has been used to reduce residual stress. [72] Island scanning is a checkerboard pattern of alternating unidirectional fills and reduces temperature gradients in the scan plane (x-y plane) by distributing the process heat. PBF systems tend to have lower inertia to beam movement than DED (due to no feeding mechanism) and can also melt in a pulsed, spot mode (Figure 15(d)). This spot mode is typically used in EBM to melt contours (Figure 15(e)), which are boundaries between infill and the powder bed. Contours follow the edges of the part, melting along free surfaces of

the part geometry. LM systems also used contours, though the contour melting strategy is typically linear (Figure 15(f)). Contour passes are done after melting in LM to refine surface finish [72], whereas the passes are done before melting in EBM. In EBM, the melt process heats up the build material; contours that are run after melting tend to form more satellites due to higher temperature, yielding a rougher surface finish. Most machines offer operators the choice of contour order and it is one of many parameters optimized by the machine manufacturer before releasing parameters for a material. The scan strategy for a given build may be adjusted by layer or by part. Unidirectional, bi-directional, and island scanning strategies are typically rotated at an angle between each layer.

Scan strategy has a direct impact on process parameters; heat source power and velocity must be optimized for a given scan strategy. The relationship between applied heat source power and the heat source velocity is a key parameter of PBF and DED processes and will be addressed in more detail with heat transfer, solidification, and thermal cycles. This relationship is important for eliminating process-induced porosity and determining grain morphology.

3.7. Deposition Strategy

The way in which feedstock is delivered to the melt surface determines deposition rate and can have a strong impact on material defect and properties. In wire-fed DED, the vertical angle (α) and the horizontal angle (β) of the wire feed are related to deposition efficiency, surface roughness, incomplete melting, rippling, and other processing defects. [60] Similarly, the angle for powder spraying is important to powder-fed processes. In both powder-fed and wire-fed DED, the deposition rate is critically important. Deposition rate and the velocity of the heat source both determine how much material gets deposited in a given pass. In DED, the build-up of material must be considered to appropriately choose the z-axis layer height, or layer thickness. In PBF, layer thickness determines how much powder can be raked out. In PBF, a "rake" is a metal, ceramic, or polymer-coated bar that sweeps out powder onto the build surface. The number of passes of the rake, mechanical type of rake, and the amount of powder being retrieved per pass determine the efficiency of the PBF powder delivery system.

3.8. Cracking, Delamination, & Swelling

The formation of defects is essentially dependent on process temperature. Cracking of the microstructure may occur during solidification or subsequent heating. Macroscopic cracks may relate to other defects, including porosity. Delamination is a lack of layer adherence due to incomplete melting (melt temperature not high enough). If the process temperature is too high, a combination of melt pool size and surface tension may lead to swelling or melt balling. If processing conditions are tightly controlled, most of these defects can be avoided. Cracking of the microstructure is material dependent as well, and there may be some processing cases where cracking is unavoidable.

There are different material-dependent mechanisms for which cracks form in AM material. [72] *Solidification cracking* can occur for some materials if too much energy is applied, and arises from the stress induced between solidified areas of the melt pool and areas that have yet to solidify. This type of cracking is dependent upon the solidification nature of the material (dendritic, cellular, planar). *Grain*

boundary cracking is cracking that nucleates or occurs along grain boundaries of the material. The origins of this type of cracking are material dependent and depend on the formation or dissolution of precipitate phases and the grain boundary morphology. The process parameters required to minimize process induced porosity may differ from those required to minimize the formation of cracks. [72] Solidification cracking and grain boundary cracking are both phenomena that occur within the microstructure. More generally, *cracking* is sometimes used to describe macroscopic cracks in the material. These cracks may nucleate due to other macroscopic defects such as delamination that are not related to excessive energy input. [73]

Delamination is the separation of adjacent layers within parts due to incomplete melting between layers. This may occur due to incomplete melting of powder or insufficient re-melting of the underlying solid. Whereas the effects of lack-of-fusion defects may be localized within the interior of the part and mitigated with post-processing, the effects of delamination are macroscopic and cannot be repaired by post-processing. Delamination leading to interlayer cracking is shown in Figure 17. Reduction in macroscopic cracking has been demonstrated in LM by using substrate heating. [73]

Excess energy input can lead to overheating of the material. This may occur due to small features or overhangs in the part geometry as shown in Figure 16. Overhangs in PBF are typically made using support structures such as wafers. Lattice support structures have been recently explored. [74] There are two kinds of supports: mechanical support and thermal support. Mechanical supports help prevent overhangs from deformation from gravity or growth stresses. Thermal supports allow applied energy a conductive path away from the melt surface in PBF. *Swelling* is the rise of solid material above the plane of powder distribution and melting. This is similar to the humping phenomenon in welding and occurs due to surface tension effects related to the melt pool geometry. [16] *Melt ball formation* is the solidification of melted material into spheres instead of solid layers, wetted onto the underlying part. Surface tension is the physical force that causes melt balling, which is directly related to the melt pool dimensions. [75] When the length over diameter ratio is great than 2.1 ($\ell/d > 2.1$), the melt pool will transition from a weld bead (half cylinder) to a melt ball (sphere). Melt ball formation, as shown in Figure 18, is an extreme condition typically only observed during material development. It occurs with higher temperatures or alongside delamination with lower temperatures. In EBM of stainless steel, a trade-off has been noted between “balling” and delamination. [76] Wetting forces and capillary forces have been identified as contributors to both balling and swelling. [77, 78] It may be difficult to identify the cause of defects post-build, as one type of defect may change the local heat transfer conditions and lead to the compounding of defects. An example of this is the formation of porosity, which can lead to reduced thermal conductivity, causing melt ball formation or swelling on subsequent layers due to unexpected thermal resistance.

3.9. Substrate Adherence & Warping

The use of a substrate to deposit material on is standard practice in DED and PBF but typically adds additional work during post-processing. Metal AM processes typically build on top of a metal substrate to achieve mechanical adherence of the first layers of the melted part.[16] The substrate may be left at room temperature, heated by internal heaters, or heated by an electron beam. Most metal deposits form ductile interfaces and must be cut off of the substrate during post-processing. Ti-6Al-4V deposited

on Stainless Steel 304 substrate forms a more brittle interface that can be removed by application of force, without cutting. This kind of interface is desirable for decreasing the number of post-processing steps.

Additionally, some substrates may warp during use as shown in Figure 19. [79] This can be due to the operating temperature of the AM process, the heat treatment of the substrate prior to use, or due to differential coefficients of thermal expansion. Some processes use a substrate of the same material as the build, like stainless steel, to reduce this effect. The ultimate result of substrate warping is distortion of part geometry within the affected layers and possible lack-of-fusion or delamination at the transition region back to unaffected material. Substrate warping is a form of stress relief that results in permanent plastic deformation. The same mechanisms that cause substrate warping can also lead to major issues with residual stress.

3.10. Residual Stress

Residual stress is common in metal AM materials due to large thermal gradients during processing, can negatively impact mechanical properties, and can act as a driving force for changes in grain structure. Residual stress is a stress within a material that persists after the removal of a stressor. Macroscopic residual stresses can have a dramatic effect on the bulk behavior of AM parts, whereas the effects of microscopic residual stresses from precipitates or atomic dislocations are more localized. Macroscopic residual stress can be thermally introduced in metal AM by (1) differential heating of solid and (2) differential cooling during and after solidification. [80] Residual stress is a concern because it can negatively affect the mechanical properties of as-fabricated parts or lead to geometrical distortions. A number of techniques have been applied to measure residual stress in AM parts and are discussed below. Studies have shown that magnitude of residual stress, and the ways to reduce it, are process dependent. Residual stress may influence recrystallization, which is discussed in detail later with post-processing.

Residual stress tends to be compressive in the center of DED and PBF parts, tensile at the edge, and more highly concentrated near the substrate interface. [81-84] Axially, peak tensile residual stresses were measured near the top surface and were noted to be balanced by compressive stresses in the sample interior. [81] Support structure, used to separate the build from the substrate, may slightly reduce residual stress due to having a higher initial temperature than the bare substrate. [81] Upon removal from the substrate, residual stress is relieved but may result in deformation of the part. [80] Modeling of thermal cycles for wire-fed DED using finite element methods has demonstrated accuracy and agrees with the measurement of higher residual stress is near the substrate interface. [85]

Residual stress tends to be higher in room temperature processes (DED, LM) than those that operate at higher temperature (EBM). DED residual stress measurements using neutron diffraction have shown that residual stress in parts was 50-80% of the 0.2% yield stress. [82] Island scanning in LM reduces porosity in parts but leads to increased residual stress. [79] Smaller islands result in less tensile residual stress than larger islands, but continuous scanning results in the least amount of tensile residual stress. All scan strategies result in roughly equivalent compressive residual stress. It is noted that porosity in parts can act to self-relieve stress, complicating analysis. Heating of the substrate helps reduce residual

stress, as does in-situ heating of the material using the primary heat source. [80] A defocused electron beam can operate with enough speed and power to accomplish this (and does via the preheat step), but most LM and DED systems cannot. As a result, LM and DED parts generally have much more residual stress than EBM parts due to a lower operating temperature. The lower operating temperature means that thermal gradients between the peak melting temperature and the powder bed temperature may be increased. Recent work has shown that residual stress in EBM parts is 5-10% of UTS. [83] The potential for multiple lasers to accomplish in-situ process heating is addressed later, within the discussion of future AM systems. Understanding the origins of residual stress requires a more detailed knowledge of process thermal history, while understanding methods for eliminating or reducing residual stress will be discussed in more detail with post-processing.

Residual stress can be measured using a variety of techniques: micro-hardness [86, 87], the contour method [88], x-ray diffraction [80], neutron diffraction [89], or other methods. For alloys that do not have significant precipitates and are dominated by a single matrix phase, the shape of micro-hardness indents can be used to quantify the presence of residual stress. However, micro-hardness only reveals information about stress near the surface that is tested. The contour method measures the deflection of surfaces after cutting via EDM and has been shown to give comparable results to neutron diffraction. [90] Additionally, the contour method is noted to be less chemistry dependent than neutron diffraction. X-ray diffraction and neutron diffraction can both be used to measure bulk stress variation, but are more expensive and require specialized equipment. Residual stress formation may also be modeled. Finite element analysis [91] has demonstrated the ability to predict LM residual stresses. Additionally, simplified thermal cycles have been shown to qualitatively match experimental results of substrate warping. [92]

4.0. Heat Transfer, Solidification, and Thermal Cycles

The metallurgy of AM parts is determined by the feedstock chemistry and the temperatures that the material experiences, or the thermal history. There are different heat transfer mechanisms for different classifications of AM, but the use of full melting means that the metallurgical principles are the same for both DED and PBF. Solidification determines the initial phase distribution and grain morphology of the metal deposit. Heat source speed, power, and size determine melt pool geometry, which in turn determines solidification kinetics. After solidification, thermal cycling and cool down path determine further precipitation kinetics, phase growth, and grain growth.

4.1. Modes of Heat Transfer

Although limited information exists, it is important to understand how the modes of heat transfer differ between AM processes. DED processes transfer heat primarily through conduction to the substrate, conduction to the build material, and convection to the shield gas. These modes of heat transfer are the same as those for welding. In LM processes, conduction may be inhibited by powder acting as a thermal insulator surrounding the part. Additionally, the fill gas in LM has a lower velocity (<2 m/s) [49] than the shield gas in DED (37.1 m/s). [54] This should result in reduced convective heat transfer in LM when compared with DED. EBM conduction mechanisms are similar to LM, but the near-vacuum environment

significantly reduces convective heat transfer during the melting process. This means that, for EBM processing, radiative loss from the build surface and conductive loss to the machine are the principle modes of heat transfer. Since EBM operates at elevated temperatures (400-1000°C), the thermal history of EBM material must be considered with respect to solidification *and* the hold temperature during the build; the fused metal solidifies from a molten pool and then is kept at elevated temperature until all layers have finished melting. DED and LM processes may use heaters to increase the temperature of the build envelope to 100-200°C. This may help reduce residual stress and warping but is not high enough to significantly impact the phase and grain structure of typical AM alloys.

4.2. Solidification

Solidification is governed by the melt pool geometry, which is mostly determined by the relationship of the beam velocity to beam power. This relationship is extremely important in all AM processes, and, using EBM as an example, may be defined by a function to select an appropriate speed based off of power (or current). The "speed function" is such a relationship for EBM and is shown in Figure 20. [93] The slope and the translation of this relationship must position the selected speed and applied power within a certain processing window. Various combinations of speed and power allow for fully dense material (Figure 21) that is free of defects. Similar process mapping of defects using heat source power and speed has been used in welding for years to map process windows as shown in Figure 22. The relationship between speed and power is material-dependent and should be measured during new material development. LM and DED define a simple relationship between speed and power that is constant, whereas the EBM parameters account for differences in part geometry and other effects by dynamically changing the speed-power relationship.

4.3. Speed-Power Relationship

The relationship between speed and power that is needed to avoid defects varies depending on several factors: edge effects, scan strategy, part geometry, and thickness of powder beneath the scan area. All of these factors amount to changes in the initial conditions or boundary conditions for heat transfer. After a heat source passes near an edge, it may return to the edge before the heat from the previous pass has time to dissipate. The scan strategy can have a similar impact on heat flow, depending on how the strategy allows for cool down between heat source passes. Part geometry effects include those associated with a variation in the size of the part. A small part will reach a higher peak temperature during melting than a larger part, given constant power and speed. This can lead to more defects in smaller parts or features. For PBF, the state of the material underneath the melt area (powder vs. solid) can drastically affect heat transfer. A powder (non-sintered or sintered) has relatively poor thermal conductivity and can be considered thermally insulating compared to the solidi part of the substrate. As heat is applied, it flows more slowly through the powder, which can lead to overheating of the melt surface located above the powder. The influence of all these phenomena means that applied energy density alone may not be the best indicator of porosity due to local variations. [94]

4.4. Columnar-to-Equiaxed Transition

The power and speed of the heat source also affect the thermal gradient (G) and liquid-solid interface velocity (R) of the melt pool. The process window of solidification can be estimated for an AM process

and used to predict the nature of the grain structure as shown in Figure 23. The columnar-to-equiaxed transition (CET) can be calculated based on established methods [95] and plotted for various materials. [96] Recent work in PBF [97] has been increasingly focused on controlling the CET and is addressed in a discussion of AM microstructures later in this paper. The CET can be transformed into a process map so that appropriate powers and velocities can be selected. [98] Further work is needed to combine the maps for defects and the CET, so that the process space can be fully understood for each material.

4.5. Process Thermal History

There are other consequences of melt pool geometry. Modeling has shown that poor powder thermal conductivity has a large impact on the size of the melt pool. [99] The heat sources in PBF move so fast that recent work has suggested that though the heat source is a point, a linear heat source may be a reasonable approximation. [100] Increasing beam diameter is a way to decrease thermal gradient of the melt pool and slow down solidification, but the effect of beam diameter on grain size has not yet been explored. The effect of beam diameter, measured as "focus offset" in mA, has been related to melt pool width in EBM. [93] Such work is crucial to the development of accurate process modeling.

PBF and DED processes involve simultaneous melting of the top powder layer and re-melting of underlying layers. This creates thermal cycling, as the material reheats and cools. This cycling has been measured experimentally and modelled as shown in Figure 24. [101, 102] DED and LM are both typically performed at, or close to (heaters can get to 100-200°C), room temperature; the material cools quickly, within seconds to minutes. In EBM, the process operates at an elevated temperature and experiences a distinct thermal history as measured by the substrate temperature in Figure 25. The EBM process can take 5-80 hours, depending on part geometry, so the effect of hold time and hold temperature on material properties must be considered. [103] The impact on an precipitate hardened material like IN718 may be spending ~100 hours (EBM) in the nominal aging range as opposed to ~100 seconds (DED).

5. Post-processing

When metal comes out of an AM process, there are many steps that are typically used to make the as-fabricated part into an end-use part; parts are not simply ready for use out of a machine. Excess powder must be removed, parts must be removed from the build substrate, support structures must be removed, thermal treatments may be required to improve mechanical properties, and the surface of parts must be finished to achieve the desired surface finish and geometrical tolerance.

5.1. Powder, Support, & Substrate Removal

After a part is fabricated, excess powder, support structures, and substrate material must be removed. Powder-bed processes require powder to either be vacuumed out of the part (LM) or blasted off using loose powder (EBM). DED processes may require machine clean-up, but the finished parts are not encased in feedstock. Support structures, for mechanical and thermal support, are frequently used in PBF and must be mechanically removed by application of force or cutting. The build substrate is typically adhered to the finished part, and must be cut off using a saw. The stainless steel and Ti-6Al-4V interface is the exception, in that parts may be fractured off of the substrate by application of force.

5.2. Thermal Post-Processing

After parts are removed from the substrate and support material, thermal post-processing can be used to relieve residual stress, close pores, and/or improve the mechanical performance of the material. As-fabricated metals typically require some form of heat treatment to achieve the desired microstructure and mechanical properties required for service. Material may be treated by hot isostatic pressing (HIP) to reduce porosity and internal cracks, furnace heating to solution treat, and/or furnace heating to age. Standard treatments for the commonly processed materials Ti-6Al-4V and IN718 are given in Table 3. The various treatment options can effect changes in grain size, grain orientation, precipitate phases, porosity, and mechanical properties. Heating AM metal in a furnace to effect changes in microstructure is the general goal of thermal post-processing. Thermal post-processing of metal affects grains through recovery, recrystallization, and growth. Phases are affected by dissolution, precipitation, and growth.

5.3. Stress Relief

Stress relief (Figure 26) involves recovery; atomic diffusion increases at elevated temperatures, and atoms in regions of high stress can move to regions of lower stress, which results in the relief of internal strain energy. LM and DED parts are typically annealed for stress relief, commonly prior to removal from the substrate. Stress relief treatments must be performed at a high enough temperature to allow atomic mobility but remain short enough in time to suppress grain recrystallization (unless desired) and growth (which is usually associated with a loss of strength). Recrystallization may be desirable in metal AM to promote the formation of equiaxed microstructure from columnar microstructure. This has been observed in LM iron, where it was theorized that thermal residual stress acts as the driving force (in the absence of cold working) for observed recrystallization. [87] Similar phenomena have been noted in wire-fed DED Ti-6Al-4V. [104, 105]

5.4. Recrystallization

One of the most important effects of post-processing is effect on the grain structure of the processed material. Metal AM parts typically have a columnar, oriented microstructure (especially in PBF), which can sometimes be recrystallized to form an equiaxed microstructure. In EBM Ti-6Al-4V, it has been shown that HIP processing can lead to grain coarsening, but not recrystallization. [106] Pre-straining the material prior to HIP creates a driving force, and recrystallization is then observed. Research on LM [87] and DED [104, 105] have noted recrystallization of as-fabricated microstructure during annealing (no HIP). In the materials studied (Iron, Ti-6Al-4V), residual stress is proposed as a likely driving force for this recrystallization. Lower amounts of residual stress in EBM material means that this driving force should be less notable in EBM parts, as seen in the Ti-6Al-4V work by Facchini et al. This is not always the case, as HIP processing of Inconel 625 [107] and Inconel 718 [108] have led to recrystallization of EBM material. In both cases material was subjected to HIP without a homogenization treatment. Both cases had significant amounts of intragranular Ni_3Nb precipitation in the as-fabricated conditions that was eliminated during HIP processing. While residual stress cannot explain the recrystallization in EBM precipitate hardened alloys, further investigation of the role of prior phase formations may offer explanation. Post-processing may thus cause recrystallization of AM material, but the driving force may be process specific. If equiaxed grain structure is desired, residual stress formation in LM and DED may be a processing benefit to act as a driving force. For maintaining columnar grain structure,

consideration of the specific alloy system may be necessary in order to use specific phase formations to limit grain growth (while limiting other phases that may drive recrystallization).

5.5. HIP

Most AM metal parts are treated by HIP to close internal pores and internal cracks. Internal pores, or "closed" pores, are surrounded by material in the center of the sample. When pores occur at the surface, they are considered "open" pores. Open pores caused by surface defects are a problem for post-processing, as they allow deeper infiltration into material from air during high heat cycles as shown in Figure 28. Internal cracks may also be closed by HIP, as has been shown in LM nickel-based superalloy parts. [72] The use of HIP may significantly alter the grain structure of AM parts. Standard HIP cycles may yield very large grains, as published in recent work on EBM of Inconel 718. [108] There is also evidence that AM material responds differently to HIP than traditional material; LENS Inconel 718 was deposited on Inconel 718 substrate and characterized before and after HIP, and it was noted that grain growth occurred in the substrate during HIP but not the deposited material, possibly due to carbides or other high temperature phases not dissolved during HIP. [109] This means that characterization of as-built microstructure is critical to applying the correct HIP post-processing of AM parts. Alternatively, the homogenization of AM alloys prior to HIP or other post-processing could lead to standard post-processing procedures that are independent of processing conditions. Most post-processing of AM parts is currently performed this way, but the use of standard wrought or cast post-processing procedures may not be ideal for AM processed alloys.

5.6. Solution Treatment & Aging

For precipitate hardened materials (like Inconel 718), a solution treatment (ST) can be used to dissolve unwanted phases and aging can be used to form and grow precipitate phases. Sometimes, these processes are performed sequentially and referred to as solution treated and aged (STA). The ST temperature should be selected above the solvus temperature at which all undesired phases will dissolve. The ST time should be long enough to dissolve precipitates but short enough to limit grain growth. After a material is solutionized, the matrix of the material is essentially "reset". Aging can now be done on the reset material, without the need to consider prior phase structure. The purpose of aging is to precipitate harden a material. These steps are common for cast and wrought materials, and have been performed on AM material. [108, 110-112]

5.7. Surface Finishing

AM parts bound for service are typically machined to achieve a smooth surface finish. As-fabricated parts typically have high surface roughness, the origins of which have been discussed previously in this review. The most common way to machine near net shapes of AM parts is to use CNC machines associated with subtractive manufacturing. Simple rotary-tool polishing or grinding with a belt sander (flat surfaces) may be adequate for some applications, but do not typically meet the standards required for high-quality parts. Chemical polishing has been explored on mesh structures and future work on electrochemical polishing is recommended. [113]

Parts to be used in service typically undergo thermal post-processing, which can oxidize the surface of the metal. Post-HIP parts are shown in Figure 27, before and after surface machining. [114] If open

pores are present, oxidation can extend into the interior of the part as shown for thin-wall EBM samples in Figure 28. Defects like this can be, and must be, avoided because they may not get removed by surface machining. CNC of freeform surfaces has been extensively reviewed in relation to tool path selection, tool orientation, and tool geometry. [115]

AM and CNC have been explored for operation in tandem [116], which is commonly referred to as Hybrid Manufacturing. Hybrid systems typically pair a DED process with CNC, using the same mounting position to position the CNC tools. This type of hybrid process is currently in use for part repair of aerospace components, capable of repairing compressor blades and other complex service parts. [117] Turbine blade repair using this method is shown in Figure 29.

6. New Materials Development

The feedstock for metal AM processing must meet some general requirements. It must be in a powder, wire, or sheet form and must be machine compatible (e.g. exposable to air, electrically conductive, etc.). A wide range of candidate materials meet these broad requirements, although current AM hardware makes the fabrication of parts from oxidation-prone materials difficult (powder is frequently loaded in open air). There are currently a limited number of commercially available alloys for AM. A handful more have been researched, but there remains tremendous opportunity in processing new material and in developing new alloys specifically for AM.

For powder feedstock, the initial powder composition is very important in determining the chemistry of final parts; any pick-up of oxygen or loss of metals to vaporization must be accounted for. Powders can be either pre-alloyed or mixtures. Pre-alloyed powder is produced from a feedstock (ingot, bar, etc.) of the desired alloy. Mixtures are made by mixing powders of different chemistries together as shown in Figure 30, forming the final alloy during the AM melting process. Mixtures of elemental powders are common in the powder metallurgy (PM) field and are termed blended elemental (BE). Pre-alloyed (or "PA" in PM) powders are the most common, although work has been done to demonstrate processing of mixtures. [118]

Some currently available commercial materials and previously researched materials for AM are summarized in Table 4. The commercially available materials are mostly steels, stainless steels, structural aerospace material (Ti-6Al-4V), bio-compatible implant materials (Ti, Ti-6Al-4V, CoCr), and high-temperature materials (Inconel 626, Inconel 718, CoCr). Promising research has been done on refractory materials (Ta, W-Ni, Nb). Bulk amorphous metallic glasses have also been demonstrated [119], but little information is available, presumably due to proprietary considerations (e.g., a recent patent by Apple Inc.).[120] SL has the potential to join many dissimilar metals through ultrasonic joining (Figure 32). DED research is developing hydrogen storage materials [121, 122], ceramics [123], and WC. [124] The high energy of some DED systems allows for melting of some of these exotic materials. BJ has only recently demonstrated pure alloys (IN625), but more research is expected to be seen in this area. Pure alloys and ceramic materials both have significant development work to be done in understanding the consolidation/sintering process to produce fully dense parts using BJ. Some research samples are pictured in Figure 31.

Recent alloy development has focused on alloy systems that have uses in high impact industries (e.g., titanium alloys and nickel-based super alloys). While this trend will likely continue, more emphasis is expected for alloy design specifically for AM processes. Alloys designed for AM would potentially accommodate large thermal gradients during solidification, facilitate the control of columnar or equiaxed grain formation, facilitate the control of orientation, and facilitate the control of in-situ phase precipitation. While development of new alloy compositions for AM processes is yet to be realized, some researchers have experimented with additives to existing alloys; an example of this is the use of boron to control β-grain growth in EBM Ti-6Al-4V. [125]

7. Microstructure and Mechanical Properties

A large amount of work has been put into characterizing the microstructure and mechanical properties of PBF and DED materials. Grain morphology, grain texture, and phase identification are typically accomplished via LOM, SEM, EBSD, XRD, or some combination thereof. Tensile properties and hardness are the most commonly reported and measured mechanical properties, although some studies of fatigue life and creep have been done. To discuss the importance of microstructure and mechanical properties, it is useful to focus on two different alloy systems, Ti-6Al-4V and Inconel 718, as there is much published research on PBF of these alloys.

7.1. Microstructure

Due to the nature of AM processing, the microstructure of AM produced metals has unique properties. Columnar grain structure dominates, with high amounts of grain orientation. Phase formation is process and material specific. Axial variation of grains and phases may occur due to subsequent heating and cooling cycles of the material. Scan strategy can be used to control the microstructure in theory (G vs. R) [126, 127], and recent results show significant progress towards demonstrating control. Porosity is a concern with all processes, though < 1% porosity can be achieved using DED, LM, or EBM by optimizing process parameters.

7.1.1. Grain Structure

Grain structure in AM alloys is dominated by highly oriented, columnar grains. These structures are common in Ti-6Al-4V produced by EBM [128], LM [129], and DED [105, 130, 131], as well as Inconel 718 produced by EBM [16, 108], LM [83, 112, 132], and DED [133]. DED grain structure is not always as oriented or columnar as LM or EBM. In fact, DED grain structure is highly influenced by the nature of the scan strategy, as shown in Figure 33. [133] The results shown show some difference based on scan strategy, but the most pronounced difference is with higher energy melting. The resulting larger, more columnar grains should be expected; more applied energy means a larger and deeper melt pool. This will include more layers during remelting, which should promote epitaxial grain growth and a more oriented microstructure (as observed). This result can be extrapolated to other systems, given knowledge of the power per area [W/mm^2]. Discussed in more detail later, EBM and LM have much higher power per area capabilities than DED systems. This has a direct impact on the amount of remelting and epitaxy. The large layer thickness of DED makes finer control of microstructure difficult due to a larger minimum feature size. DED of IN718 has been noted to form non-equilibrium Laves

eutectic heterogeneities that transform into δ-needles during solution treatment (solution treatment should reset the phase structure). [52] Such needles are typically associated with over-aging. Such solidification Laves formations have been noted in LM but not EBM. In LM, the typical scan strategy used (island scanning) has evolved to reduce residual stress and cracking. The island scanning technique has recently been noted to cause repeating patterns in grain orientations. [100] This differs significantly from the oriented columnar structure seen using a rectilinear raster (no islands). Depending on the desired grain structure, this may be a limitation. In general, residual stress impacts grain structure from the standpoint of the scan strategies used to avoid it or as a driving force for heterogeneous recrystallization. In EBM, very high (001) orientation in the build direction is normal in both Ti-6Al-4V and Inconel 718. Work to study the origins of this texture discovered the effect of grain nucleation from powder particles. [134] Additionally, this work demonstrated a clear distinction between the fine grained, equiaxed microstructure of the contour region and the highly oriented, bulk melt. Grain size and orientation has also been noted to vary from the edge to the center of a melt pool [135], which agrees with common knowledge from welding and casting. Grain nucleation can occur at edges from powder particles in PBF (Figure 34), which can result in increased misorientation near edges or in thin walled structures.

7.1.2. Phase Formation

Phase formation during solidification and solid-state phase transformation during cyclic process heating have been studied for DED [102, 136] and EBM [103]. Phases that form during rapid solidification of the melt material may coarsen and/or dissolve during subsequent passes of the heat source. This effect was discussed previously and is shown in Figure 24. In EBM, the powder bed temperature used for processing was shown to directly impact the width of α-phase grains, or laths, in Ti-6Al-4V and, correspondingly, tensile properties. [128] Furthermore, axial variation of lath width in Ti-6Al-4V has been noted in EBM.[137] The higher powder bed temperatures (400-1000°C) of EBM are unique, and similar effects are not noted in the lower temperatures (20-200°C) of LM or DED processing.

7.1.3. Microstructure Control

Local control of microstructure is possible with metal AM processes, and recent research is just beginning to demonstrate the possibilities. PBF processes have produced especially interesting results due to the accuracy and the speed of lasers and e-beams. Manipulation of G vs. R (see previous section on thermal history) has been known to modify grain structure of material during traditional processing, and applies to AM processes through manipulation of scan strategy. Control of microstructure can be discussed with respect to either grains or phases.

Control of grain morphology and size can be achieved through manipulation of G vs. R. While G vs. R curves may predict mixed grain morphology, it has been difficult to produce experimentally. It is speculated that this is due to a preference toward columnar growth once it has been established. [128] Many papers have addressed the benefits of controlled grain structure [98, 138], but demonstration has not occurred until recently in DED [133] and EBM [139, 140]. Beam modulation in wire-fed, e-beam DED has shown that beam modulation (rapid variance of the beam power) can be used to produce finer grain structure. [141] This alternative method causes a dynamic melt pool due to a rapidly changing heat flux.

The clearest demonstration of local control of grain orientation was achieved using EBM of IN718 to embed the letter D-O-E in misoriented grains within a highly oriented matrix (Figure 35). [142]

Phase control is more complex, as formation can be influenced by solidification and solid state phase transformation. Solidification structures are affected by subsequent heat source passes (as discussed previously). EBM control of Cu_2O precipitates in low-purity copper has been suggested as a possible area of future work [143], slower scan speeds in LM can cause increased Aluminum segregation in Ti-6Al-4V and form Ti3-Al [144], and columnar precipitate architectures have been reported in both EBM and LM by Murr et al.[46]. These works mostly address phase formation during solidification. Recent work has rationalized solid state phase transformation in DED [136] and EBM [103]. Solid state phase transformation can amount to in-situ aging of material. In DED this is done on subsequent beam passes. In EBM subsequent passes and holding at elevated temperature cause this change. The complex thermal histories present have allowed researches to rationalize phase formations due to solid state phase transformation, but more work is needed to be able to predict microstructures. No work has truly demonstrated process control of precipitate formations via solidification or solid state phase transformation.

7.2. Mechanical Properties

The mechanical properties of a part dictate its uses, and the performance of AM material is still being measured and understood. A large portion of the literature on AM focuses on mechanical properties, specifically tensile behavior and hardness. Tensile tests to measure yield strength (YS), ultimate tensile strength (UTS), and elongation are the most commonly used tests to compare AM mechanical properties to traditionally processed materials (cast and wrought). The location and orientation from which mechanical testing samples are taken from builds is important and should always be reported with results. ASTM standards exist, but are typically process and alloy specific. Defects, such as porosity, that affect mechanical properties may influence the test results of as-fabricated material but can typically be improved by post-processing.

Porosity, residual stress, test specimen orientation, and thermal history are particularly important factors to consider when discussing mechanical test results of AM materials. Unfortunately, not all reported research includes these necessary details. Orientation of the build direction relative to the test direction, quality and production method of feedstock, void fraction of porosity, thermal history during processing, and post-processing thermal history should all be included with any test results. This section focuses on mechanical properties of bulk material (as opposed to mesh or foam structures). Porosity can negatively affect mechanical properties due to a reduction in cross sectional area. [145] Aligned pores (non-random) or pores with sharp edges are more detrimental than homogeneously dispersed spherical pores. The effect of porosity on tensile properties is most notable in the reduction of elongation. [146] Residual stress in non-stress-relieved parts can also lead to early failure. Part thermal history (in-situ history for EBM, post-processing history for other parts) is especially important for precipitate hardened materials. The presence of columnar grains in most AM alloys means that the relationship of grain orientation to mechanical property anisotropy must be considered.

Different machines may have very different thermal histories of material, which may manifest in as-fabricated mechanical properties as variance in hardening through coarsening or aging. Similarly, the details of any post-processing heat treatments are equally important in determining mechanical properties. Data for many AM processes is only given in the stress relieved or heat treated states, which tend to have better mechanical properties. As a result, the amount of published data on as-fabricated samples (samples as they come out of the machine) is sparse. Previous work has compiled some mechanical properties, focusing on Ti-6Al-4V and Inconel 718/625. [69] A summary of tensile properties for DED, LM, and EBM is presented in Table 5 for Ti-6Al-4V and Inconel 718.

When as-fabricated samples are tested, the geometry of test specimens, surface finish, and type of measurement (global vs. extensometer) can all have a significant impact on resulting data. Comparisons of such data must therefore take testing methodology into account. Sample geometry, as discussed previously, can impact local heat transfer conditions, which can impact solidification, defects, and microstructure. It is therefore important to know how the parts were built (including what other parts they were built with) to determine the complete build geometry. For the use of as-fabricated material (not machined), surface finish is typically poor compared to well-polished test specimens. Rough surface finish can introduce stress risers or crack nucleation sites at surface defects or flaws. Using parts straight out of the machine has been observed to negatively affect mechanical performance.[129]

The reported values of UTS, YS, and elongation tend to be very similar in the X-Y versus Z directions, with the X-Y results being slightly better in some cases (see Table 5). This is unexpected, as tensile properties of directionally solidified material (columns oriented along the Z direction) should be superior to those in the X-Y direction. To understand why this is unexpected, the effect of grain orientation on mechanical properties must be considered. In nickel-based superalloys, directionally solidified material is highly oriented with the [100] direction. This high orientation is associated with an increase in primary creep, rupture life, and ductility performance. [147] The same orientation structure is seen in most metal AM parts (not just the nickel-based ones), but the increase in performance (in elongation, since orientation dependent creep data is not as common in the AM literature) is not seen. In fact, the opposite effect is seen in AM; elongation is less in the oriented [100] direction. This effect is notably seen in EBM Ti-6Al-4V, where UTS and YS remain unaffected by orientation, but elongation is 30% higher in the X-Y direction. [148] For this specific case, it was noted that the effect of “thermal mass” or in-situ aging may have influenced results. In fact, in-situ aging in EBM has been noted to influence mechanical properties in IN718 as well. [16, 103] Depending on the material, this effect appears to more strongly influence mechanical properties than the orientation of the material. EBM is unique in this in-situ aging, and such an explanation cannot be applied to similar orientation variation in DED and LM processing. In fact, the underlying mechanism for the unexpected mechanical performance due to orientation variation has not been well studied or identified for DED or LM. The mechanism is likely material and process dependent.

Post-processing can improve mechanical properties, but must be applied correctly for a given starting microstructure. The starting microstructure can vary based on process parameters (which may impact solidification kinetics), which may cause need for non-standard post-processing. Having to determine a post-processing procedure for each batch is not ideal or feasible. Work must be done to characterization the range of microstructures that may form for a given material in a given machine. If a

treatment can be applied across this variance in microstructure with acceptable results, then it can be applied uniformly. If not, then processing windows must be set to insure quality control on the material coming out of the machine. For processes without in-situ aging (LM, DED), processing parameters mostly impact solidification microstructure. For EBM, which undergoes in-situ aging, variable amounts of aging may lead to issues in solution treatment. [103] Processing windows for EBM or precipitate hardened materials must therefore include process parameters that determine solidification kinetics and the size of the part (how long it will hold in the machine). Standard post-processing with HIP will typically change tensile properties (elongation may improve at the expense of UTS/YS in precipitate hardened materials), but can close pores (should improve fatigue life).

Recent work has focused on development of standardized testing procedures for AM processes. ASTM standards have been developed for PBF Ti-6Al-4V [149], Inconel 718 [150], and Inconel 625 [151]. The ASTM guidelines offer criteria for material, but allow for agreed upon specifications between the manufacturer and end-user. For researchers, there is no official standard for reporting test results. Work by NIST using Ti-6Al-4V has been done to develop a standardized test procedure for EBM material to account for variation of mechanical properties within the build volume [148, 152, 153] but has yet to be written into an official standard. To improve the usefulness of published research results, authors should be diligent to report: orientation of build direction, process thermal history (if applicable), exact conditions of any post-processing, and the nature of the mechanical test specimen (machined, etc.).

Outside of tensile test and hardness data, other mechanical properties of AM materials are less well studied. Fatigue and creep are of strong importance to industry for certain alloys, as they are often considered a limiting property of materials (whereas YS or UTS are not limiting for many applications of aerospace parts, for example). The most complete set of fatigue data exists for Ti-6Al-4V, with tests run on powder-fed DED [154], LM [129], and EBM. [106] While differences in testing (orientation, geometry, technique, etc.) make direct comparison difficult, most as-fabricated material from DED, LM, or EBM, falls in the lower range of the performance of cast parts as shown in Figure 36. Post-processing improves material to a level of performance comparable to annealed wrought or cast with HIP material.

Fatigue properties are highly influenced by surface finish and porosity, with samples that were processed by HIP and machined exhibiting comparable fatigue properties to wrought material. [69] Machining samples (as opposed to using the as-fabricated finish) typically improves mechanical performance, but the result can be difficult to observe if material has significant porosity and residual stress. [129] Efforts to understand underlying dislocation motion and model fatigue performance are limited, but have demonstrated accuracy compared to experimental results. [155] Other testing of crack growth, creep [156], corrosion [108], and other performance properties are also limited, making these tests a likely area of future work.

8. Novel Methods of Metal AM

Having fully discussed current technologies in this paper, there are some methods for producing metal parts that have not been as fully explored: chemical vapor deposition (CVD), physical vapor deposition (PVD), liquid metal material jetting, and friction stir AM. Machine modifications to existing systems

offer the chance to improve material properties, speed up deposition rates, or both. Either by development of novel methods or incremental improvements to existing technology, innovation will continue to change the metal AM landscape.

8.1. PVD & CVD

Vapor deposition has been used for many decades to deposit coatings, among other applications. CVD is accomplished via a chemical reaction at the deposition surface with the particles in a vapor stream. PVD is accomplished solely through the condensation of metal vapor on the substrate and requires vacuum, whereas CVD may operate within a range of atmospheres. Though CVD and PVD are typically used for coatings, the use of CVD for metal AM has been considered using an e-beam [45] or laser-jet. [157, 158]

8.2. Cold Spray

Another purely physical process is known as cold spray and is being studied for use in AM. [159] Cold spray technologies typically works by acceleration of powder particles in a high-speed gas stream. This powder adheres to a substrate via plastic deformation, forming a deposit. [160] Correspondingly, residual stresses in cold spray deposits are primarily due to impact and are compressive in nature. Residual stresses have not been reported for bulk deposits, which may be a significant material defect to address considering the large amount of deformation put into the deposit. The technology also appears constrained to simple, near net shapes at present. There have been recent success stories in demonstrating cold spray techniques as shown in Figure 37 [161], and deposition rates are expected to be faster than existing metal AM processes. Though microstructures are not well characterized for cold spray processes, recent work has noted abnormalities in the precipitation kinetics of Inconel 625; typical phase precipitation was inhibited or sluggish within ranges expected to form precipitates in traditional material. [162]

8.3. Material Jetting

Metal Material Jetting deposits droplets of liquid metal that either solidify upon deposition to form a part [163] or remain liquid at room temperature to form arrays of liquid metal. [164] Demonstration has been limited to micron-scale or smaller structures, and neither technique has been demonstrated for millimeter-scale parts. Friction stir welding has been proposed for AM [165], which operates by the method of sheet lamination. Forming of an actual part using friction stir welding has not been demonstrated either and would require pairing with CNC tools to machine of each layer of deposited material before subsequent deposits are made.

8.4. Hardware Improvement & Large-Scale

Machine modifications to existing hardware typically support incremental improvements, but several developments could make large gains in the development of current technologies. The use of a combined feed of powder and wire for DED was demonstrated to increase deposition efficiency, improve surface finish, and reduce porosity under certain conditions studied.[60] The use of multiple heat sources for DED and PBF could speed up deposition times or be used to help preheat material, reducing residual stresses. Alternatively, multiple small power lasers have been combined to produce a

cheaper power source for DED laser systems. [166] Another technique is to heat the feedstock prior to deposition; wire-fed DED can be modified to heat the wire (using an arc) while creating a molten pool with a laser. [167] Initial results suggest that this method can help increase deposition rate and may reduce cracking and segregation. This method may be an enabling technology for addressing one of the major limitations of metal AM: achieving large, meter-plus-scale parts.

The ability to produce large-scale, metal AM parts is limited by machine size and materials considerations. Scaling current PBF techniques to produce large-scale parts would be very expensive and require redesigning existing processes for removing and cleaning parts. Deposition rates are prohibitively slow for scaling up existing hardware processes and the cost of the powder feedstock is very high. DED process have led the way for producing large-scale parts [168], but there are still limitations in producing overhangs, thick walls, and other features. Polymer AM has had many of the same problems as metal AM (residual stress formation, high feedstock costs, slow deposition rates), but solutions were found [169] to make a system that sacrificed resolution (surface finish) for speed and cost. [170] A similar technique could be employed for metals; a specific alloy could be identified or developed that allows for open-air DED, while maintaining acceptable amounts of residual stress. Alternatively, in-direct methods of manufacture are could be used (using large-scale polymers as molds or substrates for forming metal).

8.5. Open Source & Low Cost

3D printing is a mainstay of the open-source hardware movement, centered on the RepRap project famous for its plastic material extrusion process. The use of open-source hardware to make research cheaper and better across a wide range of disciplines is promising. [171] A major limitation of current open-source hardware is the lack of a widely used 3D metal printer. The most exciting developments in low-cost metal AM have come in the Direct Energy Deposition category. Researchers at Michigan Tech University have demonstrated a stationary welder that deposits metal on top of a moving substrate. The welding machine used is a gas metal arc welding (GMAW) or metal inert gas (MIG) machine. The machine is reported to cost <$2000. [172] The problem is that weld deposition has poor resolution, producing only *near-net shapes*. Promisingly, researchers in India have demonstrated a low-cost CNC machine to machine near-net shapes produced using a welder. [116] Using a welding machine as a desktop printer may be limited due to safety issues, but the combination of open-source weld deposition with CNC could be an important step for open-source hardware development. PBF LM machines capable of smaller resolution may develop in the future, as related patents continue to expire.

9. Process Monitoring & Quality Control

Process monitoring can be used to identify the formation of defects and measure the thermal history of the material. Infrared thermography, standard cameras, high speed video, and pyrometry have all been used for in-situ monitoring. Ultrasonic imaging, the Archimedes principle, x-ray computed tomography (XRCT), and neutron tomography have all been used as nondestructive means of quality control. The most common goal of defect detection is to determine the presence of porosity, although inclusions, swelling, and other defects can also be detected in this manner.

Optical monitoring can yield useful data for defect identification, but IR imaging is required for temperature profiling. Images from a standard camera can be taken during powder distribution during PBF processes, but not during continuous DED processes. Standard images, and high speed videos, pick up the difference in light emission due to temperature variation. This has shown usefulness in measuring melt pool dynamics. [173]

To better understand solidification and thermal history, IR imaging, pyrometry, and thermocouple measurement have been applied. Thermocouples can be used to effectively measure substrate temperature, but cannot be used to measure variation in part temperature or surface temperature, due to the nature of AM processes. Pyrometers have been used in DED [57], EBM [174], and LM. [175] The details of the sample location of the pyrometer are important to note, as the heat source may or may not pass in the measured area, depending on part geometry. For full layer thermal analysis, IR or near-IR imaging must be used and is very important in understanding metal AM metallurgy. [176] IR imaging is particularly useful for EBM, as it can be used to measure the elevated surface temperature or the powder-bed temperature as shown in Figure 39. [174] Process corrections using the average temperature from near-IR have been tested in a feedback system that adjusts process parameters during the build. [137] Differences in emissivity between powder and the melted part must be taken into account, among other details. [177]

Post-build, non-destructive techniques can be used to detect internal defects. [178] The Archimedes principle of immersion in liquid can be used to detect the presence of large amounts of porosity, but it may overestimate low amounts of porosity due to entrapment of air bubbles. XRCT and neutron tomography do not have bubble entrapment issues but will still have associated counting statistical error. XRCT and the Archimedes principle have been shown to be in general agreement, but the Archimedes method is noted to be faster and more economical for bulk measurements. [179] The benefit of XRCT and neutron tomography is that porosity mapping can be done to determine the locations of defects. Ultrasonic transducers are capable of detecting smaller amounts of porosity (~0.5%) and should also be capable of porosity mapping.

Some monitoring techniques have been implemented commercially, while others not. Pyrometry has been implemented with some DED processes to affect process control. Layer imaging using standard cameras has been implemented commercially on some EBM systems. Effective IR imaging and process feedback has yet to be implemented in any commercial system, but is a good option for users demanding better quality assurance.

10. Comparison

Now that the general processing science of metal AM has been explored, this background can be used to compare the technical aspects of existing technologies. A tabulated comparison of LM, EBM, powder-fed DED, wire-fed DED, BJ, and SL is given in Table 6. Discussion will focus on just a few of the more interesting differences. For example, porosity can be kept to low levels in PBF and DED but is inherently present in BJ. BJ must address the porous nature of the material by either infiltration of consolidation. EBM and BJ are notable for low levels of residual stress induced during processing. This can be

attributed to a high operating temperature for the EBM process (effectively in-situ stress relief) and no applied temperature during BJ processing. The high operating temperature of EBM does reduce residual stress levels, but can lead to concerns with in-situ aging of the microstructure. While BJ does have many advantages, is also has its own set of concerns associated with fragile green bodies and post-processing. PBF and BJ are the more capable techniques for producing complex geometries such as overhangs and meshes. Surface finish may be best on LM and SL systems but, as mentioned before, all metal AM parts should be considered net shapes; machining must be done after thermal post-processing for most uses. SL achieves a machined finish because machining is done as part of the process, after each layer. Process clean-up is really only a concern in PBF and BJ processes. Powder must be sieved and handled appropriately. Additionally, EBM powder must be blasted away from the surface of finished parts (adds an additional step). The use of DED for deposition on top of existing structures enables its unique use for part repair. Multi-material parts can only be produced using SL (layers of different materials), BJ (infiltration), or potentially DED (multiple wire or powder feeds).

Process speed, or deposition rate, is a major limitation of current metal AM techniques. Current deposition rates are presented in Table 7. The fastest deposition rate is using BJ, which does not melt or sinter the metal. The increase in deposition speed comes at the cost of additional post-processing steps (curing, sintering, etc.). Powder-fed DED can be fast- if a larger power laser is used. The same principle is true of all processes that use a heat source; faster deposition rates can be achieved with higher power input. Higher power allows for faster scan speeds to achieve the same energy density needed for full melting. EBM is reportedly faster than LM, making it the faster PBF technique. LM deposition rate can be increased at the expense of surface finish. Depending on part requirements, LM operators should consider this to decrease build time. Unless higher power heat sources are used, wire-fed DED is reportedly about three-times faster than powder-fed DED. More efficient deposition of material can explain this, as some powder is lost during the spray process (and cooling incurred by the gas flow). For comparison to consumer polymer hardware, the RepRap deposition rate was included. All metal AM machines are on the same order of magnitude as these polymer printers, except for the high-power LENS and ExOne systems. In addition to deposition rate, the maximum power input is another usualy figure of merit. This value is helpful for describing how much power can be applied to a given area. Though there is no clear relationship between max power input and deposition rate, max power input is useful for determining process efficiency and deducing the impact on microstructure (see previous section).

11. Applications & Economics

Metal AM has found a range of applications within the aerospace, biomedical, automotive, robotics, and many other industries. Applications in part repair are mostly limited to the aerospace industry, whereas all industries mentioned are beginning to use metal AM for end-use part production. However, limited build volumes, slow deposition rates, and high machine costs limit the current use of the technology. With these constraints, AM technologies are limited to uses in low-volume production, material use reduction, and cases of necessity. Process improvements and quality controls may help to lower the costs associated with AM production in the future.

Market analysts predict the overall market for AM (metal and polymer) parts will grow by 18% a year until 2025, reaching a market size of $8.4 billion. [180, 181] The largest growth areas are projected to be aerospace, biomedical, and automotive. Due to the nature of the parts needed by these industries, a significant portion of that growth can be expected to come from metal AM processes. In fact, the aerospace and medical industries have been early adopters and users of metal AM parts for end-use. The material of choice for these industries has been Ti-6Al-4V, for use as a light-weight structural material and as a bio-compatible material. Case studies for aerospace parts have demonstrated AM brackets [114] and landing gears. [182] Case studies for biomedical parts have demonstrated AM bone replacements for jaws [183], hips, and other parts. The application of mesh structures is attractive for biomedical parts [46] and also has applications for other uses, such as lithium ion batteries. [184] The use of light-weight Ti-6Al-4V has been demonstrated for use in robotics (Figure 41), as the use of AM can enable additional degrees of freedom and allow for internal routing of hydraulic and electrical lines. [185]

The development of Inconel 718 and other superalloys has been sponsored for use in aerospace components, but could be used in any industry that has the need for high temperatures or superalloy components. GE Aviation, a large company in the aerospace field, has committed to production of fuel injectors for the LEAP engine [186] and γ-TiAl turbine blades for the GEnX engine. [187] The aerospace industry has also found use for DED systems in turbine blade repair [117], including repair of single crystal material. [188] The use for part repair is limited to cases of high-cost parts, where the cost of repair is lower than the cost of replacement. For this reason, most AM research focuses on the production of end-use parts, fabricated without an existing component.

To analyze the economics of AM, a comparison to traditional methods and subtractive manufacturing is necessary. Cost models for LM have been developed and can calculate costs for multiple parts in a batch. [189] When comparing LM to die casting, AM is more economical only for low volumes (less than 31 parts for the geometry studied). [190] Compared to subtractive manufacturing, AM also only makes sense for small volumes or where the “buy-to-fly” ratio (amount of material consumed compared to the amount that is actually used in the final product) is high. [191] Figure 42 shows a comparison of additive manufacturing to subtractive manufacturing (where parts are machined from a block of starting material). According to this model, the cost of labor/design and the failure rate are extremely important to the viability of AM. Increasing deposition rate can also dramatically increase the range of cases where AM is viable.

These analyses mean that AM is currently economically limited for end-use parts, for small quantities of parts or parts that require large billets to be used during machining. For the remaining uses, the viability of AM comes down to economy versus necessity (which is not completely unrelated). By enabling new geometries that reduce the number of components in a part (like the GE LEAP nozzle) or mesh structures that promote body acceptance of implants (for medical implants), metal AM has the potential to make economic sense by displacing parts with inferior performance. This nuance (that AM then becomes a necessity to make the new, more efficient part design) is lost in some analyses of manufacturing economics (only looking at volumes, raw material costs, and manufacturing efficiency).

This means that the key for the growth of metal AM is to find more design improvements that are enabled by AM and/or finding ways to reduce the driving costs of using metal AM for production.

Of paramount importance is the reduction of failure rates in AM processes, which are held as proprietary information and not typically published or quoted. It has been shown that a failure rate of just 10% can make AM processes un-economical. [191] Better quality control and improved hardware/software designs will surely help. For those familiar with equipment from the last decade, there is a "Rule of 4" that has been used to describe the success rate of AM; it can take up to three iterations to produce a successful outcome, but after that the desired parts can be produced reliably. While this is viable for a standardized batch of parts, the trial and error associated with delivering new geometries must be eliminated to make AM viable for one-off parts. Hardware reliability must improve across all systems. For example, the result of selective powder fetching (only fetching powder from one hopper) in EBM is shown in Figure 40. For this build, powder distribution sensors failed to recognize powder as present in both hoppers. The machine then fetched powder from only one hopper, leaving the other completely full. The build then failed due to running out of powder (the left side of the build can be seen a depressed). There are many other machine reliability problems across platforms, and this example should be taken to highlight the kind of problems that must be overcome. Developments in technology continue to improve success rates, as does the development of a workforce skilled in AM. A skilled operator can boost success rates tremendously for most metal AM processes.

The application area is not just limited by cost, but also by capabilities of AM machines. Small build volumes mean that parts of or greater than the meter-scale are not possible with the current technology (some thin walled samples are the exception, using DED processing). Slow deposition rates are a limiting feature in some processes from the standpoint that there are hardware limitations on extremely long build times. For example, EBM processing is limited in the maximum time possible by filament lifetime (typically replaced every 100 hours of burn time). Similarly optics in laser based systems must not get dirty or heat up during long build operations. From this viewpoint, extremely long build times (>100 hours) are not just uneconomical but also not possible due to hardware constraints. Very small parts cannot be made due to limitations on machine resolution based on material feedstock and heat source size. Overhangs and complex geometries continue to be a limitation; though PBF and BJ have mostly enabled parts with this feature (supports are typically necessary in PBF).

Input costs (hardware, feedstock, maintenance, etc.) are high for metal AM and significantly limit the current metal AM market to researchers and large industrial users. Machine costs are not widely reported and vary based on model type. Some available hardware cost information has reported the following values: ExOne models range from $145,000-950,000 [192, 193], the EOS M270/M280 is $800,000 [194], Arcam models range from $0.6-1.3 Million [195], and the Renishaw AM250 is $750,000. [196] Based on these reported prices, hardware costs appear pretty similar across platforms. Costs for DED and SL systems remain unreported, but are expected to be similar to LM, EBM, and BJ. At a price of $0.5-1 Million, metal AM hardware is a significant capital investment for most companies. Hardware is not the only major cost in operating a system; feedstock costs can be a significant investment as well. Powder feedstock costs are typically higher than wire costs, and are a significant investment for powder-base processes. The powder used in EOS metal machines has been reported to vary from $120/kg for

stainless steel to $735/kg for Ti-6Al-4V ELI. [197] LM processes require a smaller particle size distribution, which tends to cost a premium due to the yields of current powder production techniques. EBM powder is less expensive due to a large particle size distribution, though exact costs are not reported. Cost is highly dependent upon atomization technique, which can determine powder quality. Typical techniques used for AM powders are gas atomization ($165-330/kg), plasma atomization, and plasma rotating electrode ($407-1210/kg). [198] BJ particle size distributions are not well known and costs are not reported. Based on similar particle size requirements to EBM, powder-fed DED powder is expected to have similar costs.

12. Conclusion

This review details processing defects, thermal histories, post-processing, microstructure, and mechanical properties associated with DED and PBF techniques. The various metal AM techniques were described, with a focus on comparison of processing strengths and weaknesses. Previous work identified future directions for metal AM within specific areas: limited deposition rate, surface finish, residual stress, and microstructural variations. [199] It is useful to consider the progress that has been made in these areas since the publication of the report in 2007 and identify new directions that the technology may take.

Higher power lasers have increased the deposition rate of some DED hardware. Currently, surface finish and deposition rate are inversely related, which is an undesirable trade-off. Many experiments try to improve surface finish, despite the fact that most-end use parts will be post-processed (thermally and mechanically) and surface finish will be determined by the polishing or machining techniques used. If this is the intended use, surface finish almost does not matter.

Residual stress continues to be a defining problem for DED and LM, but new technologies like EBM (and potentially BJ) have succeeded in producing parts with low amounts of residual stress. Residual stress can impact post-processing and mechanical properties. Acting as a driving force for recrystallization, residual stress in DED and LM parts may limit the ability to engineer grain structures using those approaches. Conversely, residual stress may be able to be used to help promote recrystallization and the formation of equiaxed microstructures.

The understanding of the microstructure, mechanical properties, and processability of new alloys has been the main advance in metal AM in the past five years. While microstructural heterogeneities are still observed, characterization work has shown certain features (columnar grains, high orientation, amount of porosity, etc.) to persist across technologies and materials. Improved process control and processing experience have allowed for the reduction of process-induce porosity to levels of frequently >99% dense parts.

Two current mindsets for metal AM material exist: (1) as-fabricated properties matter because there are customers who intend to use them without post-processing and (2) as-fabricated properties are not important because material will be post-processed to eliminate pores and cracks, change the grain structure, and change phase fractions. Both of these schools of thought are relevant, but it is important

to note that as-fabricated microstructure is still important to characterize even if post-processing is to be used; post-processing needs to consider the as-fabricated properties in order to achieve the desired final material. For this reason, work to characterize as-fabricated material will continue to be important to both schools of thought. As processes improve, the process metallurgy is likely to change the condition of as-fabricated material (even for those materials previously characterized).

Niche product applications (hip replacements, GE LEAP nozzles, GE turbine blades) have found recent success for the use of PBF parts. Previous success was mostly in the DED repair of traditional parts for the aerospace industry. (REF blades) Applications to the robotics industry are promising, as metal AM has been shown to enable performance characteristics, like increasing the degrees of freedom of rotating parts. All of these developments suggest that metal AM may really be about "giant engineering firms turning out sophisticated parts". [200]

12.1 Future Directions

The future of the technology is bright. Improvements on the high end will enable the production of higher quality AM parts, while the expiration of patents and falling costs of heat sources will help to lower the cost of the technology. New materials will be processed, offering a wider range of available alloys. Recent work on the control of grain structure and phase formation suggests that improvements in processing controls will enable metal AM to achieve microstructural engineering on a scale not previously possible.

Having explored the current state of metal AM, it is useful to look back on where limitations exist. The authors have identified the following areas as being of general importance for the continued improvement of metal AM:

- Faster Deposition rates
- Quality Control
    - NIST roadmap almost entirely falls within this category
- Machine Reliability
- Cost Reduction
- New Capabilities/Materials

Faster deposition rates are directly related to costs and feasibility. Faster rates mean more parts can be produced per machine per unit time; each machine can be made more efficient with faster deposition rates. Any decrease in process time is impactful, but jumps of orders of magnitude are needed to truly revolutionize metal AM production. To achieve faster deposition rates, limitations on the amount of power input available for the process must increase. This is possible by increasing the power or number of heat sources available. Faster deposition must not incur too much residual stress, or significant warping issues may occur. Some increase in the amount of defects (like porosity) may be tolerated, if post-processing can be done.

Quality control is a significant concern and problem for industry in suing metal AM processes. Metal AM processes are new (compared to traditional processes) and are just beginning to enter the time-frame

for qualification for many aerospace companies, though biomedical qualification may offer a shorter timeline. Quality control must understand the details of the AM process to be qualified. For this reason, advances in process technology may not get incorporated as fast (as industry is likely to qualify certain machines and older software versions). A NIST roadmap for metal AM focuses entirely on quality control concerns: standards and protocols, measurement and monitoring techniques for data, fully characterized material properties, modeling systems that couple design and manufacturing, and closed loop control systems for AM. [201] These are all extremely important efforts, but quality control is only one piece of the big picture. Developing quality control, and keeping it up-to-date, is likely to remain a focus of metal AM.

Machine reliability of all metal AM systems must improve, and the operator burden should be reduced. High failure rates are common in many systems, though these rates are hardware, operator, and design dependent. Though improvement of machine reliability must come from hardware manufacturers, researchers and operators should come together to present best practices to reduce the effect of operator error on failure rates. Improved software simulation could also play an important role in determining optimal build orientations for successful builds. As more technicians learn how to use existing hardware, operator errors will also be reduced.

The impact of cost cannot be understated. It can be argued that faster deposition rates, quality control, and machine reliability are really just sub-sets of cost. Cost is considered separately here, as reduction in hardware and feedstock costs can open up the metal AM market to completely new customers. While consumer metal printers are not likely to happen anytime soon (though open source efforts are making progress), a significant drop in hardware cost could open up the machine shop market; machine shops are a significant player in local manufacturing and have more resources to support hardware than typical consumers. Continued costs reductions should be expected to open up metal AM to more users, while increasing the number of uses considered economical.

New hardware and new materials development have the most direct impact to the research community. Development of new ways of processing metal into parts could potentially dramatically increase deposition rates and lower costs of metal AM (in the way in which large-scale polymer systems have changed what is possible with polymer printing). New materials development is research intensive but necessary to increase the number of uses for metal AM. New alloys will have uses for new industries and new parts. AM specific alloys may be able to increase performance beyond what is capable with traditional wrought or cast alloys. The ability to manipulate grain and phase structures offers the potential for microstructural engineering and will likely see continued efforts. Fundamental processing science is important to all of these development efforts.

13. Acknowledgments

Research sponsored by the U.S. Department of Energy, Office of Energy Efficiency and Renewable Energy, Advanced Manufacturing Office, under contract DE-AC05-00OR22725 with UT-Battelle, LLC. This research was also supported by fellowship funding received from the U.S. Department of Energy, Office of Nuclear Energy, Nuclear Energy University Programs. The United States Government retains and the

publisher, by accepting the article for publication, acknowledges that the United States Government retains a non-exclusive, paid-up, irrevocable, world-wide license to publish or reproduce the published form of this manuscript, or allow others to do so, for United States Government purposes.

14. References

[1] C. R. Deckard, "Part generation by layer-wise selective laser sintering," M.S., Univeristy of Texas - Austin, Austin, TX, 1986.

[2] A. Lou and C. Grosvenor. (2012, 4/11/2014). *Selective Laser Sintering, Birth of an Industry*. Available: http://www.me.utexas.edu/news/2012/0712_sls_history.php

[3] C. R. Deckard, "Selective Laser Sintering," Ph.D., Univeristy of Texas - Austin, Austin, TX, 1988.

[4] D. L. Bourell, H. L. Marcus, J. W. Barlow, and J. J. Beaman, "Selective laser sintering of metals and ceramics," *International journal of powder metallurgy,* vol. 28, pp. 369-381, 1992.

[5] H. L. Marcus, D. L. Bourell, J. J. Beaman, A. Manthiram, J. W. Barlow, and R. H. Crawford, "Challenges in laser processed solid freeform fabrication," pp. 127-127, 1994.

[6] K. Skiba, E. J. Hirst, and A. Sachdev. (2014). *Obama formally annouces Chicago as site for digital manufacturing lab*. Available: http://articles.chicagotribune.com/2014-02-26/site/ct-digital-lab-obama-0226-biz-20140226_1_president-barack-obama-institutes-advanced-manufacturing-partnership

[7] C. R. Deckard, "Method and apparatus for producing parts by selective sintering," WO1988002677 A2, 1986.

[8] M. J. Cima, J. S. Haggerty, E. M. Sachs, and P. A. Williams, "Three-dimensional printing techniques," US5204055 A, 1989.

[9] R. Larson, "Method and device for producing three-dimensional bodies," US5786562 A, 1993.

[10] EOS-GmbH. (April 16). *History*. Available: http://www.eos.info/about_eos/history

[11] Sandia-National-Laboratories. *Creating a complex metal part in a day is goal of commercial consortium*. Available: http://www.sandia.gov/media/lens.htm

[12] D. White, "Ultrasonic object consolidation," US6519500, 1999.

[13] Arcam-AB. (April 16). *Arcam History*. Available: http://www.arcam.com/company/about-arcam/history/

[14] A. International, "Standard Terminology for Additive Manufacturing Technologies," ed: ASTM International, 2012.

[15] J. P. Kruth, X. Wang, T. Laoui, and L. Froyen, "Lasers and materials in selective laser sintering," *Assembly Automation,* vol. 23, pp. 357-371, 2003.

[16] W. J. Sames, F. Medina, W. H. Peter, S. S. Babu, and R. R. Dehoff, "Effect of Process Control and Powder Quality on Inconel 718 Produced Using Electron Beam Melting," in *Superalloy 718 and Derivatives*, Pittsburgh, PA, 2014.

[17] M. L. Griffith, D. L. Keicher, J. T. Romero, J. E. Smugeresky, C. L. Atwood, L. D. Harwell*, et al.*, "Laser Engineered Net Shaping (LENSTM) for the fabrication of metallic components," in *Proceedings of the 1996 ASME International Mechanical Engineering Congress and Exposition, November 17, 1996 - November 22, 1996*, Atlanta, GA, USA, 1996, pp. 175-176.

[18] R. P. Mudge and N. R. Wald, "Laser Engineered Net Shaping Advances Additive Manufacturing and Repair," *Welding Journal,* vol. 86, pp. 44-48, 01// 2007.

[19] J. E. Matz and T. W. Eagar, "Carbide Formation in Alloy 718 during Electron-Beam Solid Freeform Fabrication," *Metallurgical and Materials Transactions A,* vol. 33A, pp. 2559-2567, 2002.

[20] B. Baufeld, E. Brandl, and O. van der Biest, "Wire based additive layer manufacturing: Comparison of microstructure and mechanical properties of Ti–6Al–4V components fabricated

by laser-beam deposition and shaped metal deposition," *Journal of Materials Processing Technology,* vol. 211, pp. 1146-1158, 6/1/ 2011.
[21] J. Xiong and G. Zhang, "Adaptive control of deposited height in GMAW-based layer additive manufacturing," *Journal of Materials Processing Technology,* vol. 214, pp. 962-968, 4// 2014.
[22] ExOne. (4/15/2014). *Metal*. Available: http://www.exone.com/en/materialization/what-is-digital-part-materialization/metal
[23] P. Vallabhajosyula and D. L. Bourell, "Indirect Selective Laser Sintered Fully Ferrous Components - Infiltration Modeling, Manufacturing and Evaluation of Mechanical Properties," in *Solid Freeform Fabrication Symposium*, Austin, TX, 2009.
[24] S. Kumar and J. P. Kruth, "Effect of bronze infiltration into laser sintered metallic parts," *Materials & Design,* vol. 28, pp. 400-407, // 2007.
[25] G. N. Levy, R. Schindel, and J. P. Kruth, "RAPID MANUFACTURING AND RAPID TOOLING WITH LAYER MANUFACTURING (LM) TECHNOLOGIES, STATE OF THE ART AND FUTURE PERSPECTIVES," *CIRP Annals - Manufacturing Technology,* vol. 52, pp. 589-609, // 2003.
[26] T. Obikawa, M. Yoshino, and J. Shinozuka, "Sheet steel lamination for rapid manufacturing," *Journal of Materials Processing Technology,* vol. 89–90, pp. 171-176, 5/19/ 1999.
[27] S. Yi, F. Liu, J. Zhang, and S. Xiong, "Study of the key technologies of LOM for functional metal parts," *Journal of Materials Processing Technology,* vol. 150, pp. 175-181, 7/1/ 2004.
[28] H. Thomas, T. Anja, N. Steffen, and B. Eckhard, "Recent developments in metal laminated tooling by multiple laser processing," *Rapid Prototyping Journal,* vol. 9, pp. 24-29, 2003/03/01 2003.
[29] B. Xu, X.-y. Wu, J.-g. Lei, F. Luo, F. Gong, C.-l. Du*, et al.*, "Research on micro-electric resistance slip welding of copper electrode during the fabrication of 3D metal micro-mold," *Journal of Materials Processing Technology,* vol. 213, pp. 2174-2183, 12// 2013.
[30] B. Mueller and D. Kochan, "Laminated object manufacturing for rapid tooling and patternmaking in foundry industry," *Computers in Industry,* vol. 39, pp. 47-53, 6// 1999.
[31] T. Himmer, T. Nakagawa, and M. Anzai, "Lamination of metal sheets," *Computers in Industry,* vol. 39, pp. 27-33, 6// 1999.
[32] D. R. White, "Ultasonic Consolidation of Aluminum Tooling," *Advanced Materials & Processes,* vol. January, pp. 64-65, 2003.
[33] Fabrisonic, "Ultrasonic Additive Manufacturing," ed, 2011.
[34] R. J. Friel and R. A. Harris, "Ultrasonic Additive Manufacturing – A Hybrid Production Process for Novel Functional Products," *Procedia CIRP,* vol. 6, pp. 35-40, // 2013.
[35] S. Masurtschak, R. J. Friel, A. Gillner, J. Ryll, and R. A. Harris, "Fiber laser induced surface modification/manipulation of an ultrasonically consolidated metal matrix," *Journal of Materials Processing Technology,* vol. 213, pp. 1792-1800, 10// 2013.
[36] G. D. J. Ram, C. Robinson, Y. Yang, and B. E. Stucker, "Use of ultrasonic consolidation for fabrication of multi-material structures," *Rapid Prototyping Journal,* vol. 13, pp. 226-235, 2007/08/07 2007.
[37] M. R. Sriraman, S. S. Babu, and M. Short, "Bonding characteristics during very high power ultrasonic additive manufacturing of copper," *Scripta Materialia,* vol. 62, pp. 560-563, 4// 2010.
[38] R. Hahnlen and M. J. Dapino, "NiTi–Al interface strength in ultrasonic additive manufacturing composites," *Composites Part B: Engineering,* vol. 59, pp. 101-108, 3// 2014.
[39] D. E. Schick, R. M. Hahnlen, R. Dehoff, P. Collins, S. S. Babu, M. J. Dapino*, et al.*, "Microstructural Characterization of Bonding Interfaces in Aluminum 3003 Blocks Fabricated by Ultrasonic Additive Manufacturing," *Welding Journal,* vol. 89, pp. 105s-115s, 2010.
[40] R. R. Dehoff and S. S. Babu, "Characterization of interfacial microstructures in 3003 aluminum alloy blocks fabricated by ultrasonic additive manufacturing," *Acta Materialia,* vol. 58, pp. 4305-4315, 8// 2010.

[41] H. Fujii, M. R. Sriraman, and S. S. Babu, "Quantitative Evaluation of Bulk and Interface Microstructures in Al-3003 Alloy Builds Made by Very High Power Ultrasonic Additive Manufacturing," *Metallurgical and Materials Transactions A,* vol. 42, pp. 4045-4055, 2011/12/01 2011.

[42] K. Sojiphan, S. S. Babu, X. Yu, and S. C. Vogel, "Quantitative Evaluation of Crystallographic Texture in Aluminum Alloy Builds Fabricated by Very High Power Ultrasonic Additive Manufacturing," presented at the Solid Freeform Fabrication Symposium, Austin, TX, 2012.

[43] M. R. Sriraman, M. Gonser, H. T. Fujii, S. S. Babu, and M. Bloss, "Thermal transients during processing of materials by very high power ultrasonic additive manufacturing," *Journal of Materials Processing Technology,* vol. 211, pp. 1650-1657, 10// 2011.

[44] A. Herr, J. Pritchard, and M. J. Dapino, "Interfacial shear strength estimates of NiTi-Al matrix composites fabricated via ultrasonic additive manufacturing," in *Industrial and Commercial Applications of Smart Structures Technologies* 2014.

[45] I. Gibson, D. W. Rosen, and B. Stucker, *Additive Manufacturing Technologies*: Springer, 2010.

[46] L. E. Murr, S. M. Gaytan, D. A. Ramirez, E. Martinez, J. Hernandez, K. N. Amato*, et al.*, "Metal Fabrication by Additive Manufacturing Using Laser and Electron Beam Melting Technologies," *Journal of Materials Science & Technology,* vol. 28, pp. 1-14, 1// 2012.

[47] F. A. List, R. R. Dehoff, L. E. Lowe, and W. J. Sames, "Properties of Inconel 625 mesh structures grown by electron beam additive manufacturing," *Materials Science and Engineering: A,* vol. 615, pp. 191-197, 10/6/ 2014.

[48] K. A. Mumtaz and N. Hopkinson, "Selective Laser Melting of thin wall parts using pulse shaping," *Journal of Materials Processing Technology,* vol. 210, pp. 279-287, 1/19/ 2010.

[49] B. Ferrar, L. Mullen, E. Jones, R. Stamp, and C. J. Sutcliffe, "Gas flow effects on selective laser melting (SLM) manufacturing performance," *Journal of Materials Processing Technology,* vol. 212, pp. 355-364, 2// 2012.

[50] A. Santomaso, P. Lazzaro, and P. Canu, "Powder flowability and density ratios: the impact of granules packing," *Chemical Engineering Science,* vol. 58, pp. 2857-2874, 7// 2003.

[51] X. Zhao, J. Chen, X. Lin, and W. Huang, "Study on microstructure and mechanical properties of laser rapid forming Inconel 718," *Materials Science and Engineering A,* vol. 478, pp. 119-124, 2008.

[52] H. Qi, M. Azer, and A. Ritter, "Studies of Standard Heat Treatment Effects on Microstructure and Mechanical Properties of Laser Net Shape Manufactured INCONEL 718," *Metallurgical and Materials Transactions A,* vol. 40A, pp. 2410-2422, 2009.

[53] AP&C. (2014). *Designed for Additive Manufacturing*. Available: http://advancedpowders.com/our-plasma-atomized-powders/designed-for-additive-manufacturing/

[54] S. Zekovic, R. Dwivedi, and R. Kovacevic, "Numerical simulation and experimental investigation of gas–powder flow from radially symmetrical nozzles in laser-based direct metal deposition," *International Journal of Machine Tools and Manufacture,* vol. 47, pp. 112-123, 1// 2007.

[55] J. Karlsson, A. Snis, H. Engqvist, and J. Lausmaa, "Characterization and comparison of materials produced by Electron Beam Melting (EBM) of two different Ti–6Al–4V powder fractions," *Journal of Materials Processing Technology,* vol. 213, pp. 2109-2118, 12// 2013.

[56] H. Tan, F. Zhang, R. Wen, J. Chen, and W. Huang, "Experiment study of powder flow feed behavior of laser solid forming," *Optics and Lasers in Engineering,* vol. 50, pp. 391-398, 3// 2012.

[57] D. D. Gu, W. Meiners, K. Wissenbach, and R. Poprawe, "Laser additive manufacturing of metallic components: materials, processes and mechanisms," *International Materials Reviews,* vol. 57, pp. 133-64, 05/ 2012.

[58] S. Stecker, K. W. Lachenberg, H. Wang, and R. C. Salo, "Advanced Electron Beam Free Form Fabrication Methods & Technology," in *AWS Welding Show*, Atlanta, GA, 2006, pp. 35-46.
[59] V. I. Murav'ev, R. F. Krupskii, R. A. Fizulakov, and P. G. Demyshev, "Effect of the quality of filler wire on the formation of pores in welding of titanium alloys," *Welding International,* vol. 22, pp. 853-858, 2008.
[60] W. U. H. Syed, A. J. Pinkerton, and L. Li, "Combining wire and coaxial powder feeding in laser direct metal deposition for rapid prototyping," *Applied Surface Science,* vol. 252, pp. 4803-4808, 4/30/ 2006.
[61] A. F. H. Kaplan and J. Powell, "Spatter in laser welding," *Journal of Laser Applications,* vol. 23, pp. -, 2011.
[62] E. C. Santos, M. Shiomi, K. Osakada, and T. Laoui, "Rapid manufacturing of metal components by laser forming," *International Journal of Machine Tools and Manufacture,* vol. 46, pp. 1459-1468, 10// 2006.
[63] S. Li, G. Chen, S. Katayama, and Y. Zhang, "Relationship between spatter formation and dynamic molten pool during high-power deep-penetration laser welding," *Applied Surface Science,* vol. 303, pp. 481-488, 6/1/ 2014.
[64] T. R. Mahale, "Electron Beam Melting of Advanced Materials and Structures," Ph.D., North Carolina State University, 2009.
[65] C. Eschey, S. Lutzmann, and M. F. Zaeh, "Examination of the powder spreading effect in Electron Beam Melting (EBM)," in *Solid Freeform Fabrication Symposium*, Austin, TX, 2009, pp. 308-319.
[66] M. Kahnert, S. Lutzmann, and M. F. Zaeh, "Layer Formations in Electron Beam Sintering," in *Solid Freeform Fabrication Symposium*, Austin, TX, 2007.
[67] C. Korner, A. Bauereiss, and E. Attar, "Fundamental consolidation mechanisms during selective beam melting of powders," *Modelling Simul. Mater. Sci. Eng.,* vol. 21, p. 18, 2013.
[68] T. Vilaro, C. Colin, and J. D. Bartout, "As-Fabricated and Heat-Treated Microstructures of the Ti-6Al-4V Alloy Processed by Selective Laser Melting," *Metallurgical and Materials Transactions A,* vol. 42, pp. 3190-3199, 2011/10/01 2011.
[69] W. Frazier, "Metal Additive Manufacturing: A Review," *Journal of Materials Engineering and Performance,* pp. 1-12, 2014/04/08 2014.
[70] M. Svensson, "Ti6Al4V manufactured with Electron Beam Melting (EBM): Mechanical and Chemical Properties," in *Aeromat 2009*, Dayton, OH, 2009.
[71] P. A. Kobryn, E. H. Moore, and S. L. Semiatin, "The effect of laser power and traverse speed on microstructure, porosity, and build height in laser-deposited Ti-6Al-4V," *Scripta Materialia,* vol. 43, pp. 299-305, 7/28/ 2000.
[72] L. N. Carter, M. M. Attallah, and R. C. Reed, "Laser Powder Bed Fabrication of Nickel-Base Superalloys: Influence of Parameters; Characterisation, Quantification and Mitigation of Cracking," in *Superalloys 2012*, ed: John Wiley & Sons, Inc., 2012, pp. 577-586.
[73] K. Kempen, L. Thijs, B. Vrancken, S. Buls, J. Van Humbeeck, and J.-P. Kruth, "Producing, Crack-Free, High Density M2 HSS Parts by Selective Laser Melting: Pre-Heating the Baseplate," in *Solid Freeform Fabrication Symposium*, Austin, TX, 2013.
[74] A. Hussein, L. Hao, C. Yan, R. Everson, and P. Young, "Advanced lattice support structures for metal additive manufacturing," *Journal of Materials Processing Technology,* vol. 213, pp. 1019-1026, 7// 2013.
[75] J. P. Kruth, L. Froyen, J. Van Vaerenbergh, P. Mercelis, M. Rombouts, and B. Lauwers, "Selective laser melting of iron-based powder," *Journal of Materials Processing Technology,* vol. 149, pp. 616-622, 6/10/ 2004.
[76] M. F. Zäh and S. Lutzmann, "Modelling and simulation of electron beam melting," *Production Engineering,* vol. 4, pp. 15-23, 2010/02/01 2010.

[77] A. Bauereiß, T. Scharowsky, and C. Körner, "Defect generation and propagation mechanism during additive manufacturing by selective beam melting," *Journal of Materials Processing Technology,* vol. 214, pp. 2522-2528, 11// 2014.
[78] C. Körner, E. Attar, and P. Heinl, "Mesoscopic simulation of selective beam melting processes," *Journal of Materials Processing Technology,* vol. 211, pp. 978-987, 6/1/ 2011.
[79] A. Wu, M. M. LeBlanc, M. Kumar, G. F. Gallegos, D. W. Brown, and W. E. King, "Effect of Laser Scanning Pattern and Build Direction in Additive Manufacturing on Anisotropy, Porosity and Residual Stress," in *2014 TMS Annual Meeting & Exhibition*, San Diego, CA, 2014.
[80] P. Mercelis and J.-P. Kruth, "Residual stresses in selective laser sintering and selective laser melting," *Rapid Prototyping Journal,* vol. 12, pp. 254-265, 2006.
[81] T. Gnäupel-Herold, J. Slotwinski, and S. Moylan, "Neutron measurements of stresses in a test artifact produced by laser-based additive manufacturing," *AIP Conference Proceedings,* vol. 1581, pp. 1205-1212, 2014.
[82] P. Rangaswamy, T. M. Holden, R. B. Rogge, and M. L. Griffith, "Residual stresses in components formed by the laser-engineered net shaping (LENS&reg) process," *Journal of Strain Analysis for Engineering Design,* vol. 38, pp. 519-527, 2003.
[83] L. M. Sochalski-Kolbus, E. A. Payzant, P. A. Cornwell, T. R. Watkins, S. S. Babu, R. R. Dehoff*, et al.*, "Comparison of Residual Stresses in Inconel 718 Simple Parts Made by Electron Beam Melting and Direct Laser Metal Sintering," *Metallurgical and Materials Transactions A,* vol. 46, pp. 1419-1432, 2015/03/01 2015.
[84] C. A. Brice and W. H. Hofmeister, "Determination of bulk residual stresses in electron beam additive-manufactured aluminum," *Metallurgical and Materials Transactions A: Physical Metallurgy and Materials Science,* vol. 44, pp. 5147-5153, 2013.
[85] J. Ding, P. Colegrove, J. Mehnen, S. Ganguly, P. M. Sequeira Almeida, F. Wang*, et al.*, "Thermo-mechanical analysis of Wire and Arc Additive Layer Manufacturing process on large multi-layer parts," *Computational Materials Science,* vol. 50, pp. 3315-3322, 12// 2011.
[86] S. Suresh and A. E. Giannakopoulos, "A new method for estimating residual stresses by instrumented sharp indentation," *Acta Materialia,* vol. 46, pp. 5755-5767, 10/9/ 1998.
[87] B. Song, S. Dong, Q. Liu, H. Liao, and C. Coddet, "Vacuum heat treatment of iron parts produced by selective laser melting: Microstructure, residual stress and tensile behavior," *Materials & Design,* vol. 54, pp. 727-733, 2// 2014.
[88] M. B. Prime, "Cross-Sectional Mapping of Residual Stresses by Measuring the Surface Contour After a Cut," 2001, pp. 162-168.
[89] T. Watkins, H. Bilheux, A. Ke, A. Payzant, R. Dehoff, C. Duty*, et al.*, "Neutron Characterization for Additive Manufacturing," *Advanced Materials & Processes,* vol. 171, pp. 23-27, 2013.
[90] R. J. Moat, A. J. Pinkerton, L. Li, P. J. Withers, and M. Preuss, "Residual stresses in laser direct metal deposited Waspaloy," *Materials Science and Engineering: A,* vol. 528, pp. 2288-2298, 3/15/ 2011.
[91] M. Zaeh and G. Branner, "Investigations on residual stresses and deformations in selective laser melting," *Production Engineering,* vol. 4, pp. 35-45, 2010/02/01 2010.
[92] P. Prabhakar, W. J. Sames, R. Smith, R. Dehoff, and S. S. Babu, "Computational Modeling of Residual Stress Formation during the Electron Beam Melting Process for Inconel 718," *Additive Manufacturing,* 2015 (submitted).
[93] S. S. Al-Bermani, " An investigation into microstructure and microstructural control of additive layer manufactured Ti-6Al-4V by electron beam melting," Ph.D., University of Sheffield, Sheffield, UK, 2011.

[94] H. Gu, H. Gong, D. Pal, K. Rafi, T. Starr, and B. Stucker, "Influences of Energy Density on Porosity and Microstructure of Selective Laser Melted 17-4PH Stainless Steel," in *Solid Freeform Fabrication Symposium*, Austin, TX, 2013.

[95] J. D. Hunt, "Steady state columnar and equiaxed growth of dendrites and eutectic," *Materials Science and Engineering,* vol. 65, pp. 75-83, 7// 1984.

[96] L. Nastac, J. J. Valencia, M. L. Tims, and F. R. Dax, "Advances in the Solidification on IN718 and RS5 Alloys," in *Superalloys 718, 625, 706, and Various Derivatives*, 2001, pp. 103-112.

[97] C. Körner, H. Helmer, A. Bauereiß, and R. F. Singer, "Tailoring the grain structure of IN718 during selective electron beam melting," in *EUROSUPERALLOYS*, 2014.

[98] J. Gockel and J. Beuth, "Understanding Ti-6Al-4V Microstructure Control in Additive Manufacturing via Process Maps," in *Solid Freeform Fabrication Symposium*, Austin, TX, 2013.

[99] N. Shen and K. Chou, *Thermal Modeling of Electron Beam Additive Manufacturing Process: Powder Sintering Effects*, 2012.

[100] L. N. Carter, C. Martin, P. J. Withers, and M. M. Attallah, "The influence of the laser scan strategy on grain structure and cracking behaviour in SLM powder-bed fabricated nickel superalloy," *Journal of Alloys and Compounds,* vol. 615, pp. 338-347, 12/5/ 2014.

[101] K. Zeng, D. Pal, and B. Stucker, "A review of thermal analysis methods in Laser Sintering and Selective Laser Melting," in *Solid Freeform Fabrication Symposium*, Austin, TX, 2012.

[102] K. T. Makiewicz, "Development of Simultaneous Transformation Kinetics Microstructure Model with Application to Laser Metal Deposited Ti-6Al-4V and Alloy 718," ed: Ohio State University, 2013.

[103] W. J. Sames, K. A. Unocic, R. R. Dehoff, T. Lolla, and S. S. Babu, "Thermal Effects on Microstructural Heterogeneity of Inconel 718 Materials Fabricated by Electron Beam Melting " *Journal of Materials Research,* vol. 29, pp. 1920-1930, 2014.

[104] E. Brandl and D. Greitemeier, "Microstructure of additive layer manufactured Ti–6Al–4V after exceptional post heat treatments," *Materials Letters,* vol. 81, pp. 84-87, 8/15/ 2012.

[105] E. Brandl, A. Schoberth, and C. Leyens, "Morphology, microstructure, and hardness of titanium (Ti-6Al-4V) blocks deposited by wire-feed additive layer manufacturing (ALM)," *Materials Science and Engineering: A,* vol. 532, pp. 295-307, 1/15/ 2012.

[106] L. Facchini, E. Magalini, P. Robotti, and A. Molinari, "Microstructure and mechanical properties of Ti-6Al-4V produced by electron beam melting of pre-alloyed powders," *Rapid Prototyping Journal,* vol. 15, pp. 171-178, 2009.

[107] L. E. Murr, E. Martinez, S. M. Gaytan, D. A. Ramirez, B. I. Machado, P. W. Shindo*, et al.*, "Microstructural Architecture, Microstructures, and Mechanical Properties for a Nickel-Base Superalloy Fabricated by Electron Beam Melting," *Metallurgical and Materials Transactions A,* vol. 42, pp. 3491-3508, 2011/11/01 2011.

[108] K. A. Unocic, L. M. Kolbus, R. R. Dehoff, S. N. Dryepondt, and B. A. Pint, "High-Temperature Performance of N07718 Processed by Additive Manufacturing," in *NACE Corrosion 2014*, San Antonio, TX, 2014.

[109] P. L. Blackwell, "The mechanical and microstructural characteristics of laser-deposited IN718," *Journal of Materials Processing Technology,* vol. 170, pp. 240-246, 12/14/ 2005.

[110] C. Bampton, J. Wooten, and B. Hayes, "Additive Manufactuing by Electron Beam Melting (EBM) of Alloy 718," in *Material Science & Technology*, Montreal, Canada, 2013.

[111] A. Strondl, M. Palm, J. Gnauk, and G. Frommeyer, "Microstructure and mechanical properties of nickel based superalloy IN718 produced by rapid prototyping with electron beam melting (EBM)," *Materials Science and Technology,* vol. 27, pp. 876-883, 2011.

[112] K. N. Amato, S. M. Gaytan, L. E. Murr, E. Martinez, P. W. Shindo, J. Hernandez*, et al.*, "Microstructures and mechanical behavior of Inconel 718 fabricated by selective laser melting," *Acta Materiala,* vol. 60, pp. 2229-2239, 2012.
[113] E. Łyczkowska, P. Szymczyk, B. Dybała, and E. Chlebus, "Chemical polishing of scaffolds made of Ti–6Al–7Nb alloy by additive manufacturing," *Archives of Civil and Mechanical Engineering*.
[114] R. Dehoff, C. Duty, W. Peter, Y. Yamamoto, C. Wei, C. Blue*, et al.*, "Case Study: Additive Manufacturing of Aerospace Brackets," *Advanced Materials & Processes,* vol. 171, pp. 19-22, 2013.
[115] A. Lasemi, D. Xue, and P. Gu, "Recent development in CNC machining of freeform surfaces: A state-of-the-art review," *Computer-Aided Design,* vol. 42, pp. 641-654, 7// 2010.
[116] K. P. Karunakaran, S. Suryakumar, V. Pushpa, and S. Akula, "Low cost integration of additive and subtractive processes for hybrid layered manufacturing," *Robotics and Computer-Integrated Manufacturing,* vol. 26, pp. 490-499, 10// 2010.
[117] J. Jones, P. McNutt, R. Tosi, C. Perry, and D. Wimpenny, "Remanufacture of turbine blades by laser cladding, machining and in-process scanning in a single machine," in *Solid Freeform Fabrication Symposium*, Austin, TX, 2012.
[118] B. Vrancken, L. Thijs, J. P. Kruth, and J. Van Humbeeck, "Microstructure and mechanical properties of a novel β titanium metallic composite by selective laser melting," *Acta Materialia,* vol. 68, pp. 150-158, 4/15/ 2014.
[119] J. Landin, "Unique breakthrough in bulk metallic glass manufacturing," ed: Mid Sweden University, 2012.
[120] C. D. Prest, J. C. Poole, J. Stevick, T. A. Waniuk, and Q. T. Pham, "Layer-by-layer construction with bulk metallic glasses," US 20130309121 A1, 2012.
[121] I. Kunce, M. Polanski, and J. Bystrzycki, "Microstructure and hydrogen storage properties of a TiZrNbMoV high entropy alloy synthesized using Laser Engineered Net Shaping (LENS)," *International Journal of Hydrogen Energy,* vol. 39, pp. 9904-9910, 6/15/ 2014.
[122] M. Polanski, M. Kwiatkowska, I. Kunce, and J. Bystrzycki, "Combinatorial synthesis of alloy libraries with a progressive composition gradient using laser engineered net shaping (LENS): Hydrogen storage alloys," *International Journal of Hydrogen Energy,* vol. 38, pp. 12159-12171, 9/10/ 2013.
[123] F. Niu, D. Wu, S. Zhou, and G. Ma, "Power prediction for laser engineered net shaping of Al2O3 ceramic parts," *Journal of the European Ceramic Society,* vol. 34, pp. 3811-3817, 12// 2014.
[124] V. K. Balla, S. Bose, and A. Bandyopadhyay, "Microstructure and wear properties of laser deposited WC–12%Co composites," *Materials Science and Engineering: A,* vol. 527, pp. 6677-6682, 9/25/ 2010.
[125] T. Horn, "Material Development for Electron Beam Melting," ed: NC State University, 2013.
[126] O. Grong, *Metallurgical Modeling of Welding*, 2nd Edition ed.: The Institute of Materials, 1997.
[127] S. A. David and J. M. Vitek, "Correlation between solidification parameters and weld microstructures," *International Materials Reviews,* vol. 34, pp. 213-245, 1989.
[128] S. S. Al-Bermani, M. L. Blackmore, W. Zhang, and I. Todd, "The Origin of Microstructural Diversity, Texture, and Mechanical Properties in Electron Beam Melted Ti-6Al-4V," *Metallurgical and Materials Transactions A,* vol. 41A, pp. 3422-3434, 2010.
[129] P. Edwards and M. Ramulu, "Fatigue performance evaluation of selective laser melted Ti–6Al–4V," *Materials Science and Engineering: A,* vol. 598, pp. 327-337, 3/26/ 2014.
[130] J. Yu, M. Rombouts, G. Maes, and F. Motmans, "Material Properties of Ti6Al4 V Parts Produced by Laser Metal Deposition," *Physics Procedia,* vol. 39, pp. 416-424, // 2012.

[131] E. Amsterdam and G. A. Kool, "High Cycle Fatigue of Laser Beam Deposited Ti-6Al-4V and Inconel 718," in *ICAF 2009, Bridging the Gap between Theory and Operational Practice*, M. J. Bos, Ed., ed: Springer Netherlands, 2009, pp. 1261-1274.
[132] Z. Wang, K. Guan, M. Gao, X. Li, X. Chen, and X. Zeng, "The microstructure and mechanical properties of deposited-IN718 by selective laser melting," *Journal of Alloys and Compounds,* vol. 513, pp. 518-523, 2012.
[133] L. P. Parimi, M. M. Attallah, J. C. Gebelin, and R. C. Reed, "Direct Laser Fabrication of Inconel 718," in *Superalloys 2012: 12th International Symposium on Superalloys*, 2012, pp. 511-519.
[134] A. A. Antonysamy, J. Meyer, and P. B. Prangnell, "Effect of build geometry on the β-grain structure and texture in additive manufacture of Ti6Al4V by selective electron beam melting," *Materials Characterization,* vol. 84, pp. 153-168, 10// 2013.
[135] L. Thijs, K. Kempen, J.-P. Kruth, and J. Van Humbeeck, "Fine-structured aluminium products with controllable texture by selective laser melting of pre-alloyed AlSi10Mg powder," *Acta Materialia,* vol. 61, pp. 1809-1819, 3// 2013.
[136] Y. Tian, D. McAllister, H. Colijn, M. Mills, D. Farson, M. Nordin*, et al.*, "Rationalization of Microstructure Heterogeneity in INCONEL 718 Builds Made by the Direct Laser Additive Manufacturing Process," *Metallurgical and Materials Transactions A,* vol. 45, pp. 4470-4483, 2014/09/01 2014.
[137] J. Mireles, C. Terrazas, F. Medina, and R. Wicker, "Automatic Feedback Control in Electron Beam Melting Using Infrared Tomography," in *Solid Freefrom Fabrication Symposium*, Austin, TX, 2013.
[138] L. Thijs, M. L. Montero Sistiaga, R. Wauthle, Q. Xie, J.-P. Kruth, and J. Van Humbeeck, "Strong morphological and crystallographic texture and resulting yield strength anisotropy in selective laser melted tantalum," *Acta Materialia,* vol. 61, pp. 4657-4668, 7// 2013.
[139] R. R. Dehoff, M. M. Kirka, F. A. List, K. A. Unocic, and W. J. Sames, "Crystallographic Texture Engineering Through Novel Melt Strategies via Electron Beam Processing: Inconel 718," *Materials Science & Technology,* 2014 (Submitted).
[140] H. E. Helmer, C. Körner, and R. F. Singer, "Additive manufacturing of nickel-based superalloy Inconel 718 by selective electron beam melting: Processing window and microstructure," *Journal of Materials Research,* vol. 29, pp. 1987-1996, 2014.
[141] S. Mitzner, S. Liu, M. Domack, and R. Hafley, "Grain Refinement of Freeform Fabricated Ti-6Al-4V Alloy Using Beam/Arc Modulation," in *Solid Freeform Fabrication Symposium*, Austin, TX, 2012.
[142] R. R. Dehoff, M. M. Kirka, W. J. Sames, H. Bilheux, A. S. Tremsin, L. E. Lowe*, et al.*, "Site-Specific Control of Crystallographic Grain Orientation Through Electron Beam Additive Manufacturing," *Materials Science & Technology,* 2014 (submitted).
[143] D. A. Ramirez, L. E. Murr, E. Martinez, D. H. Hernandez, J. L. Martinez, B. I. Machado*, et al.*, "Novel precipitate–microstructural architecture developed in the fabrication of solid copper components by additive manufacturing using electron beam melting," *Acta Materialia,* vol. 59, pp. 4088-4099, 6// 2011.
[144] L. Thijs, F. Verhaeghe, T. Craeghs, J. V. Humbeeck, and J.-P. Kruth, "A study of the microstructural evolution during selective laser melting of Ti–6Al–4V," *Acta Materialia,* vol. 58, pp. 3303-3312, 5// 2010.
[145] J. F. Rudy and E. J. Rupert, "EFFECTS OF POROSITY ON MECHANICAL PROPERTIES OF ALUMINUM WELDS," vol. 49, pp. 322s-336s, 1970.
[146] R. F. Ashton, R. P. Wesley, and C. R. Dixon, "The Effect of Porosity on 5086-H116 Aluminum Alloy Welds," *Welding Journal,* pp. 95-98, 1975.
[147] J. E. Northwood, "Improving Turbine Blade Performance by Solidification Control," *Metallurgia,* vol. 46, pp. 437-439, 441, 442, 2011-11-10 1979.

[148] N. Hrabe and T. Quinn, "Effects of processing on microstructure and mechanical properties of a titanium alloy (Ti–6Al–4V) fabricated using electron beam melting (EBM), Part 2: Energy input, orientation, and location," *Materials Science and Engineering: A,* vol. 573, pp. 271-277, 6/20/ 2013.
[149] A. International, "Standard Specification for Additive Manufacturing Titanium-6 Aluminum-4 Vanadium ELI (Extra Low Interstitial) with Powder Bed Fusion," ed, 2014.
[150] A. International, "Standard Specfication for Additive Manufacturing Nickel Alloy (UNS N07718) with Powder Bed Fusion," ed: ASTM International, 2014.
[151] A. International, "Standard Specification for Additive Manufacturing Nickel Alloy (UNS N06625) with Powder Bed Fusion," ed: ASTM International, 2014.
[152] N. Hrabe, R. Kircher, and T. Quinn, "Effects of Processing on Microstructure and Mechanical Properties of Ti-6Al-4V Fabricated Using Electron Beam Melting (EBM): Orientation and Location," in *Solid Freefrom Fabrication Symposium*, Austin, TX, 2012.
[153] N. Hrabe and T. Quinn, "Effects of processing on microstructure and mechanical properties of a titanium alloy (Ti–6Al–4V) fabricated using electron beam melting (EBM), part 1: Distance from build plate and part size," *Materials Science and Engineering: A,* vol. 573, pp. 264-270, 6/20/ 2013.
[154] P. A. Kobryn and S. L. Semiatin, "Mechanical Properties of Laser-Deposited Ti-6Al-4V," in *Solid Freeform Fabrication Proceedings*, ed. Austin, TX, 2001.
[155] D. Pal, N. Patil, and B. Stucker, "Prediction of mechanical properties of Electron Beam Melted Ti6Al4V parts using dislocation density based crystal plasticity framework," in *Solid Freeform Fabrication Symposium*, Austin, TX, 2012.
[156] H. Brodin, O. Andersson, and S. Johansson, "Mechanical testing of a selective laser melted superalloy," in *13th International Conference on Fracture*, Beijing, China, 2013.
[157] C. E. Duty, D. L. Jean, and W. J. Lackey, "Design of a laser CVD rapid prototyping system," *Ceramic Engineering and Science Proceedings,* vol. 20, pp. 347-354, 1999.
[158] F. T. Wallenberger, "Rapid Prototyping Directly from the Vapor Phase," *Science,* vol. 267, pp. 1274-1275, 1995.
[159] A. Sova, S. Grigoriev, A. Okunkova, and I. Smurov, "Potential of cold gas dynamic spray as additive manufacturing technology," *The International Journal of Advanced Manufacturing Technology,* vol. 69, pp. 2269-2278, 2013/12/01 2013.
[160] E. Irissou, J.-G. Legoux, A. Ryabinin, B. Jodoin, and C. Moreau, "Review on Cold Spray Process and Technology: Part I—Intellectual Property," *Journal of Thermal Spray Technology,* vol. 17, pp. 495-516, 2008/12/01 2008.
[161] (2013, Cold Spray and GE Technology. Available: http://www.geglobalresearch.com/blog/cold-spray-ge-technology
[162] D. Srinivasan and R. Amuthan, "Modified T-T-T Behaviour of IN626 Cold Sprayed Coatings," in *Superalloy 718 and Derivatives*, Pittsburgh, PA, 2014, pp. 433-445.
[163] E. J. Vega, M. G. Cabezas, B. N. Muñoz-Sánchez, J. M. Montanero, and A. M. Gañán-Calvo, "A novel technique to produce metallic microdrops for additive manufacturing," *International Journal of Advanced Manufacturing Technology,* vol. 70, pp. 1395-1402, 2014.
[164] C. Ladd, J.-H. So, J. Muth, and M. D. Dickey, "3D Printing of Free Standing Liquid Metal Microstructures," *Advanced Materials,* vol. 25, pp. 5081-5085, 2013.
[165] S. Palanivel and R. S. Mishra, "Friction Stir Additive Manufacturing for High Structural Performance Through Microstructural Control," in *RAPID 2014*, Detroit, MI, 2014.
[166] H. J. Herfurth, "Multi-Beam Laser Additive Manufacturing (MB-LAM)," Fraunhofer USA, 2013 CTMA Annual Partners Meeting2013.

[167] B. Narayanan and M. Kottman, "Microstructural Development of Inconel 625 Deposited via Laser Hot Wire," in *RAPID 2014*, Detroit, MI, 2014.
[168] Sciaky. (2014). *Additive Manufacturing*. Available: http://www.sciaky.com/additive_manufacturing.html
[169] L. J. Love, V. Kunc, O. Rios, C. E. Duty, A. M. Elliott, B. K. Post*, et al.*, "The importance of carbon fiber to polymer additive manufacturing," *Journal of Materials Research,* vol. 29, pp. 1893-1898, 2014.
[170] C. Holshouser, C. Newell, S. Palas, L. J. Love, V. Kunc, R. Lind*, et al.*, "Out of Bounds Additive Manufacturing," *Advanced Materials & Processes,* vol. 171, pp. 15-17, 2013.
[171] J. M. Pearce, "Building Research Equipment with Free, Open-Source Hardware," *Science,* vol. 337, pp. 1303-1304, September 14, 2012 2012.
[172] G. C. Anzalone, Z. Chenlong, B. Wijnen, P. G. Sanders, and J. M. Pearce, "A Low-Cost Open-Source Metal 3-D Printer," *IEEE Access,* vol. 1, pp. 803-10, / 2013.
[173] T. Scharowsky, F. Osmanlic, R. F. Singer, and C. Körner, "Melt pool dynamics during selective electron beam melting," *Applied physics. A, Materials science & processing,* vol. 114, pp. 1303-1307, 2014.
[174] E. Rodriguez, "Development of a thermal imaging feedback control system in electron beam melting," ed: ETD Collection for University of Texas, El Paso., 2013.
[175] M. Pavlov, M. Doubenskaia, and I. Smurov, "Pyrometric analysis of thermal processes in SLM technology," *Physics Procedia,* vol. 5, Part B, pp. 523-531, // 2010.
[176] S. Moylan, E. Whitenton, B. Lane, and J. Slotwinski, "Infrared thermography for laser-based powder bed fusion additive manufacturing processes," *AIP Conference Proceedings,* vol. 1581, pp. 1191-1196, 2014.
[177] R. B. Dinwiddie, R. R. Dehoff, P. D. Lloyd, L. E. Lowe, and J. B. Ulrich, "Thermographic In-Situ Process Monitoring of the Electron Beam Melting Technology used in Additive Manufacturing," in *Thermosense: Thermal Infrared Applications XXXV*, Baltimore, Maryland, 2013.
[178] J. A. Slotwinski and E. J. Garboczi, "Porosity of additive manufacturing parts for process monitoring," *AIP conference proceedings,* vol. 1581, pp. 1197-1204, 2014.
[179] A. B. Spierings, M. Schneider, and R. Eggenberger, "Comparison of density measurement techniques for additive manufactured metallic parts," *Rapid Prototyping Journal,* vol. 17, pp. 380-386, 2011.
[180] "Building the Future: Assessing 3D Printing's Opportunities and Challenges," Lux Research2013.
[181] A. R. Thryft. (2013, Report: 3D Printing Will (Eventually) Transform Manufacturing. Available: http://www.designnews.com/author.asp?doc_id=262205
[182] E. Atzeni and A. Salmi, "Economics of additive manufacturing for end-usable metal parts," *The International Journal of Advanced Manufacturing Technology,* vol. 62, pp. 1147-1155, 2012/10/01 2012.
[183] A. Koptyug, L.-E. Rannar, M. Backstrom, S. F. Franzen, and P. Derand, "Additive Manufacturing Technology Applications Targeting Practical Surgery," *International Journal of Life Science and Medical Research,* vol. 3, pp. 15-24, 2013.
[184] Z. Bi, M. P. Paranthaman, P. A. Menchhofer, R. R. Dehoff, C. A. Bridges, M. Chi*, et al.*, "Self-organized amorphous TiO2 nanotube arrays on porous Ti foam for rechargeable lithium and sodium ion batteries," *Journal of Power Sources,* vol. 222, pp. 461-466, 1/15/ 2013.
[185] L. J. Love, B. Richardson, R. Lind, R. R. Dehoff, B. Peter, L. Lowe*, et al.*, "Freeform Fluidics," in *Mechanical Engineering - CIME*, 2013.
[186] T. Catts. (2013, GE Turns to 3D Printing for Plane Parts. *Business Week*. Available: http://www.businessweek.com/articles/2013-11-27/general-electric-turns-to-3d-printers-for-plane-parts

[187] 3ders. (2014, GE reveals breakthrough in 3D printing super light-weight metal blades for jet engine. Available: http://www.3ders.org/articles/20140818-ge-reveals-breakthrough-in-3d-printing-super-light-weight-metal-blades-for-jet-engine.html
[188] M. Gäumann, C. Bezençon, P. Canalis, and W. Kurz, "Single-crystal laser deposition of superalloys: processing–microstructure maps," *Acta Materialia,* vol. 49, pp. 1051-1062, 4/2/ 2001.
[189] L. Rickenbacher, A. Spierings, and K. Wegener, "An integrated cost-model for selective laser melting (SLM)," *Rapid Prototyping Journal,* vol. 19, pp. 208-214, 2013.
[190] S. Merkt, C. Hinke, H. Schleifenbaum, and H. Voswinckel, "Integrative Technology Evaluation Model (ITEM) for Selective Laser Melting (SLM)," *Advanced Materials Research,* vol. 337, pp. 274-280, 2011.
[191] S. S. Babu, L. J. Love, W. H. Peter, and R. R. Dehoff, "Additive Manufacturing: The Future of Manufacturing in a Flat World: Challenges and Path Forward," 2014 (in progress).
[192] D. W. Rosen. (2014, Additive Manufacturing Process Overview. Available: http://pages.wilsoncenter.org/rs/woodrowwilson/images/AMprocesses_DRosen1014_site.pdf
[193] K. Maxey. (2014, ExOne M-Flex Production Metal 3D Printer. Available: http://www.engineering.com/3DPrinting/3DPrintingArticles/ArticleID/7618/ExOne-M-Flex-Production-Metal-3D-Printer.aspx
[194] S. Rengers. (2012, Electron Beam Melting [EBM] vs. Direct Metal Laser Sintering [DMLS]. Available: http://www.midwestsampe.org/content/files/events/dpmworkshop2012/Rengers%20EBM%20vs%20DMLS.pdf
[195] M. Dahlbom. (2013, Arcam AB, A Very Promising 3D Printer Company. *Seeking Alpha*. Available: http://seekingalpha.com/article/1316271-arcam-ab-a-very-promising-3d-printer-company
[196] G. Nelson. (2013, NAMII Open House Shows Potential of 3-D Printing. *The Business Journal*. Available: http://businessjournaldaily.com/awards-events/namii-open-house-shows-potential-3-d-printing-2013-10-4
[197] L. P. Vigna, "Additive Manufacturing - 3D Printing Emerging Technologies," ed, 2012.
[198] C. G. McCracken, C. Motchenbacher, and D. P. Barbis, "Review of Titanium-Powder-Production Methods," *International Journal of Powder Metallurgy,* vol. 46, pp. 19-26, 2010.
[199] X. Wu, "A review of laser fabrication of metallic engineering components and of materials," *Materials Science and Technology,* vol. 23, pp. 631-640, 2007.
[200] (2014, 2014/05/03) Additive Manufacturing: Heavy Metal. *The Economist*.
[201] NIST, "Measurement Science Roadmap for Metal-Based Additive Manufacturing," National Institute for Standards and Technology 2013.
[202] L.-E. Andersson and M. Larsson, "Device and arrangment for producing a three-dimensional object," US Patent US 7537722 B2, 2000.
[203] F. P. Jeantette, D. M. Keicher, J. A. Romero, and L. P. Schanwald, "Method and system for producing complex-shape objects," US 6046426 A, 1996.
[204] Arcam-AB. (2015, EBM Hardware. Available: http://www.arcam.com/technology/electron-beam-melting/hardware/
[205] custompartnet.com. (2015, Direct Metal Laser Sintering. Available: http://www.custompartnet.com/wu/direct-metal-laser-sintering
[206] custompartnet.com. (2015, 3D Printing. Available: http://www.custompartnet.com/wu/3d-printing
[207] K. F. Graff, M. Short, and M. Norfolk, "Very High Power Ultrasonic Additive Manufacturing (VHP UAM) For Advanced Materials," in *Solid Freeform Fabrication Symposium*, Austin, TX, 2010.

[208] D. Dye, O. Hunziker, and R. C. Reed, "Numerical analysis of the weldability of superalloys," *Acta Materialia,* vol. 49, pp. 683-697, 2/23/ 2001.
[209] "Nickel-Base Superalloys," in *Heat Treater's Guide: Practices and Procedures for Nonferrous Alloys*, ed: ASM International, 1996, pp. 41-58.
[210] M. K. Mallik, C. S. Rao, and V. V. S. Kesava rao, "Effect of Heat Treatment on Hardness of Co-Cr-Mo Alloy Deposited With Laser Engineered Net Shaping," *Procedia Engineering,* vol. 97, pp. 1718-1723, // 2014.
[211] S.-H. Sun, Y. Koizumi, S. Kurosu, Y.-P. Li, H. Matsumoto, and A. Chiba, "Build direction dependence of microstructure and high-temperature tensile property of Co–Cr–Mo alloy fabricated by electron beam melting," *Acta Materialia,* vol. 64, pp. 154-168, 2// 2014.
[212] E. Martinez, L. Murr, J. Hernandez, X. Pan, K. Amato, P. Frigola*, et al.*, "Microstructures of Niobium Components Fabricated by Electron Beam Melting," *Metallography, Microstructure, and Analysis,* vol. 2, pp. 183-189, 2013/06/01 2013.
[213] M. Terner, S. Biamino, P. Epicoco, A. Penna, O. Hedin, S. Sabbadini*, et al.*, "Electron Beam Melting of High Niobium Containing TiAl Alloy: Feasibility Investigation," *steel research international,* vol. 83, pp. 943-949, 2012.
[214] D. Q. Zhang, Z. H. Liu, Q. Z. Cai, J. H. Liu, and C. K. Chua, "Influence of Ni content on microstructure of W–Ni alloy produced by selective laser melting," *International Journal of Refractory Metals and Hard Materials,* vol. 45, pp. 15-22, 7// 2014.
[215] Fabrisonic. (2015). *New Materials Engineered for Your Needs*. Available: http://fabrisonic.com/materials/
[216] "ExOne adds new metal 3D printing material," *Metal Powder Report,* vol. 68, p. 36, 9// 2013.
[217] D.-T. Chou, D. Wells, D. Hong, B. Lee, H. Kuhn, and P. N. Kumta, "Novel processing of iron–manganese alloy-based biomaterials by inkjet 3-D printing," *Acta Biomaterialia,* vol. 9, pp. 8593-8603, 11// 2013.
[218] S. M. Gaytan, M. A. Cadena, H. Karim, D. Delfin, Y. Lin, D. Espalin*, et al.*, "Fabrication of barium titanate by binder jetting additive manufacturing technology," *Ceramics International*.
[219] H. K. Rafi, T. Starr, and B. Stucker, "A comparison of the tensile, fatigue, and fracture behavior of Ti–6Al–4V and 15-5 PH stainless steel parts made by selective laser melting," *The International Journal of Advanced Manufacturing Technology,* vol. 69, pp. 1299-1309, 2013/11/01 2013.
[220] G. K. Lewis and E. Schlienger, "Practical considerations and capabilities for laser assisted direct metal deposition," *Materials & Design,* vol. 21, pp. 417-423, 8/1/ 2000.
[221] M. Bauccio, *ASM Metals Reference Book, Third Edition*. Materials Park, OH: ASM International, 1993.
[222] E. Rodriguez, F. Medina, D. Espalin, C. Terrazas, D. Muse, C. Henry*, et al.*, "Integration of a Thermal Imaging Feedback Control System in Electron Beam Melting," in *Solid Freeform Fabrication Symposium*, Austin, TX, 2012.
[223] ExOne. (2013, ExOne-Rapid Growth of Additive Manufacturing (AM) Disrupts Traditional Manufacturing Process. Available: http://additivemanufacturing.com/2013/06/06/exone-rapid-growth-of-additive-manufacturing-am-disrupts-traditional-manufacturing-process/
[224] RepRapPro. (2014, RepRapPro Tricolour Mendel specifications. Available: https://reprappro.com/shop/reprap-kits/tricolour-mendel/
[225] Renishaw. (2015). *About AM250*. Available: http://www.renishaw.com/en/am250-laser-melting-metal-3d-printing-machine--15253

Figures

Table 1. Original patents for the various classifications of metal AM.

Process	Patent Number	Patent Priority Date	Inventor	Original Associated Corporation
SLS [7]	WO1988002677 A2	1986	Carl Deckard	University of Texas
"3D Printing" [8] (binder deposition)	US5204055 A	1989	Cima et al.	MIT
EBM [202]	US 7537722 B2	2000	Ralf Larson	Arcam AB
LENS [203]	US 6046426 A	1996	Jeantette et al.	Sandia Corporation
UAM [12]	US6519500	1999	Dawn White	Solidica

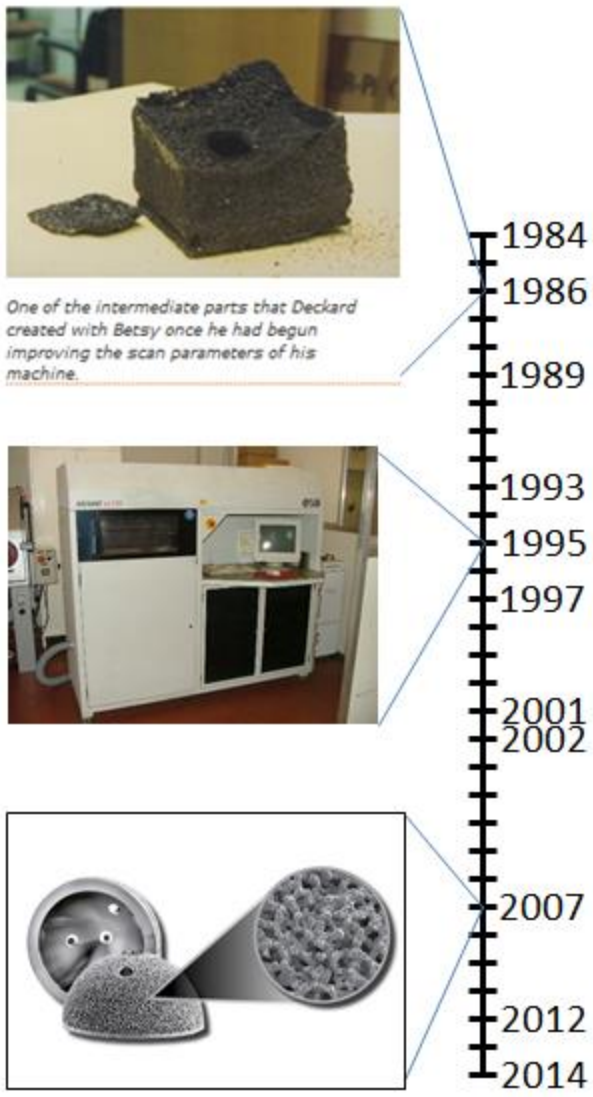

Figure 1. Timeline of significant events in metal AM development.

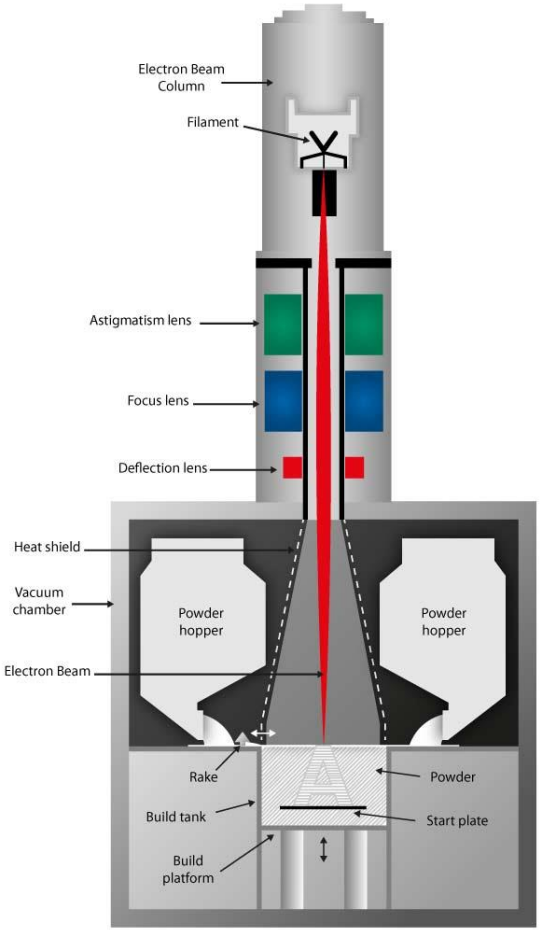

Figure 2. EBM system schematic. [204]

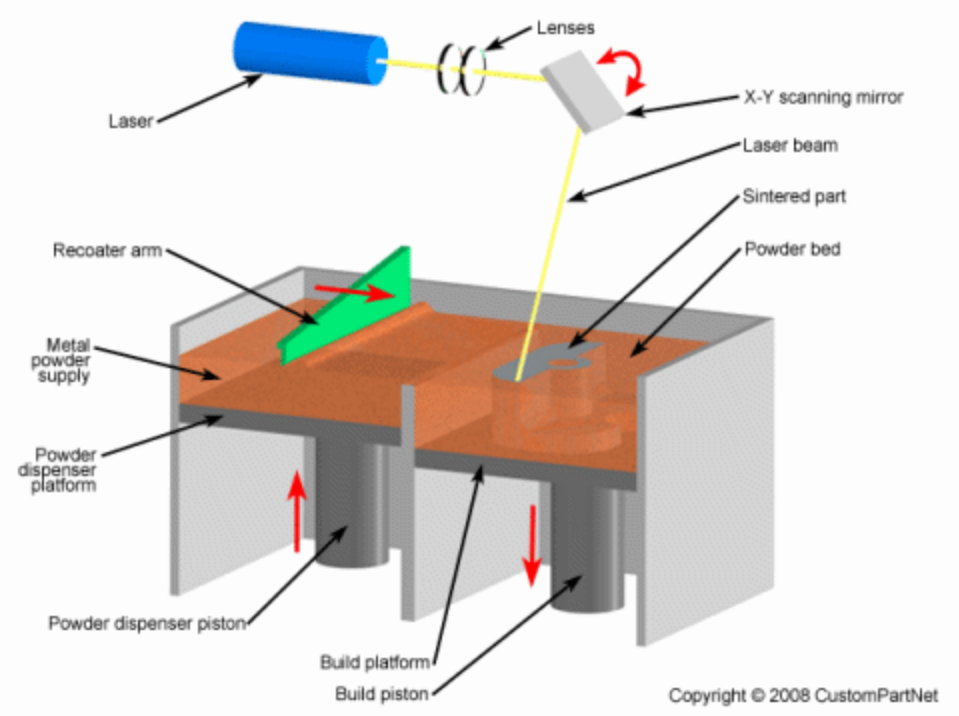

Figure 3. LM system schematic [205]

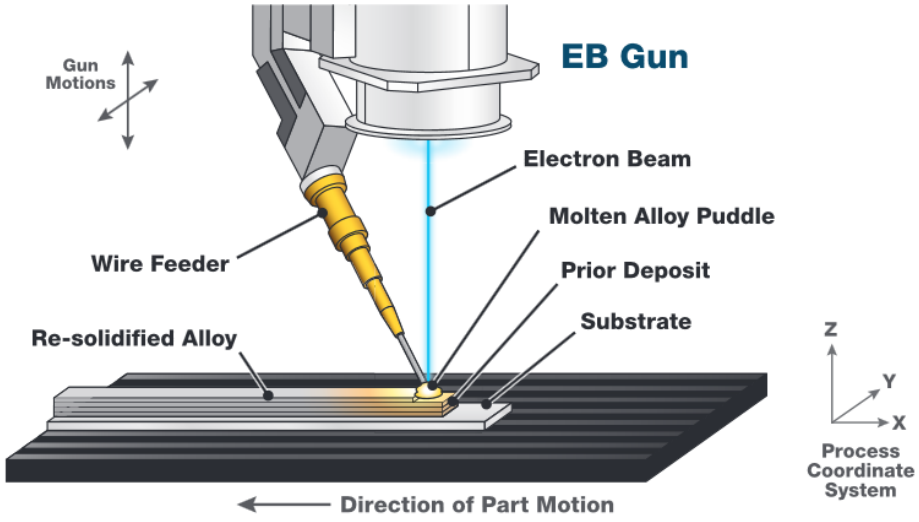

Figure 4. Electron beam, wire-fed DED system. [168]

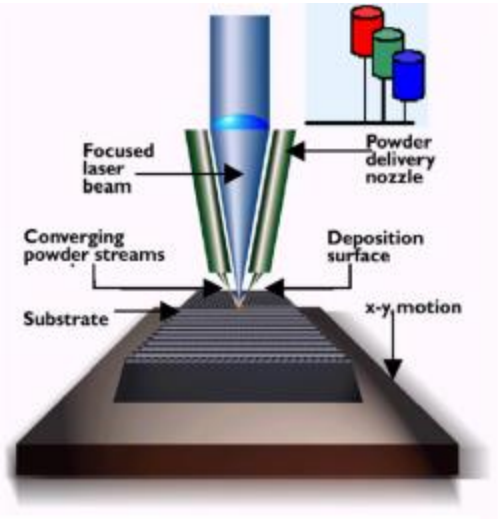

Figure 5. Laser, powder-fed DED system (LENS). [18]

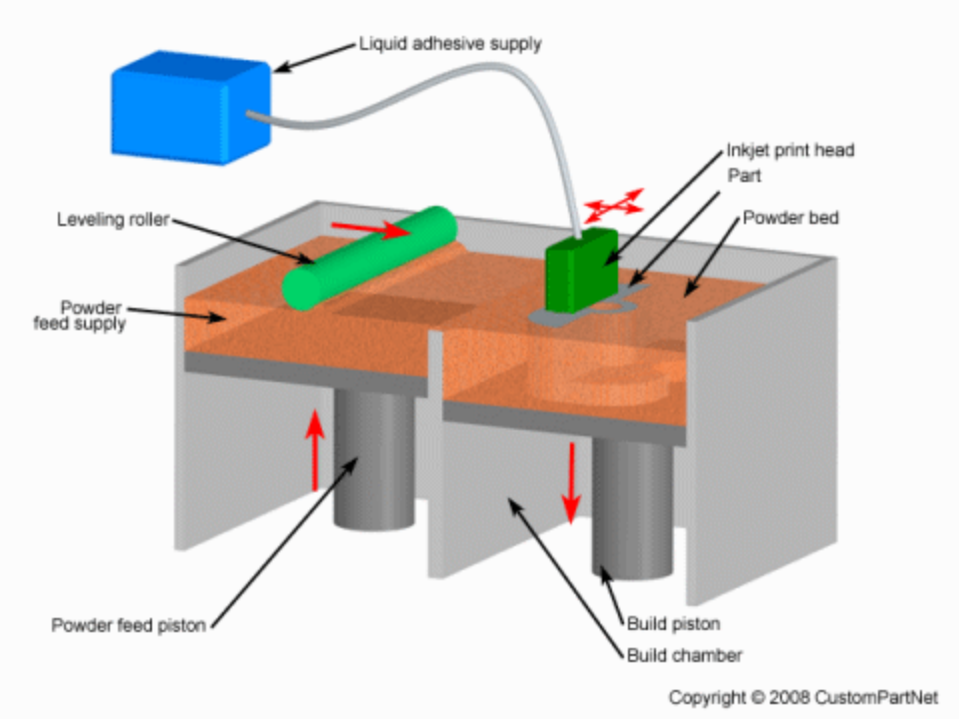

Figure 6. BJ process schematic. [206]

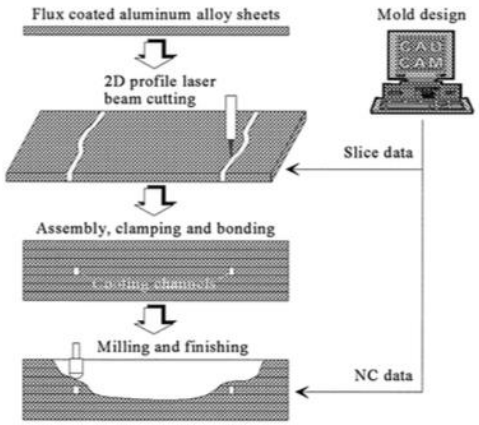

Figure 7. Schematic illustration of SL process to make injection or metal forming molds (we need permission to use this diagram) [31]

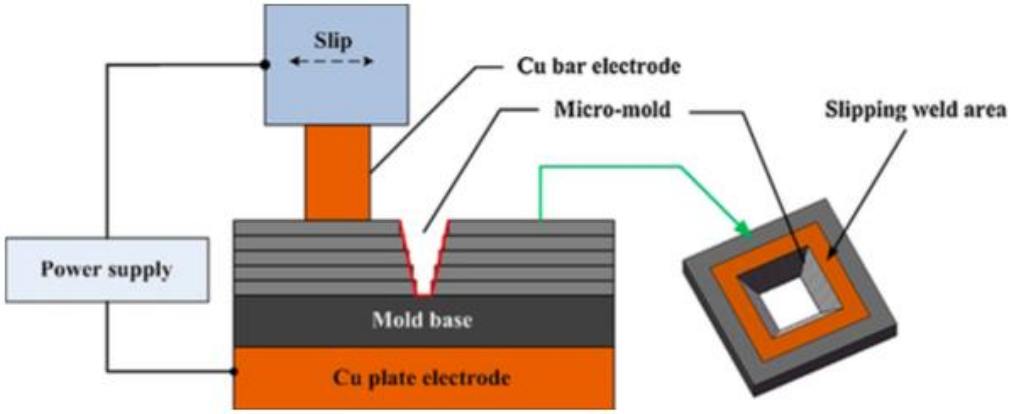

Figure 8. SL methodology with slip resistance welding to join sheets. [29]

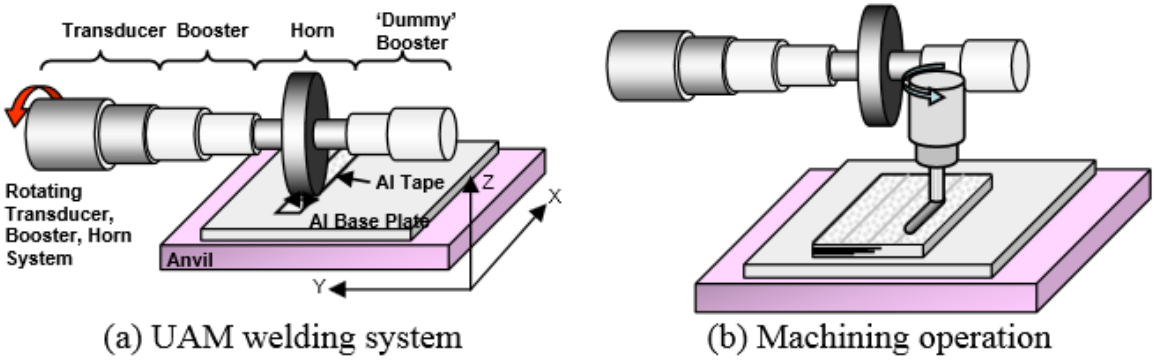

Figure 9. The UAM process forms solid metal by (a) ultrasonic welding of metal tape onto a substrate or other tape layers and (b) machining or parts edges, channels, or features as needed through the process. [207]

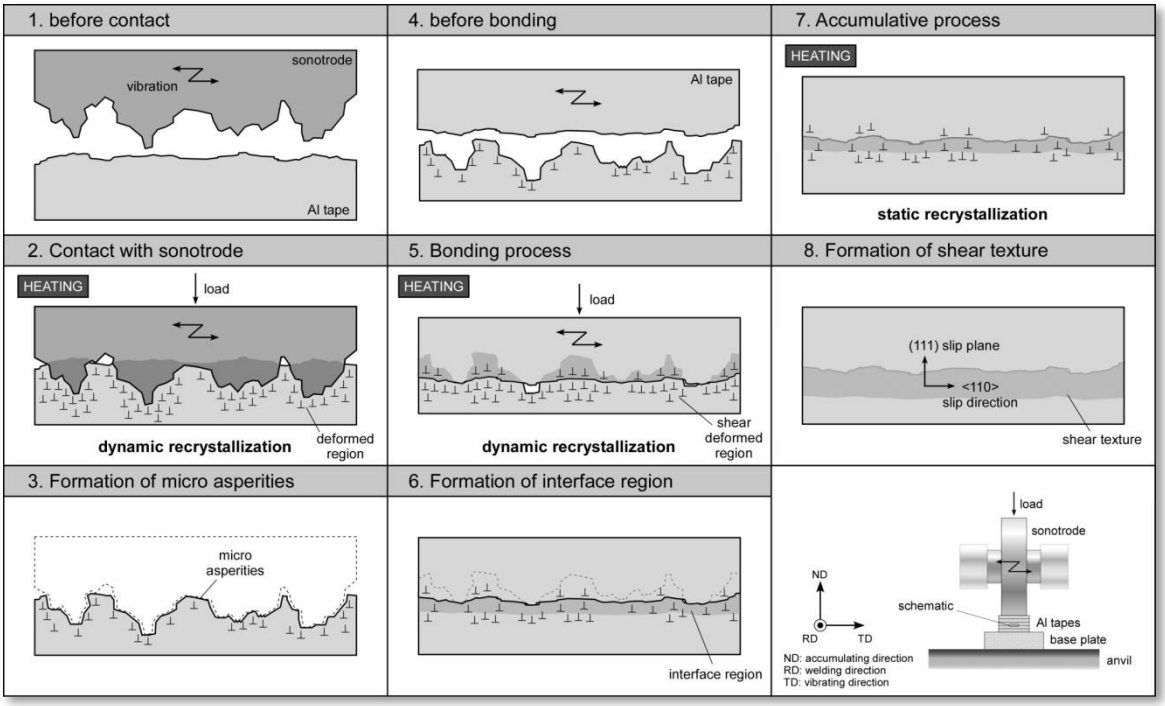

Figure 10. Schematic illustration of microstructural evolution during UAM. [41]

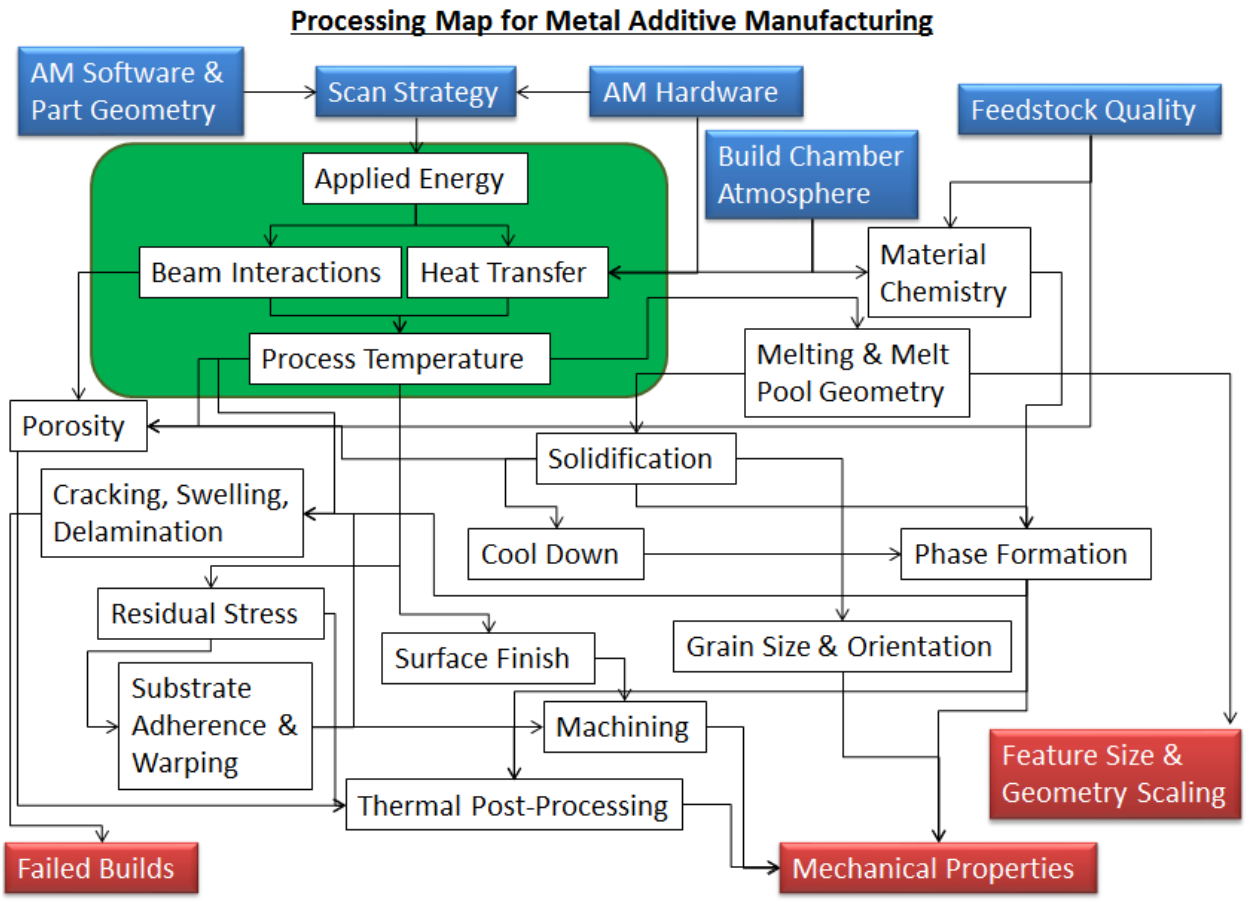

Figure 11. Processing map for metal AM.

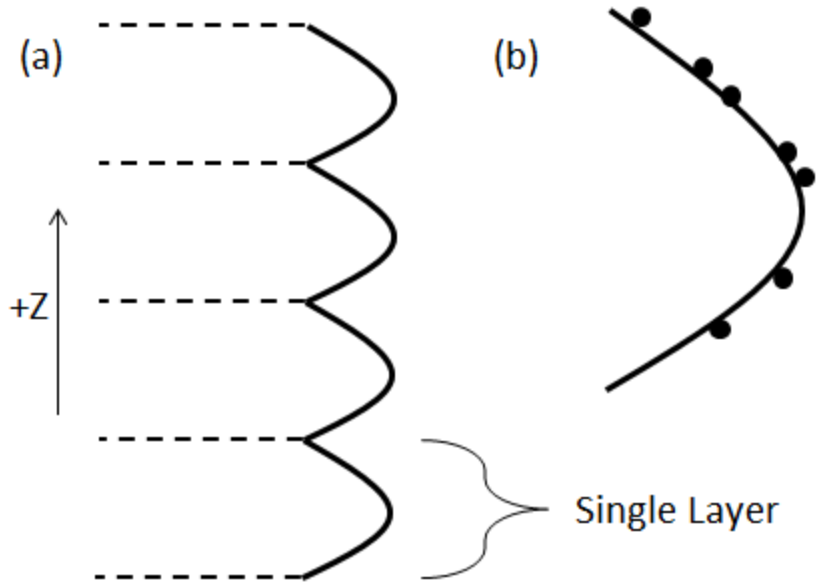

Figure 12. Sketch of the contributions to surface finish by (a) layer roughness and (b) actual surface roughness.

Table 2. Typcial layer thicknesses and minimum feature sizes of PBF and DED processes.

Process	Typical Layer Thickness [µm]	Minimum Feature Size or Beam Diameter [µm]
PBF – LM [112]	10-50	75-100
PBF – EBM	50	100-200
DED – Powder Fed [71]	250	380
DED – Wire Fed [58]	3,000	16,000

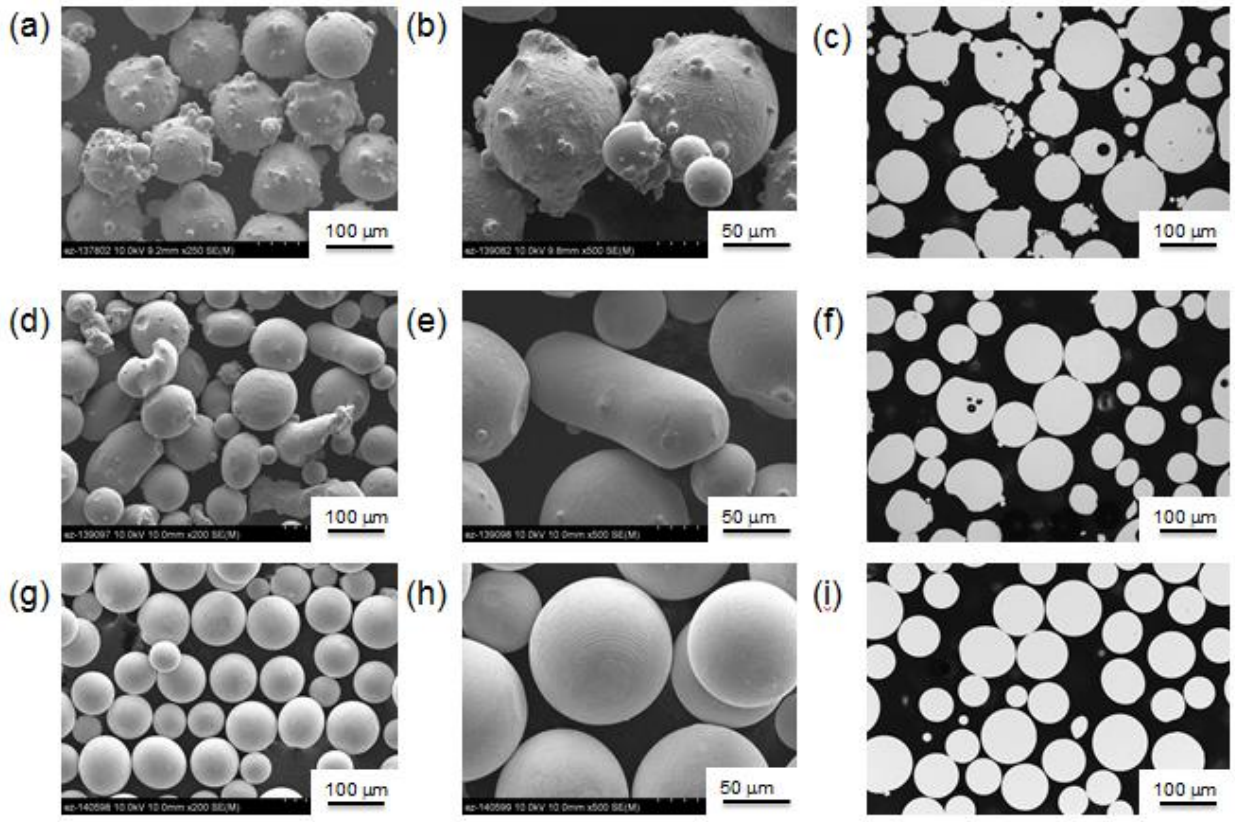

Figure 13. Comparison of powder quality before use: (a) SEM 250x of GA, (b) SEM 500x of GA, (c) LOM of GA, (d) SEM 200x of RA, (e) SEM 500x of RA, (f) LOM of RA, (g) SEM 200x of PREP, (h) SEM 500x of PREP, (i) LOM of PREP. (Used with permission) [16]

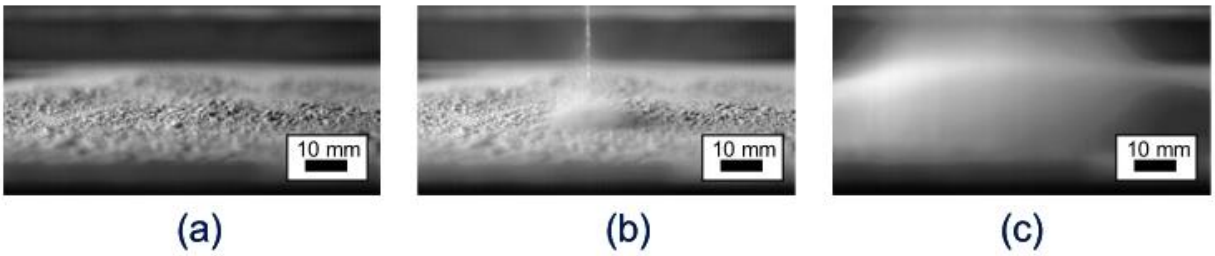

Figure 14. An event of "smoking" caused by electrostatic repulsion: (a) distributed powder bed, (b) applied beam, and (c) "smoking" or a cloud of charged powder particles. [66]

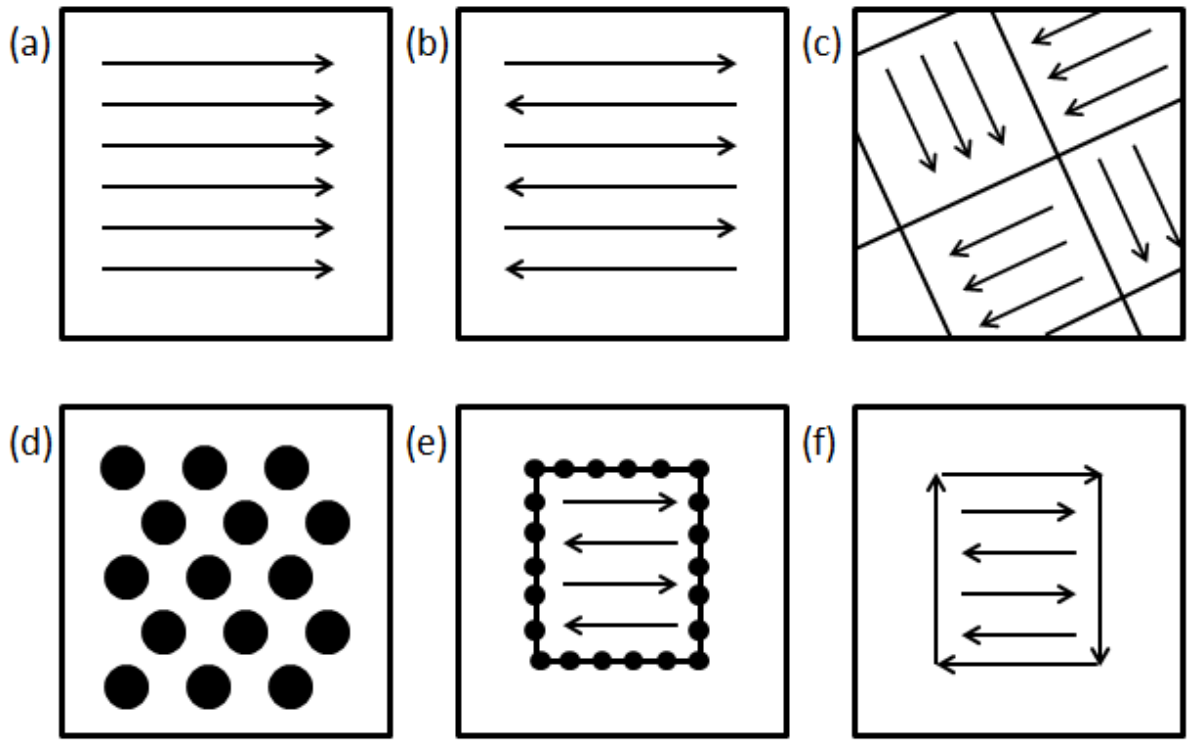

Figure 15. Scan strategies used to determine heat source path in metal AM as seen in the X-Y plane (perpendicular to the build direction): (a) unidirectional or concurrent fill, (b) bi-directional, snaking, or countercurrent fill, (c) island scanning, (d) spot melting, (e) spot melting contours with snaking fill, and (f) line melting contours with snaking fill.

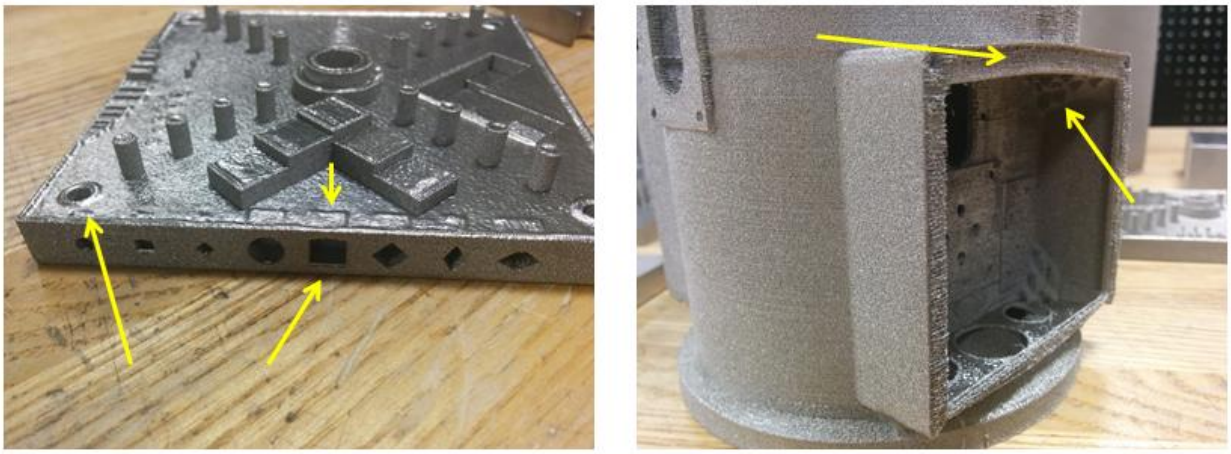

Figure 16. For EBM printed Ti-6Al-4V parts it can be seen that (Left) a NIST test artifact designed to test AM capabilities has overhangs printed in the side of the part. These are intended to test the ability of various machines to print overhangs. Minor swelling can be seen both above the overhang and near a hole on the left side on the top surface. (Right) A complex robotic part shows a slightly deformed overhang, with sintered powder and support stubs left underneath.

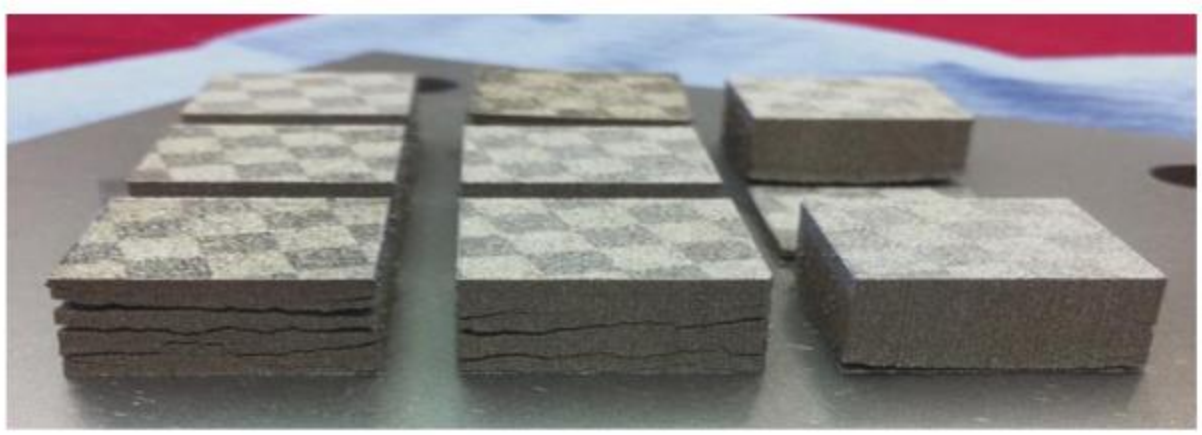

Figure 17. Layer delamination and cracking can be a problem in SLM (shown for M2 tool steel). [73]

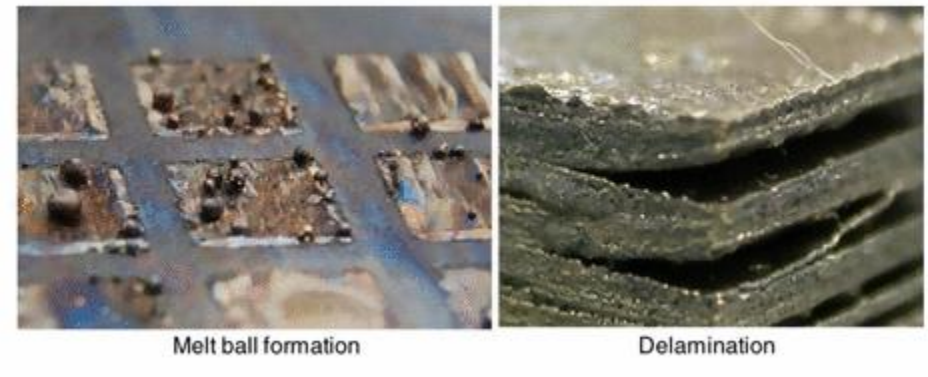

Figure 18. Melt ball formation and Delamination in EBM stainless steel. [76]

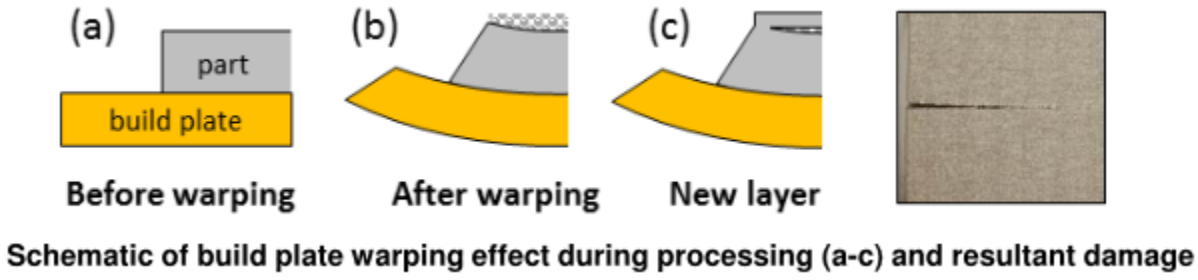

Figure 19. The effect of substrate warping can lead to lack-of-fusion or delamination. [79]

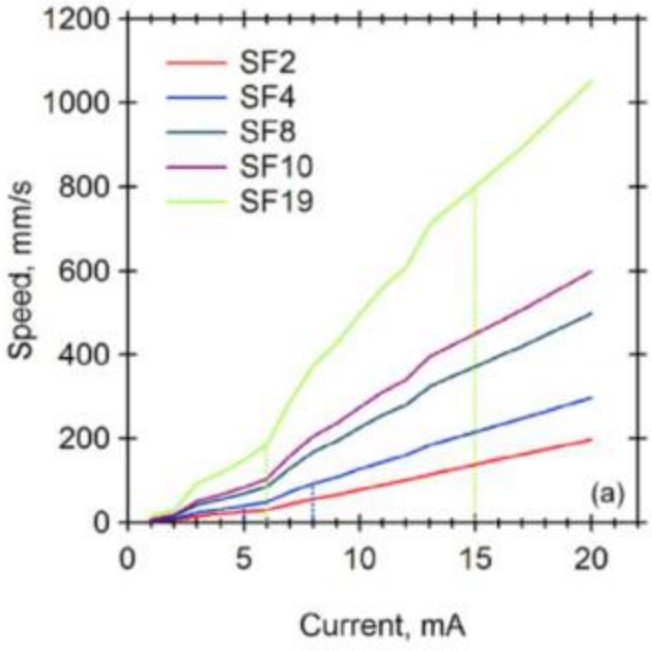

Figure 20. The relationship between speed and current for EBM is known as the "speed function". [93]

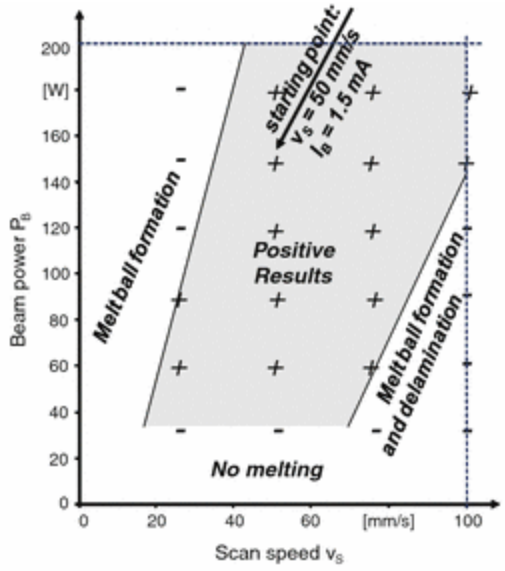

Figure 21. Process map for stainless steel EBM demonstrates importance in the relationship between applied power and beam speed. [76]

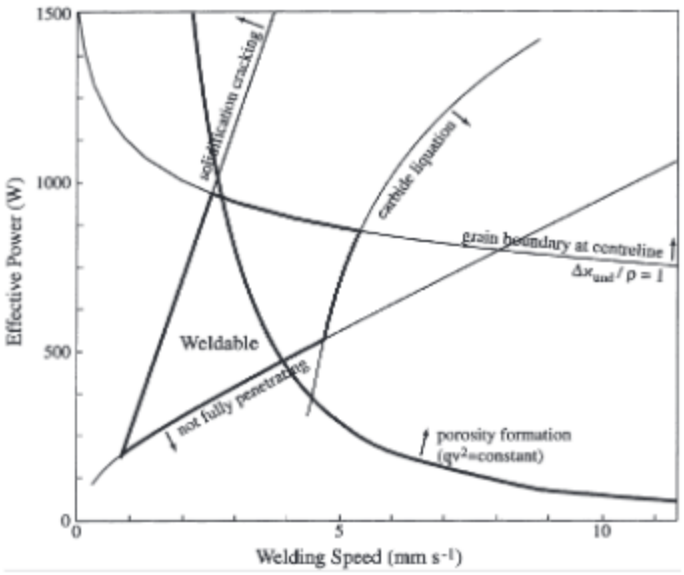

Figure 22. Relationship between effective power and speed in determining the weldability of Inconel 718. [208]

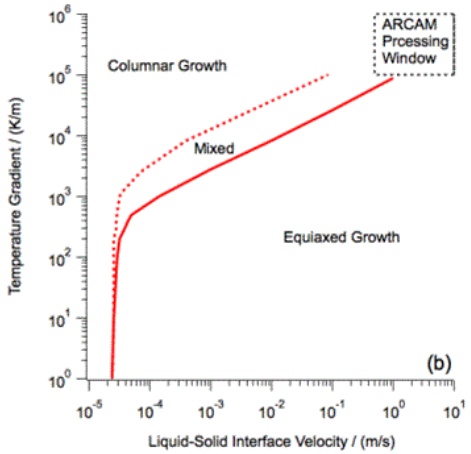

Figure 23. EBM processing window for Inconel 718 processing overlaid on G vs. R data. [103]

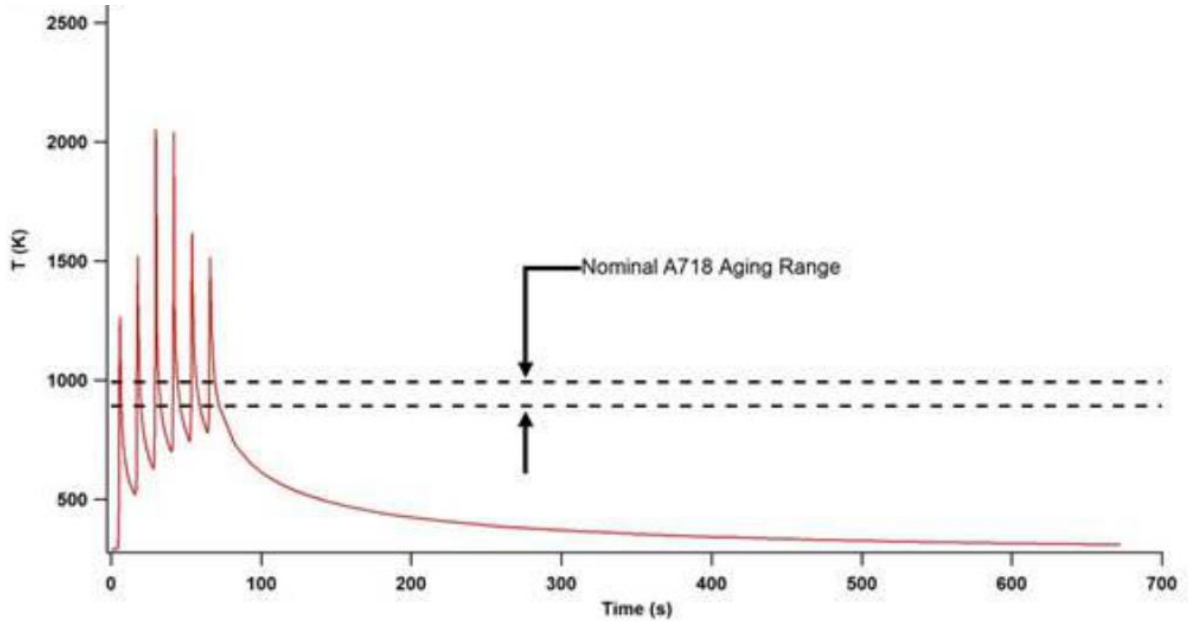

Figure 24. Thermal simulation of a point during powder-fed DED showing cyclic heating cycles. [102]

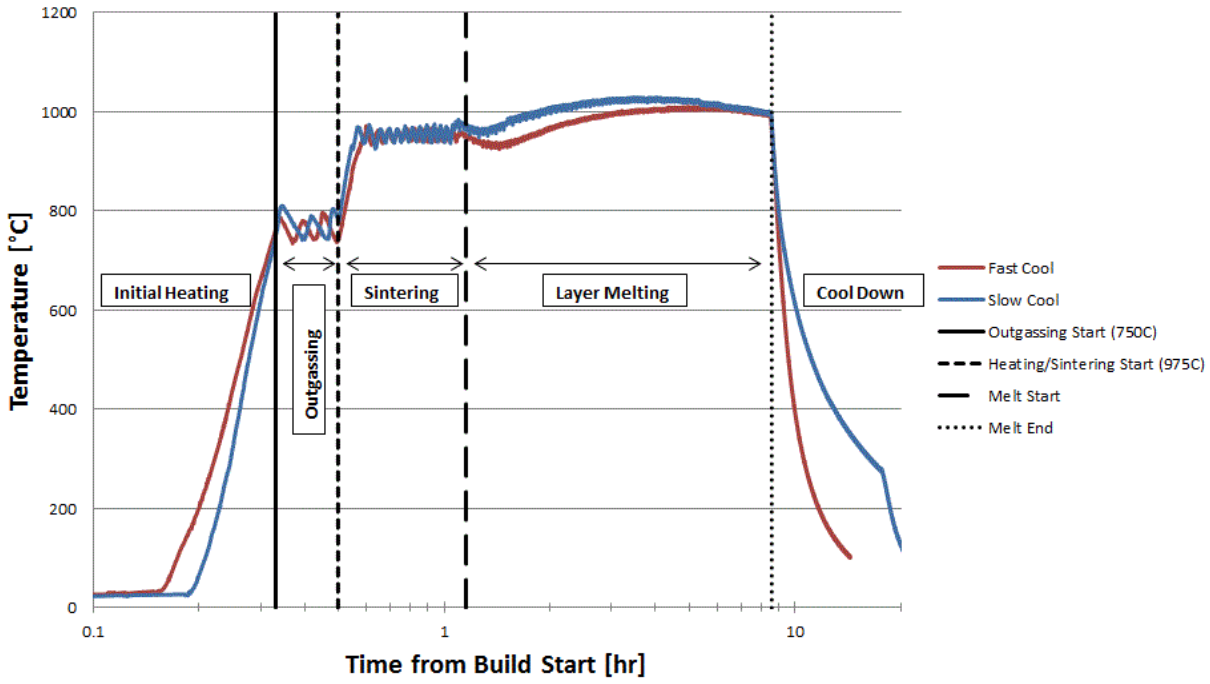

Figure 25. EBM process thermal history, as measured by the machine-standard, substrate thermocouple. [103]

Table 3. Common post-processing procedures for Ti-6Al-4V and Inconel 718.

Treatment	Ti-6Al-4V	Inconel 718
Stress Relief	2 hours, 700-730°C [154]	0.5 hours at 982°C [112] 1065±15°C for 90 min (-5/+15min) [150]
Hot Isostatic Pressing (HIP)	2 hours, 900°C, 900MPa [154] 180±60 min, 895-955°C, >100MPa [149]	4 hours at 1120°C, 200MPa
Solution Treat (ST)	Not Typical	1 hour at 980°C [209]
Aging	Not Typical	8 hours at 720°C Cool to 620°C Hold at 620°C for 18 hours total [209]

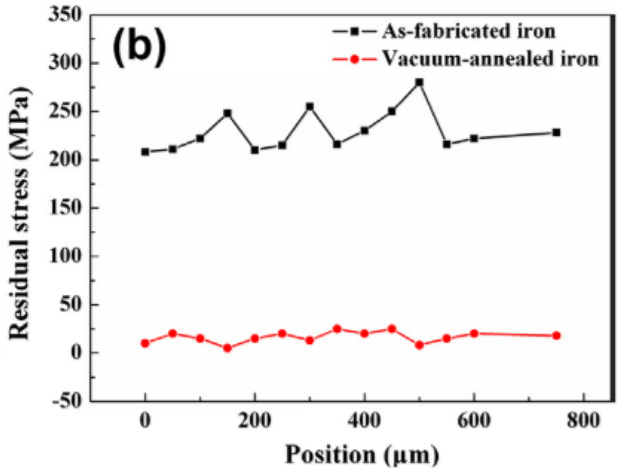

Figure 26. Stress relief through vacuum annealing can almost eliminate residual stress. [87]

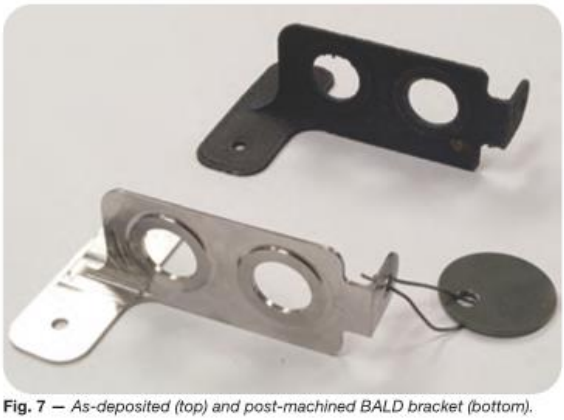
Fig. 7 — *As-deposited (top) and post-machined BALD bracket (bottom).*

Figure 27. Post-HIP Ti-6Al-4V brackets, before (Top) and after (Bottom) machining. (reprinted with permission) [114]

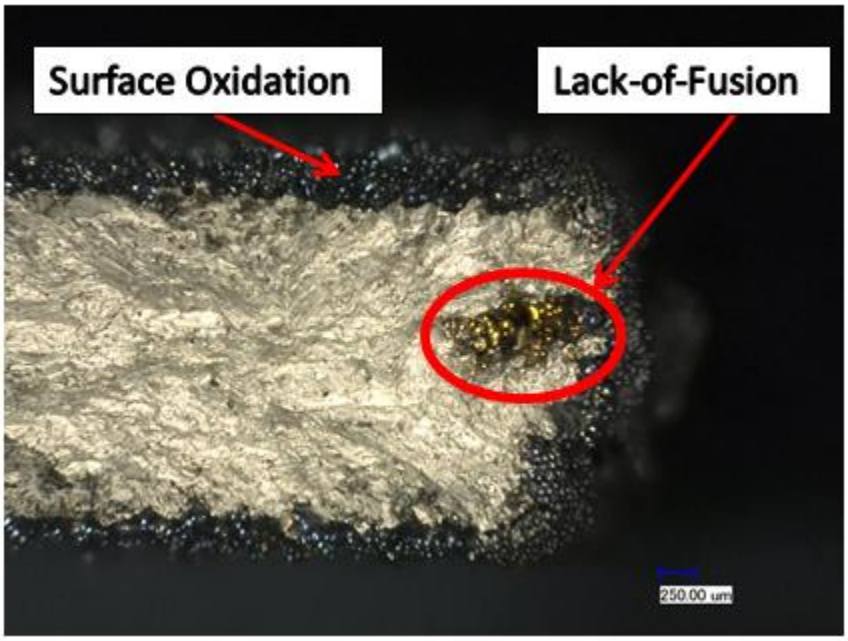

Figure 28. Thin wall EBM fracture surface of Inconel 718 from post-HIP sample with notable change in surface oxidation and oxidation of an open pore caused by lack-of-fusion near the edge.

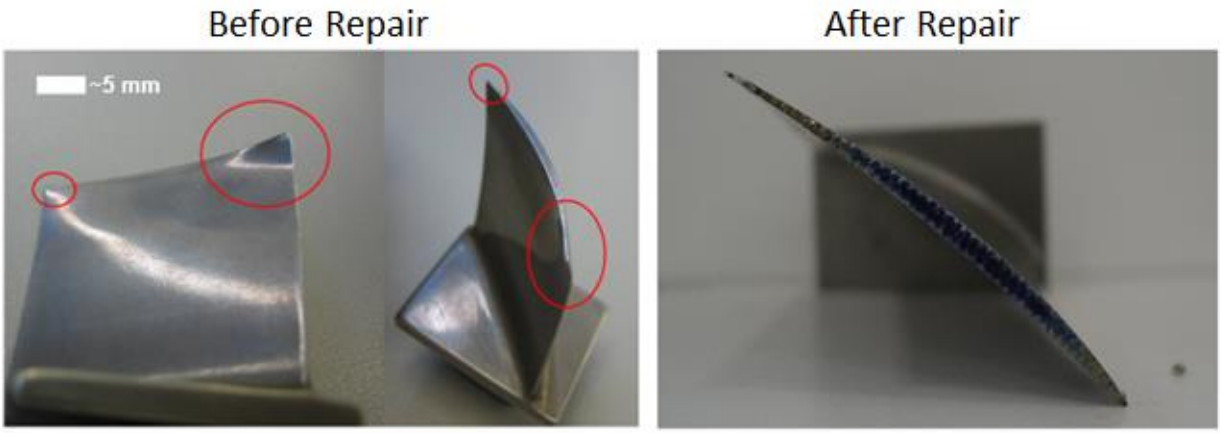

Figure 29. Airfoil repair using a hybrid DED+CNC method. [117]

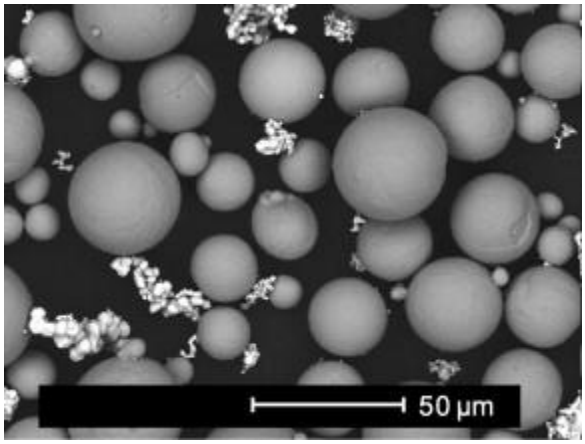

Figure 30. Ti-6Al-4V-ELI, Extra Low Interstitial, (large, round particles) mixed with 10%wt Mo (white, irregular particles). Powder mixture was processed using SLM, which led to room temperature β-phase stabilization. [118]

Table 4. There is a limited scope of currently available commercial materials, but there are ongoing R&D efforts in materials development.

Process	Commercial Materials	Researched Materials
DED	Stainless steel, Ni based alloys, tool steel, Ti alloys	FeTiNi [122], TiZrNbMoV [121], ceramics [123], CoCrMo [210], WC-Co [124]
EBM	Ti-6Al-4V, Ti, CoCr [211]	Inconel 718, Inconel 625, Al 2024 [64], high purity copper [143], GRCop-84 [125], Niobium [212], bulk metallic glass [119], stainless steel 316L [76], TiAl [213]
LM	Ti-6Al-4V, stainless steel, various steels, Ti, CoCr, Al-Si-10Mg, Bronze, precious metals, Inconel 718, Inconel 625, Hastelloy X	Tantalum [138], W-Ni [214], AlSi10Mg [135]
Sheet Lamination [215]	Al/Cu, Al/Fe, Al/Ti	Ta/Fe, Ag/Au, Ni/Stainless
Binder Deposition	316 Stainless Steel Infiltrated with Bronze, 420 Stainless Steel Infiltrated with Bronze (Annealed & Non-Annealed), Bronze, Iron Infiltrated with Bronze, Bonded Tungsten [22], Inconel 625 [216]	FeMn [217], pure alloys (no infiltration), ceramics [218]

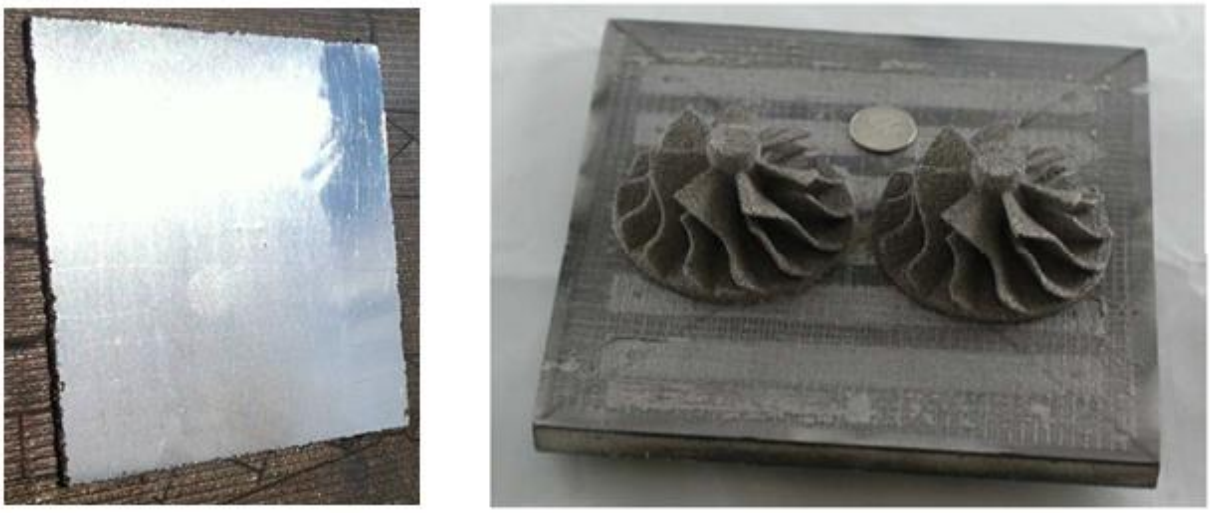

Figure 31. (Left) Bulk metallic glass made in EBM, with amorphous structure [119] and (Right) EBM fabricated Al 2024 impellers on build substrate. [64]

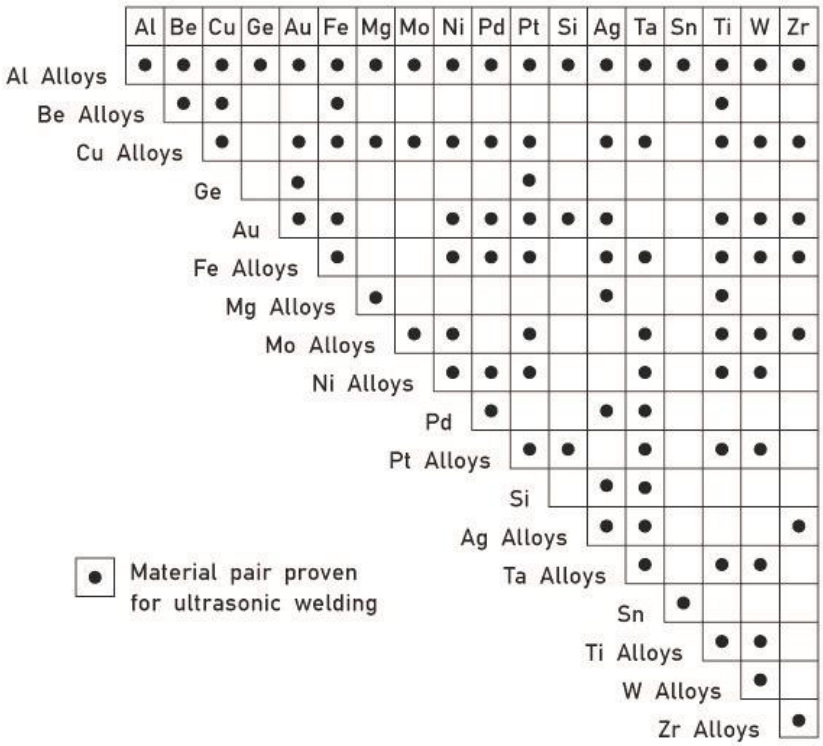

Figure 32. Tabular representation of alloys that can be joined using ultrasonic consolidation. [215]

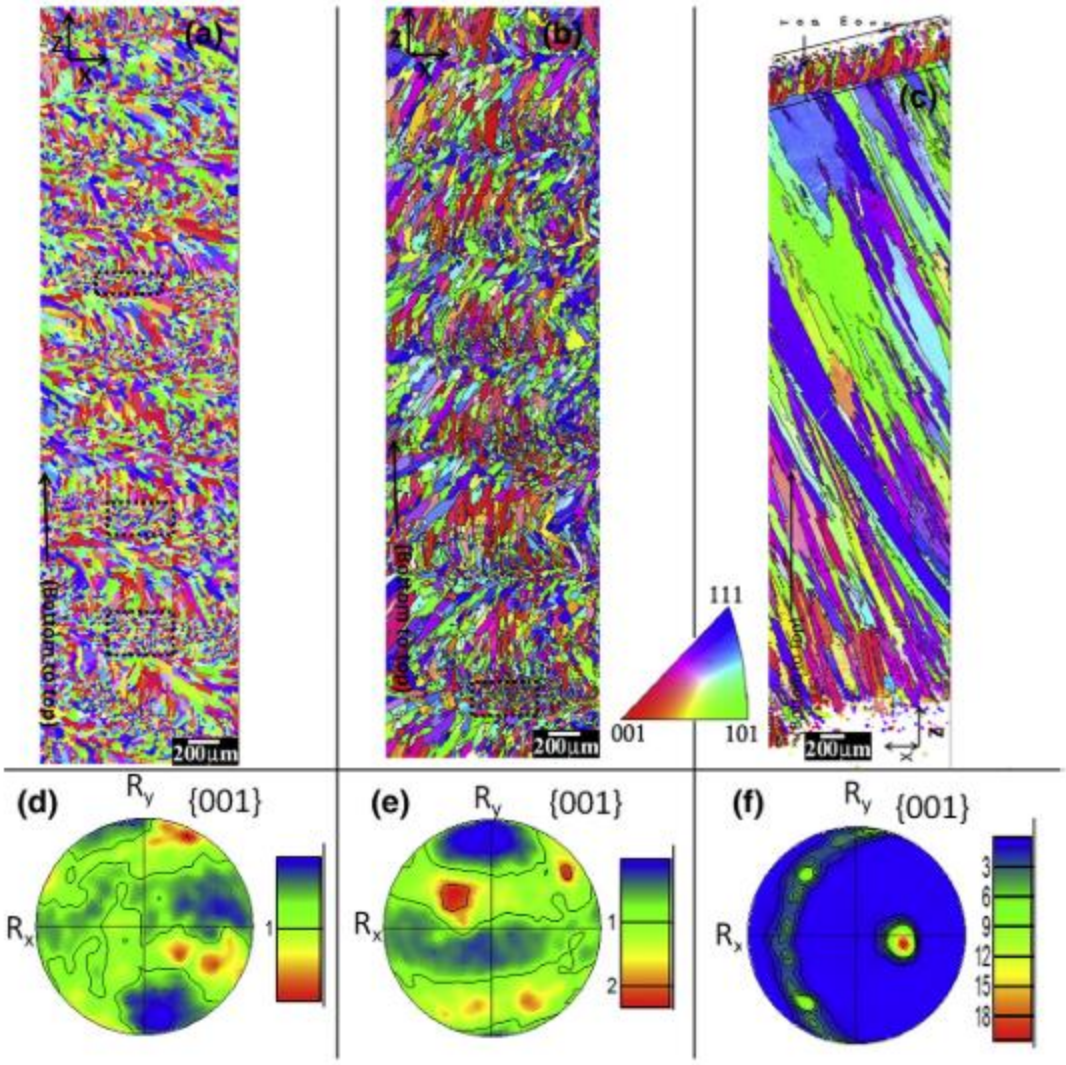

Figure 33. Grain structure in DED material is highly influenced by scan strategy. Shown is Inconel 718, produced using (a) unidirectional, (b), bi-directional, and (c) bi-directional, high power scanning. [133]

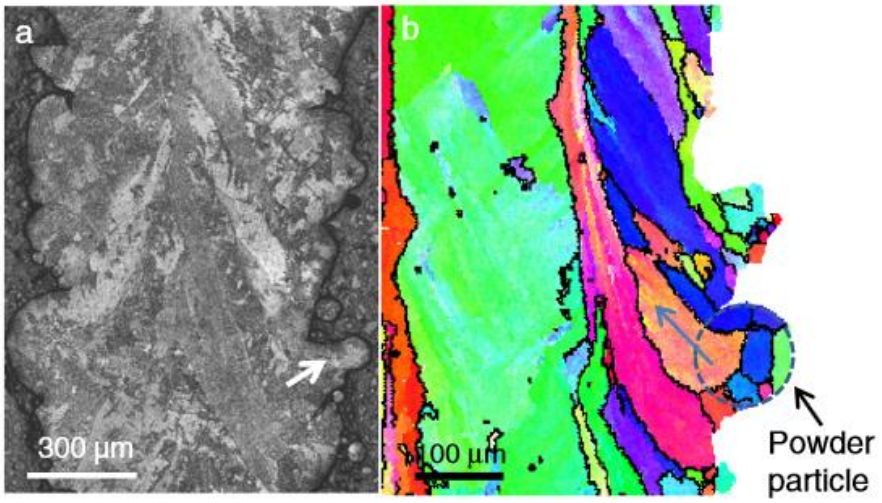

Figure 34. Effect of powder and edges on grain growth in EBM Ti-6Al-4V. [134]

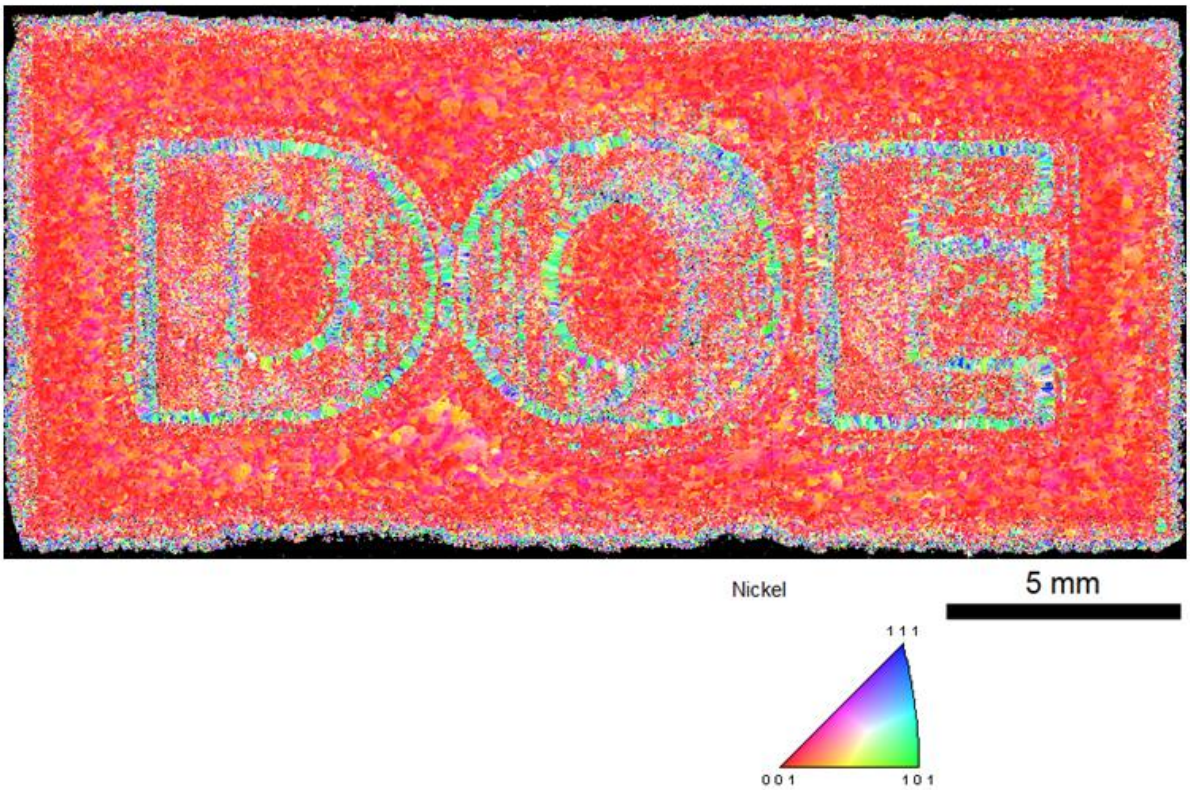

Figure 35. Local control of grain orientation in EBM of IN718. (Used with Permission) [142]

Table 5. Compilation of reported tensile results for Ti-6Al-4V and Inconel 718.

Material	0.2% YS [Mpa]	UTS [Mpa]	Elongation [%]	Reference
Ti-6Al-4V				
DED As-Deposited (X-Y)	976±24	1099±2	4.9±0.1	[130]
DED Stress Relieved (X-Y)	1065-1066	1109	4.9-5.5	[154]
DED Stress Relieved (Z)	832	832	0.8	[154]
DED HIP (X-Y)	946-952	1005-1007	13.0-13.1	[154]
DED HIP (Z)	899	1002	11.8	[154]
LM As-fabricated (X-Y)	910±9.9	1035±29.0	3.3±0.76	[129]
LM + HT (X-Y)	1195±19.89	1269±9.57	5±0.52	[219]
LM + HT (Z)	1143±38.34	1219±20.15	4.89±0.65	[219]
EBM As-fabricated (X-Y)	967-983	1017-1030	12.2	[148]
EBM As-fabricated (Z)	961-984	1009-1033	7.0-9.0	[148]
EBM As-fabricated (Z)	883.7-938.5	993.9-1031.9	11.6-13.6	[128]
EBM HIP (Z)	841.4-875.2	938.8-977.6	13.4-14.0	[128]
Wrought bar (annealed)	827-1000	931-1069	15-20	[220]
Cast+Anneal	889	1014	10	[220]
Cast+Anneal (peak aged)	1170	1310	-	[219, 221]
Inconel 718				
DED As-Deposited (NR)	590	845	11	[51]
DED STA (X-Y)	635-1107	958-1415	2.4-18.4	[131]
LM As-fabricated (NR)	889-907	1137-1148	19.2-25.9	[132]
LM STA (NR)	1102-1161	1280-1358	10.0-22.0	[132]
LM As-fabricated + stress relief (X-Y)	830	1120	25	[112]
LM HIP+anneal (X-Y)	890	1200	28	[112]
LM HIP+anneal (Z)	850	1140	28	[112]
EBM As-fabricated (X-Y)	822 ± 25	1060 ± 26	22	[111]
EBM As-fabricated (Z)	669-744	929-1207	21-22	[108, 111]
EBM HIP+STA (X-Y)	1154 ± 46	1238 ± 22	7	[111]
EBM HIP+STA (Z)	1187 ± 27	1232 ± 16	1.1	[111]
Wrought - Bar	1190	1430	21	[221]
Wrought - Sheet	1050	1280	22	[221]

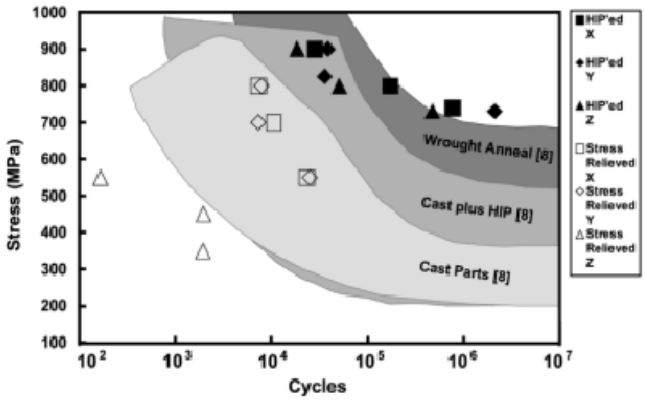

Figure 36. Fatigue test results of HIP and stress relieved DED material. [154]

Figure 37. (Left) Operator setting up cold spray AM system, which operates outside of a controlled environment, and (Right) cold spray deposit forming on the tip of a substrate tube that is rotated. [161]

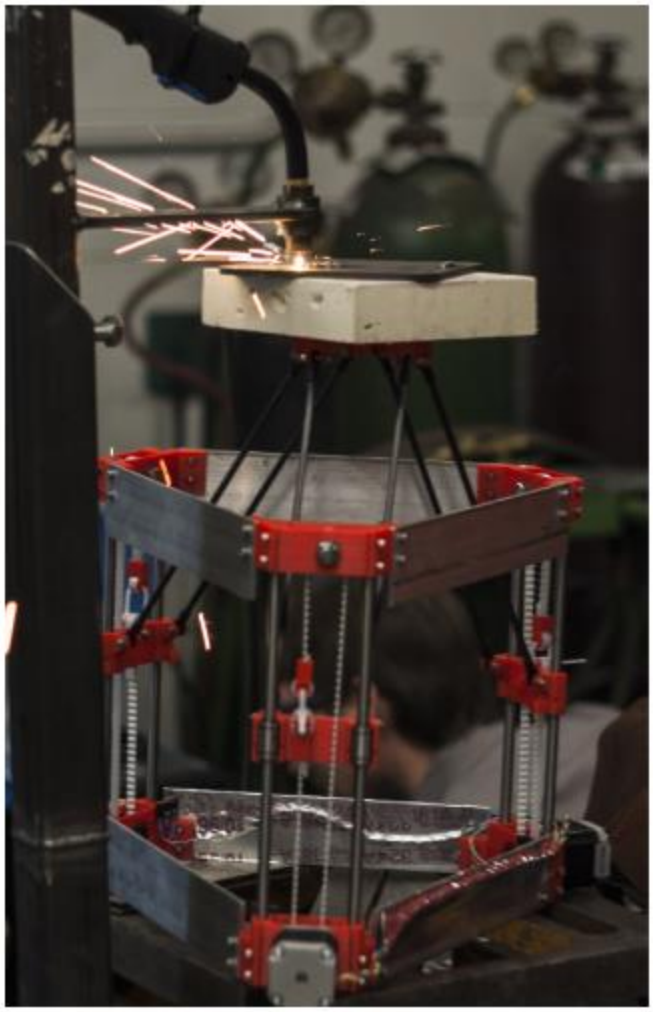

Figure 38. Open source DED system designed with a stationary GMAW/MIG welder and moving stage/platform. [172]

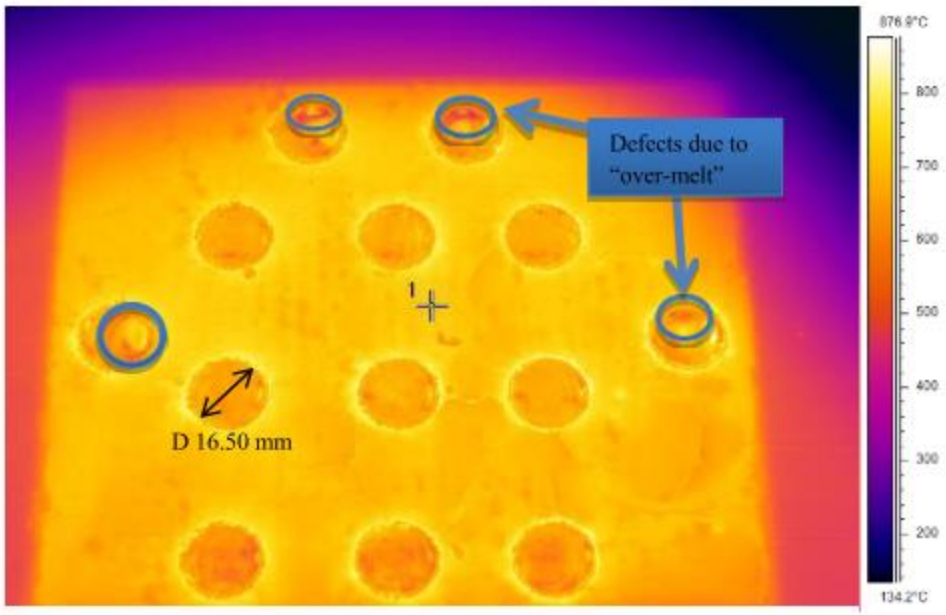

Figure 39. Near IR imaging of Ti-6Al-4V tensile specimens used to identify defects. [222]

Table 6. Comparison of defects and features across platforms.

Defect or Feature	LM	EBM	DED – Powder Fed	DED – Wire Fed	Binder Jetting	Sheet Lamination
Feedstock	Powder	Powder	Powder	Wire	Powder	Sheets
Heat Source	Laser	E-Beam	Laser	Laser/E-Beam	N/A; Kiln	N/A; Ultrasound
Atmosphere	Inert	Vacuum	Inert	Inert/Vacuum	Open Air	Open Air
Part Repair	No	No	Yes	Yes	No	No
New Parts	Yes	Yes	Yes	Yes	Yes	Yes
Multi-Material	No	No	Possible	Possible	Infiltration	Yes
Porosity	Low	Low	Low	Low	Yes	At sheet interfaces
Residual Stress	Yes	Low	Yes	Yes	No	?
Substrate Adherence	Yes	Material Dependent	Yes	Yes	?	?
Cracking	Yes	Not Typical	Yes	Yes	Fragile Green Bodies	No
Delamination	Yes	Yes	Yes	Yes	No	Yes
Rapid Solidification	Yes	Yes	Yes	Yes	No	No
In-Situ Aging	No	Yes	No	No	No	No
Overhangs	Yes	Yes	Limited	Limited	Yes	Limited
Mesh Structures	Yes	Yes	No	No	?	No
Surface Finish	Medium -Rough	Rough	Medium - Poor	Poor but Smooth	?	Machined
Build Clean-Up From Process	Loose Powder	Sintered Powder	Some Loose Powder	N/A	Loose Powder	Metal Shavings

Table 7. Reported deposition rates for various technologies

Process	Machine	Deposition Rate [cc/hr]	Maximum Power [W]	Min. Heat Source Diameter [mm]	Max Power Input [kW/mm^2]
BJ	M-Flex [223]	1200-1800	N/A	N/A	N/A
DED – Powder Fed	LENS (2500-3000W) [18]	230	3000	1	3.8
EBM	A2 [194]	60	3500	0.2	110
DED – Wire Fed	EBFFF [19]	47	408	0.38	3.6
Material Extrusion	RepRap, Polymer [224]	33	N/A	N/A	N/A
LM	Renishaw AM 250 [225]	5-20	400	0.135	28
DED – Powder Fed	LENS (400-500W) [18]	16	500	1	0.64

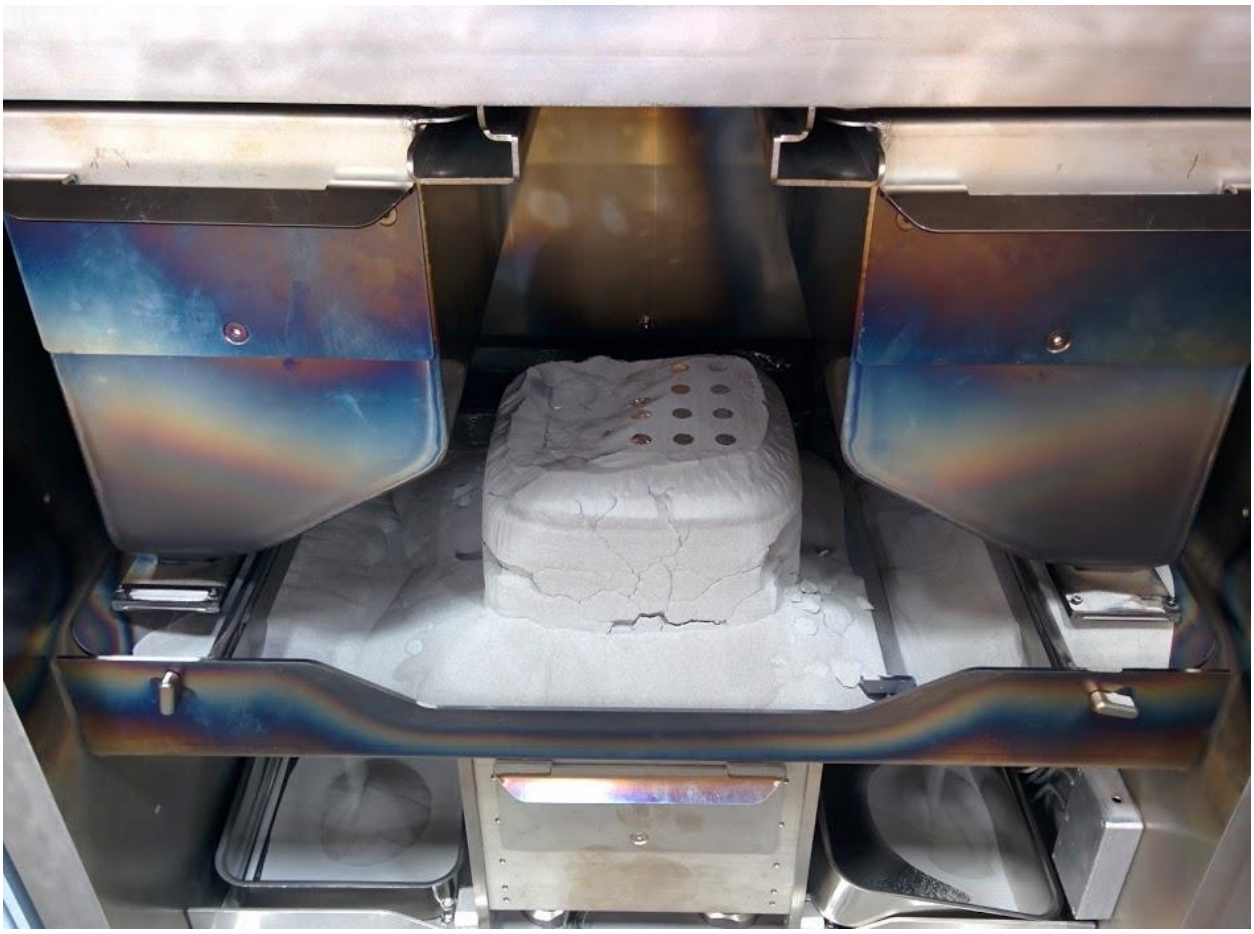

Figure 40. Failed build due to selective powder fetching in EBM. Hardware/software advances are needed to eliminate such problems.

Figure 41. Joint of a robotic arm that embeds hydraulic lines, eliminating external lines for hydraulic fluid and wiring. (used with permission) [185]

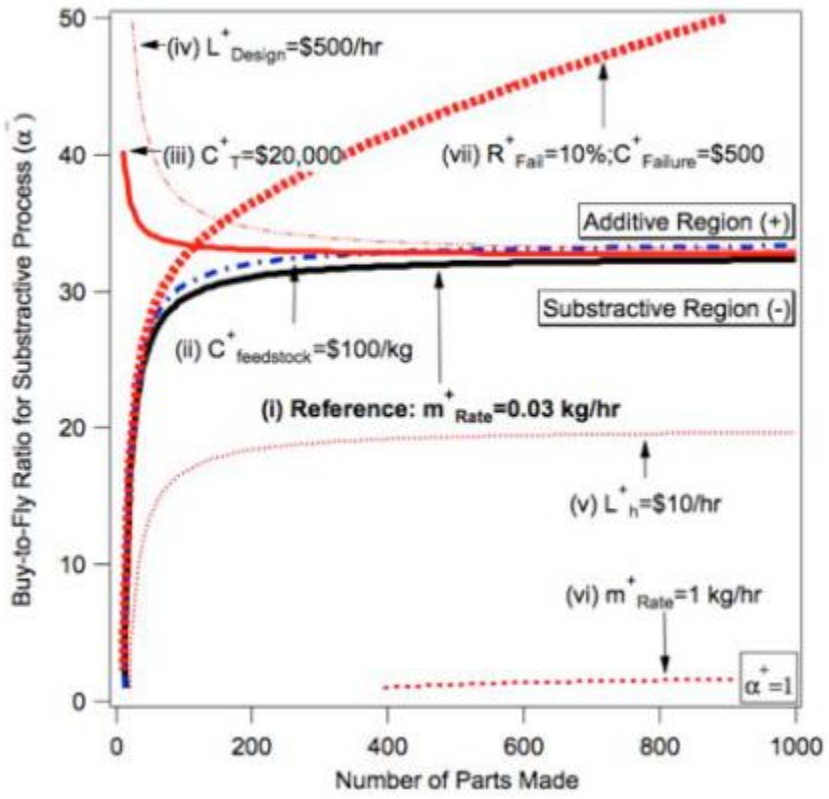

Figure 42. Comparative analysis of additive and subtractive manufacturing.